SEPARATION OF ZIRCONIUM FROM URANIUM IN U-ZR ALLOYS USING A CHLORINATION PROCESS

A Dissertation

by

ADAM JOSEPH PARKISON

Submitted to the Office of Graduate Studies of
Texas A&M University
in partial fulfillment of the requirements for the degree of

DOCTOR OF PHILOSOPHY

Chair of Committee,	Sean M. McDeavitt
Committee Members,	William Charlton
	Simon North
	Lin Shao
Head of Department,	Yassin Hassan

August 2013

Major Subject: Nuclear Engineering

ABSTRACT

The fundamental behavior underpinning a new processing concept was demonstrated which is capable of separating uranium from zirconium in U-Zr alloys through the formation and selective volatilization of their respective chlorides. Bench-scale chlorination and volatilization experiments were conducted on uranium, zirconium, and a U-50 wt% Zr alloy in order to gather the data needed to develop processing methods and equipment. It is also proposed that the demonstrated chlorination process may be coupled to a hydride/dehydride pulverization process, resulting in increased process efficiencies and simplified equipment design.

Process variables such as temperature, pressure, surface area, and reaction time were studied in an iterative manner until the variables needed for selective volatilization were discovered. This began with the design and assembly of an experimental apparatus which was capable of surviving a hot chlorine atmosphere. It was found that standard glass test-tubes were suitable as reaction vessels for these experiments. Heated and non-heated regions were established within the glass reaction vessels to allow for volatilization and condensation of the volatile chlorides through natural convection. The volatilized and non-volatilized products were collected and analyzed using EPMA to determine the relative uranium and zirconium compositions.

It was found that chlorination reactions on gram-size samples at temperatures of 320, 340, 360 °C generated a uranium product with 89.9, 95.0, and 98.8% purity, and a zirconium product with 82.1, 85.1, and 84.2% purity, respectively. These separations

were achieved through a single distillation with a U-50 wt% Zr starting material. It is anticipated that further distillations could be used to achieve increased uranium and zirconium purity, and changes in system geometry could also significantly increase these purities, specifically with the zirconium product stream.

ACKNOWLEDGEMENTS

I would like to thank my committee for their support throughout the course of this research. I would also like to thank Ray Guillemette, “The Fifth Beatle”. Thanks go to my colleagues Aaron Totemeier, Brandon Blamer, Grant Helmreich, Jeff Clemens, and Miguel Holgado who each provided their own unique contribution. I would like to extend a special thanks to Sean McDeavitt for giving me the freedom and the opportunity to pursue this research in my own way.

TABLE OF CONTENTS

Page

Page

LIST OF FIGURES

Page

Page

Page

Page

LIST OF TABLES

Page

1. INTRODUCTION

1.1 Context and Motivation

The development of new nuclear energy systems and advanced fuel cycles creates a unique set of challenges. The challenge being considered in this research is the establishment of a strategy for the disposal and/or reprocessing of uranium-zirconium alloy nuclear fuel that has been burned to relatively high burnup. Such enabling strategies are being considered to address the sustainability of nuclear power for centuries to come. The particular process being considered here enables zirconium, and perhaps other volatile species, to be separated from the uranium through selective volatilization of the chlorides of zirconium and uranium. These chlorides can be separated using a simple distillation process based on their respective boiling points of 331 and 791 °C [1].

Chemical processing of U-xZr alloys is challenging because of issues related to material handling on industrial scales which arise due to the chemistry of these two elements. The worldwide standard for reprocessing oxide fuel is the Plutonium URanium EXtraction (PUREX) process. The PUREX process consists of first dissolving the nuclear fuel in nitric acid. This acid solution is then mixed with a tributyl phosphate (TBP)/kerosene mixture in order to extract the uranium, plutonium, thorium, or whatever else might be of interest, from the waste-stream [2]. Problems arise during aqueous processing of uranium-zirconium alloys due to the relative “nobility” of zirconium in nitric acid [3]. This nobility results in sludge formation within the

reprocessing equipment. Not only does this sludge clog equipment, but it also impedes the extraction process.

The PUREX process was designed to produce pure plutonium as a product [4]. This can be viewed as a drawback when nuclear fuel reprocessing is considered. Therefore, the recovery of a "dirty" product certainly has its advantages. It should also be noted that PUREX results in an oxide product after the aqueous effluent is calcined. It can be viewed as being somewhat counterproductive from a processing standpoint to process a metal fuel into an oxide, only to reconvert the oxide back into a metal. Many of the loosely defined pyroprocessing methods, including the one being proposed, allow for the recovery of "dirty" metallic products.

The fundamental chemical behavior of uranium and zirconium enables the use of halide-based separation methods. In this study, a chloride volatilization process was demonstrated that is effective in separating zirconium from uranium-zirconium metal alloys, resulting in both uranium-rich and zirconium-rich product streams. While the project focuses on the uranium-zirconium system, the results of this study may be applied to uranium alloyed with any group-4 (e.g., Ti, Zr, Hf) species and may also have relevance to the separation of other types of alloy mixtures where there is a range of chloride species vapor pressures. This study may be used as a basis to begin development of an industrial-scale process capable of selective separation of any group-4 species from uranium alloys.

There is a strong interest in the use of metal-alloy fuels in nuclear energy systems, especially in fast reactors, where a higher uranium-density is required when

compared to conventional oxide nuclear fuels. While metallic fuels have been used in experimental fast reactors for decades, the design requirement for high uranium density fuels has recently been a key component for two applications. The first arises from the desire to convert research reactors from High Enriched Uranium (HEU) fuel to Low Enriched Uranium (LEU) fuel. A fuel with a high uranium-density is required in order for some of the higher power density reactors to maintain operation at the same power output, and/or to have neutron flux levels which meet their continued mission requirements after being converted from HEU to LEU fuel. Much of this work has been performed under the Reduced Enrichment for Research and Test Reactors (RERTR) program [5].

The second application is more relevant to this project and is related to the need for development of fuels that can survive and enable ultra-high burnup requirements. At the forefront of this need are the requirements of the Traveling Wave Reactor (TWR) concept [6]. The TWR is an ultra-high burnup reactor that requires a high uranium density fuel for a more efficient conversion of U-238 to Pu-239 as well as for the ability to counteract the neutron poison effect from buildup of fission products. The uranium-zirconium alloy system has been directly considered for use in TWR's.

1.2 Hydride/Dehydride Pulverization

The chloride volatilization project considered here may be part of a sequence of steps that will begin with a hydride pre-treatment of the alloy to be processed. It is known that both uranium and zirconium readily form brittle hydrides [7-12]. It has also been shown that hydride formation in both of these elements results in a fine hydride

powder which is easily dehydrided through heating under vacuum [13]. Formation of a powdered alloy prior to processing with chlorine should greatly increase the chlorination rate due to the dramatically increased surface area which is formed during the hydride/dehydride process. This increased reaction rate was observed in the experiments performed for this research, as discussed in Sections 3.1.2, 4.4.2, and 4.4.3, where it was shown that formation of zirconium chloride has a strong dependence on surface area.

Perhaps the greatest advantage that a hydride pulverization process offers is that it fundamentally changes the equipment required for handling and processing this material in future stages. Pulverization would allow the material to be handled in a continuous or semi-continuous manner through fluidization of the powder, which offers clear advantages when compared to other processes where batch handling of bulk alloy material is required. The advantage of processing a fluidized powder are perhaps best demonstrated in Section 3.1.2 where it is shown that prohibitively high temperatures may be reached if a bulk alloy is processed using a chlorination process.

In addition to the aforementioned advantages of handling a pulverized material when compared to a bulk alloy, it cannot be ignored that a similar fluidization process is already in use for the purification of Group-4 species. This existing process begins with a fluidized zircon ($ZrSiO_4$) feed material, and produces a purified zirconium product. The process being proposed for this research is compared to the existing process in Table 1.

Table 1: Comparison of exiting process to proposed process.

	Existing Chlorination Process	**Proposed Chlorination Process**
Starting Material	Crushed Zircon ($ZrSiO_4$)	Pulverized U-Zr Alloy
Chlorination Reaction	$ZrSiO_4 + 2C + 4Cl_2(g) = ZrCl_4(g) + SiCl_4(g) + 2CO_2(g)$	$U + Zr + 4Cl_2(g) = UCl_4 + ZrCl_4(g)$
Reaction Temperature	~1,000 °C	~200 °C
Enthalpy Change	-307 kJ	-1883 kJ
Off Gasses	CO_2 and $SiCl_4$	Fission Products (If Present)
Reduction Agent	Magnesium	Magnesium
Reduction Products (Zr)	Zirconium Sponge	Zirconium and FPs (If Present)
Reduction Products (U)	NA	Uranium and FPs (If Present)

1.3 Chloride Volatilization

Following hydride/dehydride pulverization, the powderized alloy would be processed using the chloride volatilization method demonstrated for this work. The dramatically increased surface area of the metal powder, when compared to an intact bulk alloy, will result in a rapid chlorination reaction. The near-instantaneous, highly exothermic, chloride formation will enable the system to be operated at lower overall system temperatures than would be otherwise required. It was demonstrated, and is discussed in Section 4.4.3, that zirconium chloride formation and volatilization would occur at a system temperature of 310 °C for bulk zirconium, but could be reduced to as low as 195 °C for a zirconium powder. This would allow an industrial vessel to be maintained at a lower temperature than would otherwise be possible if bulk material

were to be in contact with the vessel walls during its exothermic conversion to the volatile chloride, which would undoubtedly result in high local temperatures.

The majority of experiments performed for this project were ultimately focused on studying the chlorination and selective volatilization of zirconium from U-50Zr (all compositions will be reported in weight-percent from this point onward) bulk alloys. The results of these selective volatilization experiments show great promise that chlorine may be used to produce purified uranium and zirconium product streams from this and similar alloys. For example, it was observed that at 360 °C this chlorination process is capable of producing a uranium and zirconium product stream each with a purity of 98.8% and 84.2%, respectively, through a single distillation. These separation efficiencies are likely to be increased if a powder feed material is used instead of a bulk alloy because of the increased chloride formation rate which will result in greater control over the volatilization process.

The following chapters contain the literature foundation (Ch. 2), experimental equipment and methods (Ch. 3), and a detailed and complete presentation of the experimental results (Ch. 4). Chapter 5 contains a discussion of the implications and the potential impact of these results as they may apply to future research and/or industrial systems which utilize this or a similar process.

2. BACKGROUND

The Sections below contain descriptions of the conversion of metals to powder via hydride formation (Section 2.1), the chlorination and volatilization of metals (Section 2.2), as well as a brief description of methods involving other halides (I, Br, and F) (Section 2.3).

2.1 Hydride Formation

As noted in Section 1.2, the hydride/dehydride method may be used prior to the chlorination process evaluated in this study to significantly increase the surface area of the material. Therefore, this section will review the fundamental aspects of this method.

The chemical reaction of an active metal with hydrogen is a common method for producing reactive metal powder [14]. This method begins by hydriding the metal(s) of interest, usually via reaction with hydrogen gas at an elevated temperature, to form a brittle metal hydride which has a lower density than the original material. The formation of a low density metal hydride phase introduces stresses in the embrittled structure which results in the metal being reduced to a hydride powder. The hydride powder may then be dehydrided to produce a relatively pure metal powder, although complete removal of the hydrogen is a challenge. The dehydride process typically takes place under sub-atmospheric pressures and at even higher temperatures than the hydride formation reaction. The product of this coupled hydride/dehydride process is a powder (pure metal or alloy) that has been produced from a bulk solid piece of metal. While not

suitable for all metals, a hydride/dehydride process is capable of reducing the materials of interest to this project, namely uranium and zirconium, to a fine metal powder.

2.1.1 Zirconium Hydride Formation

It has been shown that a hydride/dehydride process can be used to reduce zirconium metal to a fine metal powder at relatively modest temperatures. Experiments were performed which studied the hydride formation rate in Zircaloy-4 (98.5%Zr-1.5%Sn-trace others) as a function of temperature [15]. The purpose of these experiments was to pulverize Zircaloy-4 into a fine metal powder for reuse in a ceramic-metal (cermet) actinide-transmutation material [16-17]. Data collected focused on determining the ideal temperature to achieve this result. While counter-intuitive, it was found that lower temperatures were more efficient at producing a pulverized metal powder, as seen in Figure 1. It was found that if hydrides were formed at temperatures lower than the 545 °C eutectoid (Figure 2), total pulverization could be achieved in as little as one hour. It is believed that this is due to the early onset of the δ-phase at these lower temperatures [10,13].

The formation of the δ-ZrH_{2-x} phase is believed to be critical to the pulverization of zirconium. As stated previously, a hydride pulverization process depends on the formation of a lower density hydride phase. As can be seen in Figure 2, the onset of the formation of δ-ZrH_{2-x} is highly dependent on the process temperature. The δ-phase begins to form at hydrogen concentrations below ~5% along the α-pathway at temperatures below 545 °C. Conversely, the brittle δ-phase does not begin to form until a hydrogen concentration of at least 28% is achieved along the β-pathway, at

temperatures above 545 °C. The effect of such a result is dramatic when the desired goal is pulverization of the material because of the strong dependence of surface area on the hydride reaction rate. The formation of a brittle hydride causes the material to fracture, thereby increasing the surface area, which accelerates the formation of the brittle hydride. The rapid onset of δ-phase formation for the α-phase pathway results in a dramatically increased pulverization rate when compared to the β-phase pathway.

Figure 1: Comparison of hydride formation along the β-path (left) and α-path (right). The sample on the left was produced at 582 °C with a hydrogen pickup of 90%. The sample on the right was produced at 432 °C with a hydrogen pickup of 86% [15].

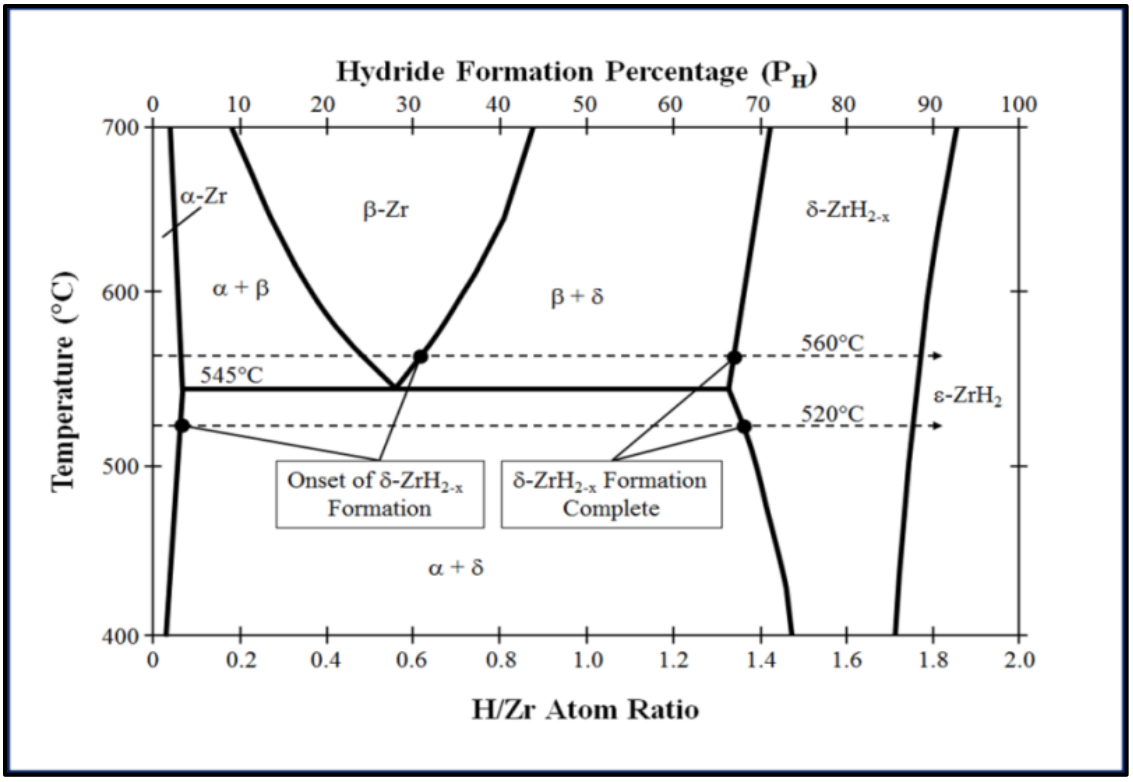

Figure 2: Zr-H phase diagram. Early onset of the δ-phase along the α-pathway results in a dramatically increased pulverization rate [13].

2.1.2 Uranium Hydride Formation

Uranium is also known to form a brittle hydride; a property which is commonly used in the creation of uranium metal powder through a hydride/dehydride process. A hydride/dehydride process is even more effective for the production of metallic uranium powder than for the production of metallic zirconium powder. This is because of the very low solubility of hydrogen in uranium metal, which results in an early formation of the brittle uranium hydride phase. While this hydride phase has been shown to naturally spall off of bulk uranium metal, mechanical action applied to the material during hydride formation would undoubtedly increase the rate of pulverization [13,18].

It has been demonstrated by Garnetti and Sames that the ideal temperature for pulverization of uranium via hydride formation is 233 °C [18]. This is in agreement with previously published rate information by Chiotti and Rogers [19]. Garnetti and Sames also demonstrated that uranium hydride powder can be easily converted to pure uranium metal by heating said powder under vacuum [18]. Uranium hydride begins the conversion to metallic uranium at temperatures of ~430 °C at atmospheric pressures. This conversion can be accelerated through heating of the material under dynamic vacuum and was found to take less than 30 minutes for nominally complete conversion to uranium metal at temperatures as low as 325 °C. This suggests that the material can be dehydrided during a preheating/purge process prior to introducing the material to the chlorination vessel which will likely be operated at ~330 °C.

2.1.3 Uranium-Zirconium Hydride Pulverization Process

For this research, it was postulated that the reaction rate for hydride formation in U-xZr alloys will more closely resemble that of pure uranium [20]. This would result in a process which can be operated at lower temperatures, similar to those encountered during uranium hydride formation processes. However, this assumption is highly dependent on the microstructure of the uranium-zirconium alloy being processed. Ideally, the pulverization process will not require the formation of zirconium hydride, but will be driven by the ease of uranium hydride formation. This is where the microstructure of the U-xZr alloy being processed is crucial.

In order for this proposed hydride pulverization process to be useful in a coupled hydride-dehydride-chlorination process, the material does not need to be fully converted

to hydride. The material only needs to be reduced to particle sizes small enough to allow near-instantaneous chloride formation once introduced into the chlorination vessel. This suggests that U-Zr alloys can be heat treated to produce microstructures which are ideal for hydride pulverization.

2.2 Halide Processing of Group-4 Elements

Processes which utilize halide volatilization of group-4 (e.g., Ti, Zr, and Hf) elements for the purpose of purification or separation have been used for well over 100 years [21,22]. The process most directly analogous to this work is the Kroll process, which is used industrially for the production of ductile zirconium and titanium [23,24]. This process utilizes the concept of chloride volatility for the formation of purified metallic titanium or zirconium.

The enabling characteristic of halide processing begins with the extreme reactivity of the halogens when in their elemental form (e.g., F, Cl, Br, and I). This reactivity is capable of separating the group-IV elements even from their stable, naturally-occurring minerals. The second enabling characteristic of halide processing is that the group-4 halides are volatile at relatively modest temperatures. All halide processing techniques of the group-4 species take advantage of these two properties. The material of interest is halogenated to form a volatile halide which is separated from its feed material through volatilization.

There have been numerous methods developed since the late 18th century which use halide processing for the purification of materials of all types. An exhaustive list of

halide methods is not practical here, so a review of selected processes deemed to be most relevant is presented in the following sections.

2.2.1 Chloride Processing

Chlorine was selected as the process halogen for this present study for several reasons. First, the proposed process is intended to be coupled to a hydride/dehydride process similar to the methods described in Section 2.1. The temperatures most likely required to hydride and dehydride a uranium-zirconium alloy (225-400 °C) are very near the temperatures needed to form and volatilize zirconium tetrachloride (331 °C). While this similarity in processing temperature may not be a prerequisite for a hydride/halogenation process to be successful, it could simplify the design of a coupled hydride-pulverization/chlorination system. The second advantage in using chlorine as the halogenating agent is that it is less reactive than fluorine, yet maintains the ability to react quickly with materials to form volatile chlorides. The construction materials for a chlorination system may also be composed of less expensive materials when compared to a fluorination system. Perhaps the most important advantage is the extensive industrial experience that has been gathered over the years in the production of titanium and zirconium sponge.

The benefits of this industrial experience with chloride volatilization of group-4 elements will be exceptionally useful if the reactions studied in Section 4 are ever reduced to practice in an industrial process and scaled up for practical use. If a new reprocessing technology is to be implemented, there is a strong advantage to basing this

new technology on industrial systems that currently exist with decades of industrial-scale operation. The Kroll process is an example of such a system [22,24].

Chloride volatility of titanium was first used to produce ductile metal with the development of the Hunter process in 1910. This process utilized the concept of chloride volatility and distillation of titanium-containing ores. The distilled chlorides were then reduced with liquid sodium, resulting in a purified titanium metal [23]. The Kroll process improved upon the Hunter process and can be credited with the widespread availability of relatively inexpensive, high purity titanium, zirconium, and hafnium [23]. This process also involves chloride volatilization of selected elements from their respective ores in order to separate and purify them. These chlorides are separated via distillation and reduced using liquid magnesium, instead of liquid sodium, resulting in a highly purified metal sponge [1]. The feed materials for the Kroll process are the naturally occurring ores of the element of interest. The most common mineral used in the production of titanium metal is rutile (TiO_2) [25]. This material is fluidized in the presence of both chlorine and carbon to form the volatile tetrachloride via

(1) $$TiO_2 + C + 2Cl_2(g) \xrightarrow{yields} TiCl_4(g) + CO_2(g)$$

Likewise, zirconium metal is typically produced by the carbothermic processing of zircon ($ZrSiO_4$) [25] to form the volatile tetrachloride as shown in

(2) $$ZrSiO_4 + 2C + 4Cl_2(g) \xrightarrow{yields} ZrCl_4(g) + 2CO_2(g) + SiCl_4(g)$$

Both $TiCl_4$ and $ZrCl_4$ may then be reduced using liquid magnesium (as well as the $SiCl_4$), which typically results in the formation of Ti or Zr metal sponge and $MgCl_2$.

The magnesium chloride is separated by volatile distillation and the metal is collected. This process is shown in Equation 3 where "X" represents any Group-4 species. This magnesium reduction is the heart of the Kroll process [1].

(3) $$XCl_4(g) + 2Mg(l) \xrightarrow{yields} X + 2MgCl_2(l)$$

The Kroll process produces high purity, ductile metal which is fully suited for use in most applications. However, upon its initial implementation, the Kroll process was incapable of producing reactor-grade zirconium due to issues with ductility and the nuclear industry's high standards for quality control [1]. For this reason, the already purified metal sponge had to be further processed into ultra-high purity zirconium using the van Arkel crystal-bar process [1,26]. The van Arkel process will be discussed in Section 2.2.4.

2.2.2 Fluoride Processing

Fluoride volatility has been used in nuclear applications since the birth of the nuclear industry during World War 2 [27-29]. Perhaps the most visible use is in the formation of UF_6 for uranium enrichment. Production of UF_6 begins with the formation of UF_4. Uranium tetrafluoride for use in UF_6 fabrication is typically produced through hydrofluorination of the oxides of uranium as shown in Equations 4 through 6. Following the formation of UF_4, this material is further reacted with elemental fluorine resulting in the highly volatile UF_6 by way of Equation 7. The hexafluoride can then be distilled from the feed material to be used in various enrichment processes [11,30]. The

distillation of uranium hexafluoride is an example of halide volatility being used to purify a feed material.

(4) $$UO_2 + 4HF(g) \xrightarrow{yields} UF_4(s) + 2H_2O(g)$$

(5) $$UO_3 + 2HF(g) \xrightarrow{yields} UO_2F_2(s) + H_2O(g)$$

(6) $$U_3O_8 + 8HF(g) \xrightarrow{yields} UF_4(s) + 2UO_2F_2(s) + 4H_2O(g)$$

(7) $$UF_4 + F_2(g) \xrightarrow{yields} UF_6(g)$$

Instead of being used in uranium hexafluoride production, uranium tetrafluoride is often reduced to metallic uranium through reduction using liquid magnesium following Equation 8 [30]. This is directly analogous to the Kroll process discussed in Section 2.2.1, and is very similar to the reduction process which will likely be used in the chloride process being considered in this dissertation.

(8) $$UF_4 + 2Mg \xrightarrow{yields} U + 2MgF_2$$

Fluoride volatility has been considered for reprocessing applications [31-37]. There are potentially promising applications for fluoride volatilization processes; however, fluorine may not be the best halogen for processing the uranium-zirconium alloy system. Fluoride processing is most useful when the materials to be reacted are in such a chemically stable form that an extremely reactive species, such as fluorine, is required. This is not the case when the starting material is metallic uranium and

zirconium. The extreme reactivity of fluorine introduces equipment design challenges to the implementation of a fluoride volatilization process.

2.2.3 Bromide Processing

While not the topic of this research, selective volatilization of group-4 metals from uranium alloys through formation of their bromides has potential. Many of the processing methods suited for chloride volatilization are also applicable for bromide processing. This includes the carbothermic reduction and volatilization of group-4 metals from their respective ores, as well as a process directly analogous to the Kroll process [38].

It may be possible that a process similar to that which is being presented in this research can be created using elemental bromine instead of elemental chlorine. The use of bromine has some advantages upon first inspection. The most obvious advantage to using bromine when compared to either fluorine or chlorine is that it is much less corrosive than either of its cousins. This would allow a bromide system to be constructed using less expensive materials. However, the decreased reactivity of bromine could result in slower reactions between the elemental bromine and the species to be volatilized. Bromide volatilization is intriguing from a theoretical standpoint; however, the advantage of having facilities which utilize chloride volatilization presently in operation and with decades of experience is hard to ignore. It is primarily for this reason that bromide volatilization was not pursued here and will not be discussed further other than to say that it is a promising concept that requires further research.

2.2.4 Iodide Processing

The final halogen to be discussed is iodine. Elemental iodine and its corresponding group-4 halides are perhaps the most unique among the four halogens. Carbothermic reduction of the oxides of titanium or zirconium, while possible with the other three halogens, cannot be done using iodine. This is a result of the much lower comparative reactivity of elemental iodine. Iodine should not be considered for, and is not suited for, any process resembling the Kroll process. That being said, iodide volatility has been used industrially for the production of certain Ultra High Purity (UHP) metals. These processes take advantage of the low stability of many iodides at high temperatures and low pressures. The van Arkel process is the most noteworthy process which utilizes iodide volatility.

The van Arkel process has been used industrially to create UHP titanium, zirconium, hafnium, vanadium, thorium, protactinium, etc. [39,40]. This industrial process relies on a semi-pure feed material to produce a truly UHP metal product. To produce reactor-grade zirconium, a reaction vessel is loaded with zirconium metal sponge created from the Kroll process. The vessel is then baked out under vacuum before pure, elemental iodine is introduced. The iodine is allowed to react with the zirconium at relatively low temperatures under reduced pressure forming the volatile ZrI_4. The zirconium tetraiodide is then allowed to naturally pass over a resistively heated hot wire (~1350 °C) where the molecule is decomposed, resulting in a continuously growing UHP metal crystal bar. The liberated iodine is then able to react with more impure metal, thus completing the cycle as seen in Figure 3 [1,39]. Examples

of crystal-bar produced using this method are shown in Figure 4. For the nuclear industry, the van Arkel process was later superseded by improvements in the Kroll process for the production of high-ductility, high-purity zirconium.

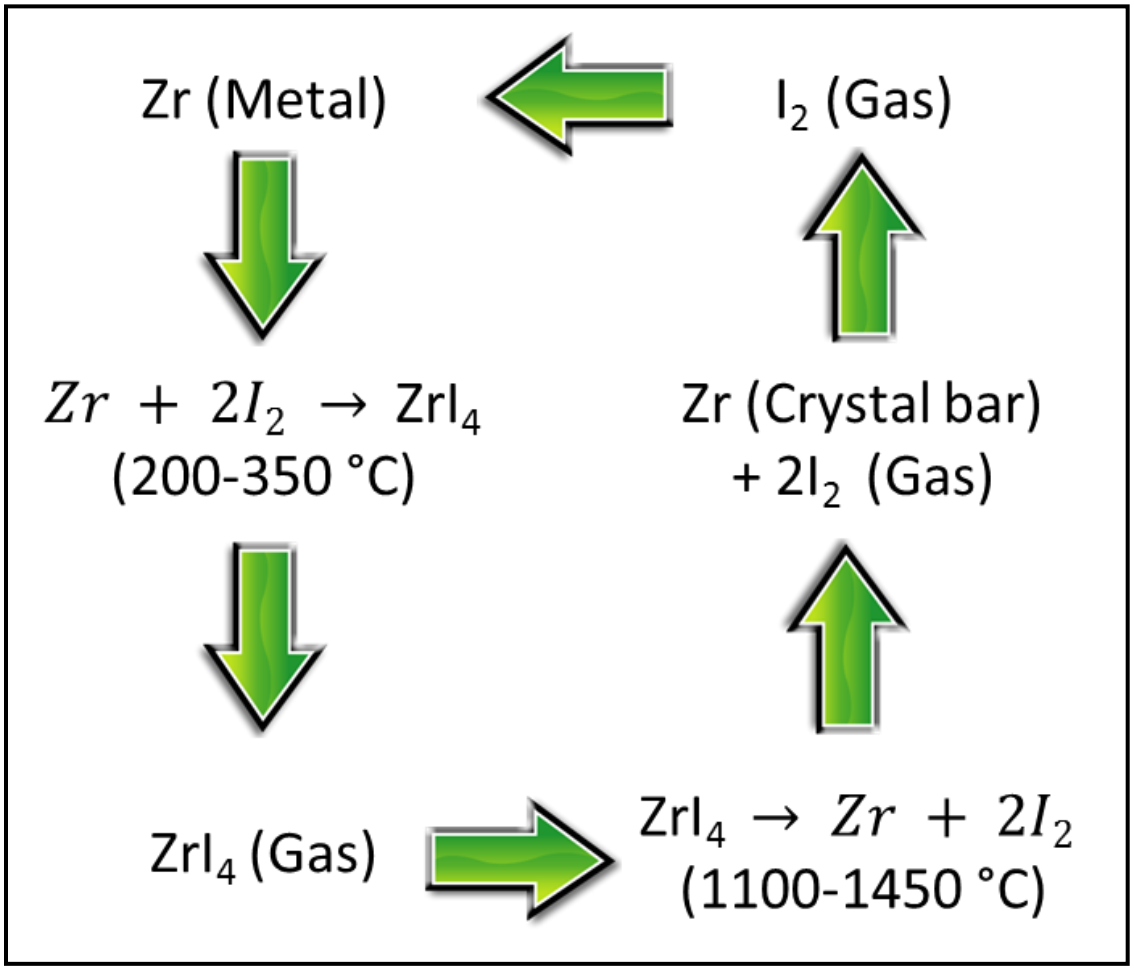

Figure 3: Zirconium crystal bar process flow diagram.

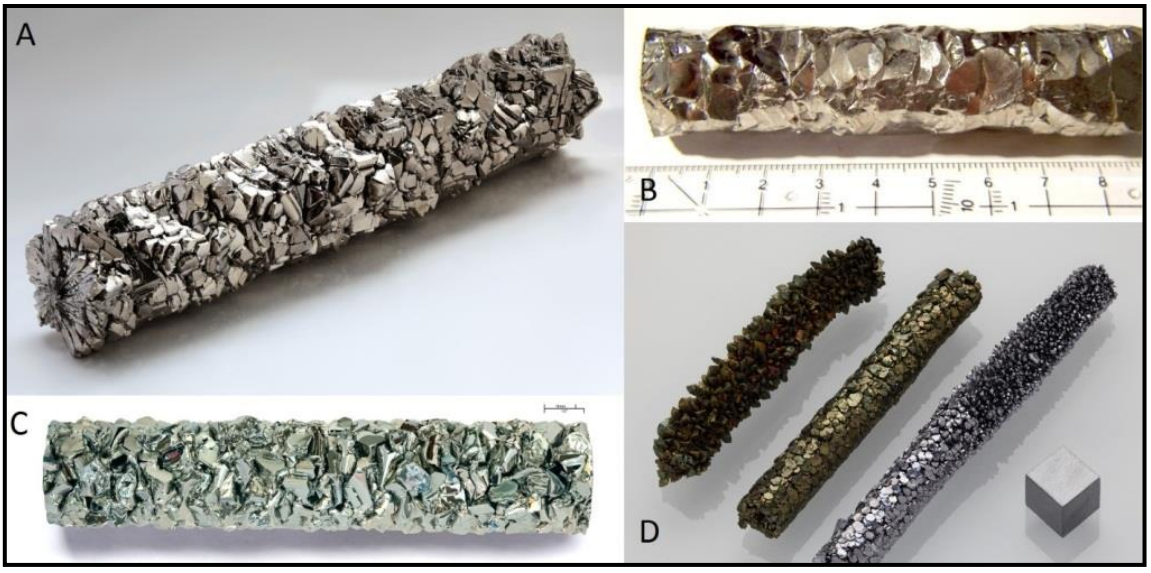

Figure 4: Examples of crystal bar produced using the iodide volatilization process. (A) Titanium. (B) Zirconium. (C) Hafnium. (D) Vanadium.

2.2.5 Uranium-Zirconium Chloride Volatilization Process

The ability of chlorine to "crack" zirconium-containing materials in order to form the volatile tetrachloride has been demonstrated industrially and is well-known. This property of chlorine is so strong that it is routinely used to break the bonds of the highly stable mineral zircon. The research being presented in this dissertation depends on chlorine being able to volatilize zirconium from a uranium-zirconium alloy; a feat which is far less challenging for chlorine than that which is accomplished on a regular basis when converting zircon to metallic zirconium, as seen in Table 1.

With the pulverization of the uranium-zirconium alloy prior to chlorination, formation of the volatile zirconium tetrachloride becomes almost trivial. In fact, this reaction should occur so quickly that a hypothetical facility will likely be more concerned with heat removal during chlorination than with supplying process heat. The

result is a process which will likely be capable of a high conversion rate when compared to the chlorination of bulk material.

3. EXPERIMENTAL DESIGN AND PROCEDURE

3.1 Experimental Design

One of the greatest challenges encountered in the development of this chloride volatilization system was in designing a system capable of surviving an environment containing hot chlorine gas. Not only must the system be able to survive this harsh environment, but it also must be designed in such a way that useful and reliable data can be extracted. The following sections describe the system details for each of the experimental configurations that were used to explore the chlorination process.

3.1.1 System 1 - All-Metal System

The initial system designs were assembled using all metal components, which turned out to be an incorrect methodology. All-metal systems do have clear advantages over glass and ceramic systems for several reasons. The first is that the majority of the metal components that may be used for assembly are standard parts which are relatively inexpensive and can be readily purchased from several manufacturers. This allows for rapid construction, deployment, and alteration of an experimental system, all of which are useful in designing a system whose purpose is to get preliminary data. Another advantage of an all-metal system is that it can operate at high pressures and relatively high temperatures, allowing for a wide range of variables to be studied within a single system.

The first system was designed to operate with a flowing Ar-Cl_2 mixture into a heated alloy-625 reaction zone. The argon and chlorine were supplied from

independent, pure gas supplies. Their respective flow rates were controlled using separate mass flow controllers prior to their mixture and introduction into the reaction zone. The argon was preheated by passing it through a copper coil of tubing which wrapped around an alloy-625 chlorine preheating coil. A 0.75 inch alloy-625 tube was used as the reaction zone and it was nested inside of both the alloy 625 chlorine preheater and the copper argon preheater. This system is depicted in Figure 5. The gasses were allowed to mix just prior to entering the reaction zone, where the mixture would flow over the sample and exit the heated zone to then be scrubbed for the removal of chlorine and chlorides.

This system underwent preliminary testing designed to determine the suitability of the materials involved for this application, including the SS304 Swagelok fittings. It was soon discovered that SS304, while suitable at lower temperatures in a chlorine atmosphere, is not suitable at elevated temperatures. Once operations began at elevated temperatures (~300 °C), it was noted that SS304 is rapidly and exothermically attacked by hot chlorine when the T-fitting connecting the preheated argon, chlorine, and reaction zone began glowing bright orange and ignited. The threshold temperature of this reaction was not determined because this particular design was never used again for safety reasons as well as for the fact that the system was completely destroyed.

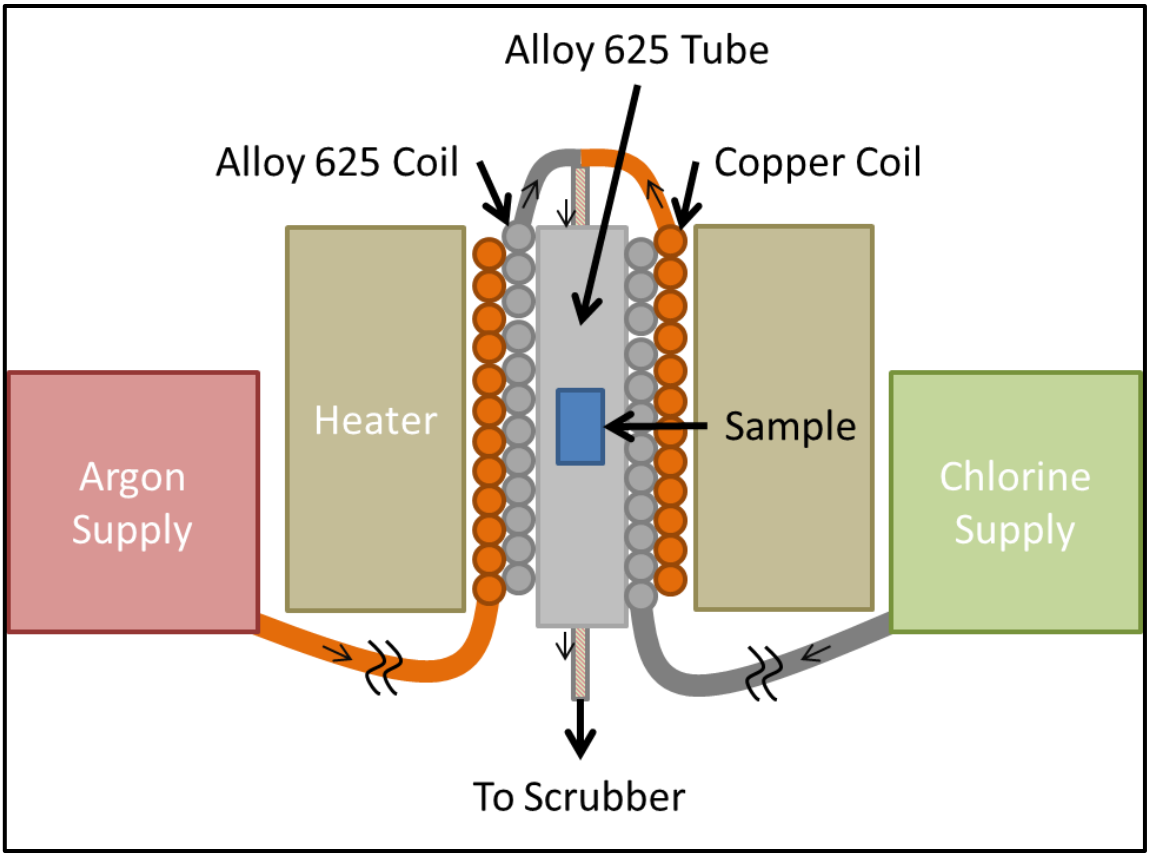

Figure 5: Schematic diagram of the initial all-metal system constructed using the Ni-based Alloy-625.

While this system may have been a technical failure, many lessons were learned. The most obvious was an appreciation by the operator for the extreme reactivity of hot elemental chlorine gas. The gas rapidly volatilized the iron in the SS304, and would have continued destroying the rest of the system if the chlorine supply had not been immediately turned off. (It was at this point that decladding of iron based steel clad nuclear fuel was seriously considered as a potential application of this process.) It naturally followed that iron-based steels should never be used, under any circumstances, in a chlorine system at elevated temperatures. In spite of the obvious incompatibility of

iron-based steels in these systems, it was observed that the alloy-625 reaction zone remained totally intact, even though this material saw a much higher temperature. It was concluded that nickel-based alloys may be considered as potential materials to be used in this chloride process.

The concept of mixing the reaction gas with a preheated carrier gas was abandoned after this initial system failure. It proved too challenging to verify exact gas flow rates. This also removed the carrier-gas to reaction-gas ratio from the list of variables which must be studied, making a more in depth study of some of the more intrinsic variables possible. This was acceptable because if this system is to be scaled up to an industrial system, the desired carrier-gas to reaction-gas ratio will likely be largely dependent on the specific equipment and process being performed.

3.1.2 System 2 - Long Glass Tube

Following the failure of the all-metal system, a series of tests were performed to qualitatively study the effects of hot chlorine on various materials. This system consisted of a three foot long, one inch diameter borosilicate glass tube connected to a pure chlorine gas supply with PTFE tubing and fittings, shown in Figure 6. The exhaust was passed through two glass water-filled vessels to filter the chlorine exhaust. The motivation behind this setup was that the glass tube would be slowly filled with a liquid capable of dissolving the chlorides, such as hydrochloric acid, to capture the volatilized material after the reaction was completed by pressurizing the glass vessels. This would result in two product streams. The first being the volatilized material in the fluid, the second being the non-volatilized material, which could then be collected separately. At

the time, it was believed that this material would need to be collected prior to its exposure to air. This ended up not being the case, as the chlorides are more stable in air than initially anticipated.

As stated previously, a select group of materials were chosen to have their behavior qualitatively studied. The purpose was to determine appropriate materials for construction of the next systems. The materials tested include crystal-bar zirconium, zirconium powder, Zircaloy-4, zirconium hydride, iron, SS316, alloy 625, copper, and molybdenum. It was found that all materials containing zirconium or iron were rapidly destroyed through volatilization. The copper was seen to react with hot chlorine, but this reaction appeared to proceed slowly, and may have been limited to a surface reaction. The molybdenum, graphite, and alloy-625 all appeared to remain totally intact. However, it was later found conclusively in Section 3.1.3 that molybdenum is not suitable for systems containing hot chlorine.

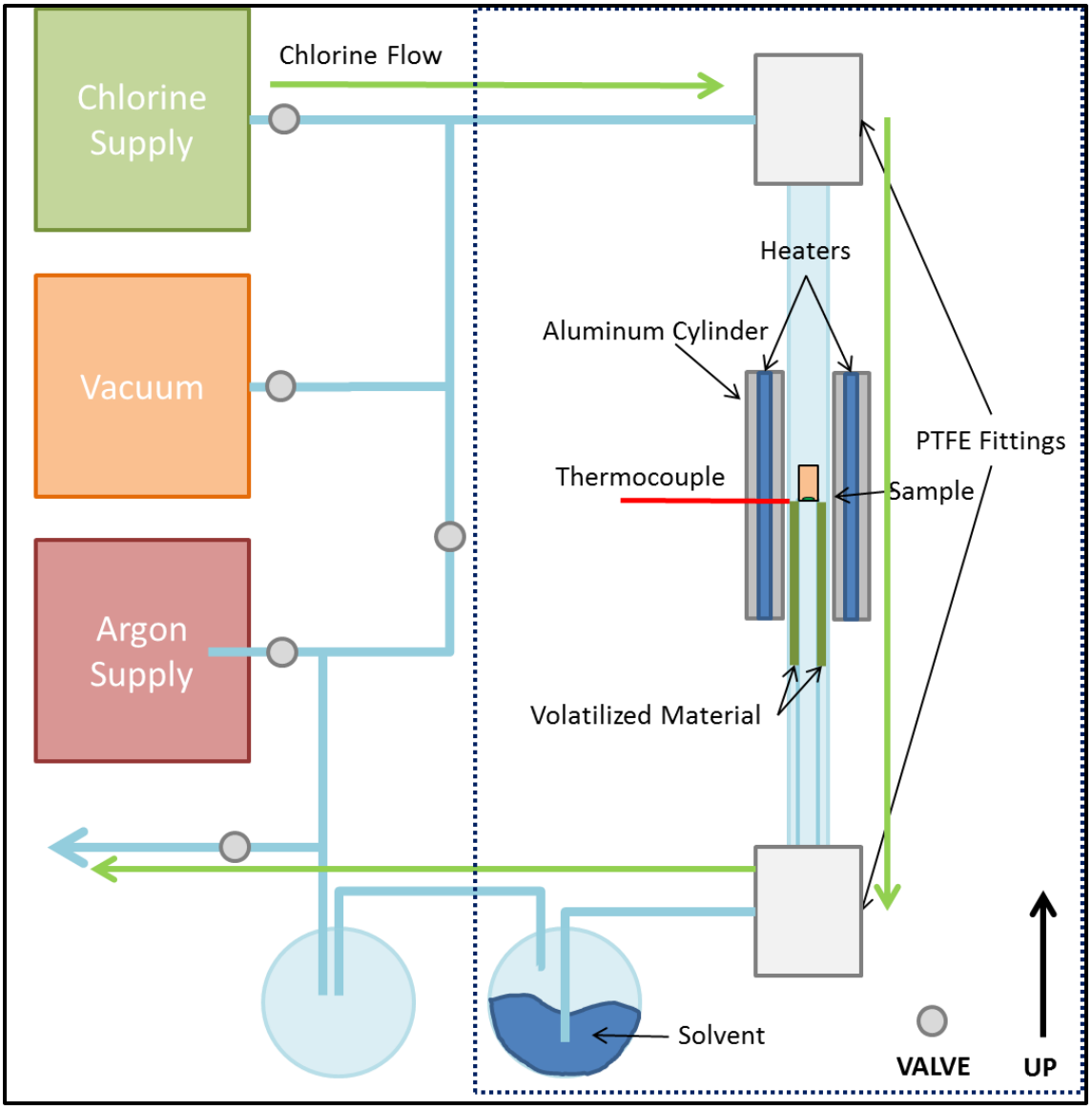

Figure 6: Schematic diagram of the second experimental system constructed using a long glass tube.

These tests showed that the only reasonable materials suitable for construction of the heated reaction zone are borosilicate glass, oxides such as alumina, alloy-625, and molybdenum. (As stated previously, molybdenum was incorrectly identified as being compatible.) This information put boundaries on the design requirements of the final

system. A glass or oxide system, while relatively inexpensive, is not suited for pressurization since these materials are brittle and can fail dramatically. Therefore, pressure could not be studied as a variable in a glass or oxide system. A system constructed of alloy-625 would likely function well, but components made from this material were prohibitively expensive for this study. Molybdenum was also considered as unreasonable as a construction material due to its cost and machinability.

In spite of the challenges which were identified here, a very promising result was obtained. It was observed that the chlorine reaction rate of bulk zirconium metal and zirconium metal powder were significantly different. The chlorine reaction with bulk zirconium metal took several minutes to complete, while the reaction with zirconium powder could be considered to be instantaneous. The reaction was so fast in fact, that the 1/8 inch thick glass tube was deformed beyond repair as a result of the rapid exothermic reaction of chlorine with zirconium powder. This was a conclusive demonstration of the potential advantages of a pulverization method such as hydriding prior to its chlorination. This idea will be further supported in future sections.

3.1.3 System 3 - Hastelloy C-22 Vessel

A system was created for a separate research project involving a similar zirconium iodide volatilization experiment. This system was capable of surviving repeated long-term exposures to elemental iodine at temperatures up to 500 °C. This custom vessel was correctly believed to be capable of surviving the harsh conditions of hot elemental chlorine. This was further supported by the results of the previous tests which indicated that an alloy related to C-22, alloy-625, is compatible with hot elemental chlorine. The

head of the C-22 vessel contained an electrical feed-through with molybdenum electrodes. The previous tests performed in a long glass tube seemed to show that molybdenum was compatible with chlorine, but tests in this C-22 system decisively proved otherwise. It was found that molybdenum would react with chlorine to form a black liquid even at modest temperatures. This black liquid deposited itself over nearly every surface within the vessel in the form of splattered drops. In spite of the problems related to molybdenum chloride formation, information which proved to be very useful was gathered using this system.

This large C-22 vessel was heated from the bottom only, using a high-temperature hot-plate. The reason for this orientation is because it was considered necessary to physically separate the volatilized phase from the non-volatilized phase, and heating from the bottom would set up distinct hot and cold zones. A zirconium sample was placed on the heated bottom surface throughout each test. Chlorine was introduced, and any material which volatilized would condense on the walls of the vessel where the temperature was below the volatilization temperature of 331 °C. This was observed as a ring of zirconium chloride being deposited above an area which was totally void of all volatiles. This was the first full demonstration during this project that chlorine could be used to controllably volatilize and deposit zirconium, that the chlorides could then be condensed in a controlled predictable manner, and that both of these phases could be separately collected.

A non-flowing system was also considered as a result of this series of tests. This arose due to the large size of the C-22 vessel. It was reasonable to regulate the pressure

of the system using the regulator connected to the gas cylinder, and allow gas to flow in as it is consumed. The reason that a constant-pressure system was not considered before was because of the requirement to predictably deposit the volatilized material in such a way that both the volatilized material and non-volatilized material could be recovered separately. A flowing system would transport all volatiles down-stream where they can be collected. However, the large size of the C-22 vessel made this unnecessary, because natural convection could produce the needed physical separation. Changing the system from a flowing system to an isostatic system dramatically reduced the filtration requirements of the exhaust gasses. Instead of being required to have an attached system capable of continuous filtration, it only became necessary to filter the volume of gas which was contained in the C-22 vessel. This greatly increased the level of experimental control over the system. This constant-pressure method was found to be so far superior to a flowing system that it was used throughout the remaining system iterations.

In spite of its advantages, this large C-22 system had some drawbacks. The most significant drawback was its size. The large thermal mass of the system greatly reduced the rate at which experiments could be performed. The system would take several hours to reach temperature before an experiment could begin, and it would have to cool overnight before the vessel could be opened. This is not just an inconvenience. Uranium and zirconium are both very reactive metals, and maintaining experimental accuracy is difficult if these highly reactive metals are subjected to elevated temperatures for several hours prior to the reaction even beginning. Another disadvantage with the C-22 system again has to do with its large size. Collection of the

non-volatile material is rather straightforward, but collection of the volatile material proved to be difficult for several reasons. First, the entire vessel is to be thoroughly washed out, and all of this liquid collected for analysis. This proved to be very difficult simply because of the awkwardness in physically handling such a massive object. This would have been compounded further in later experiments if radioactive material was introduced. Even with the system cleaned out, one then has to deal with the large volume of liquid which results from this cleansing. The sheer size of this system was prohibitive and a smaller system was considered.

3.1.4 System 4 - Narrow Glass Tube

A small reusable reaction vessel was created using a 3/8 inch glass tube which was flame-sealed at one end. The purpose of this system was to gather data needed for proper experimental design so that a final system could be constructed. This system combined the lessons learned from the previous designs, resulting in a system which was capable of gathering preliminary data.

The glass reaction vessel was designed to be partially inserted into a custom-made aluminum block which was heated using cartridge heaters, resulting in a reaction vessel with both a heated and non-heated zone. As was seen in the C-22 vessel, the volatilized chlorides would deposit on a cooler surface through natural convection, and this effect was taken advantage of in the design of the narrow glass tube system. This is the system that was used in the "ZRT" series, the results of which are presented in Section 4.1. It should be noted that the experiments conducted for the "ZRT" series were oriented in a vertical position. All other experimental series were oriented in a horizontal position.

The horizontal position was determined to be ideal for these experiments because it prevented volatilized material from falling back into the heated zone during the experiments. It was found that this system was capable of achieving the volatilization needed, but would be improved with a larger diameter glass tube.

3.1.5 System 5 - Glass Test-Tube Systems

The glass test-tube system took several forms depending on the experiment being conducted. It began as a glass test-tube containing an inner glass tube used for introducing fresh chlorine gas directly to the sample. It was quickly found that this inner glass tube was unnecessary because the system would be operated in a constant pressure condition. This made direct application of chlorine unnecessary. The presence of the inner glass tube was seen to inhibit the volatilization process because it clogged up the deposition zone.

The test-tube system was initially constructed to obtain volatilization data for two materials simultaneously. The system was arranged so that two test-tubes could be placed horizontally inside of the heated aluminum block with the bottoms of the test tubes butted against a thermocouple, as shown in Figure 7. The advantage of this double-test-tube arrangement is that all variables between samples are eliminated allowing for a direct comparison between materials. This orientation was used for the "UT" series discussed in Section 4.2.

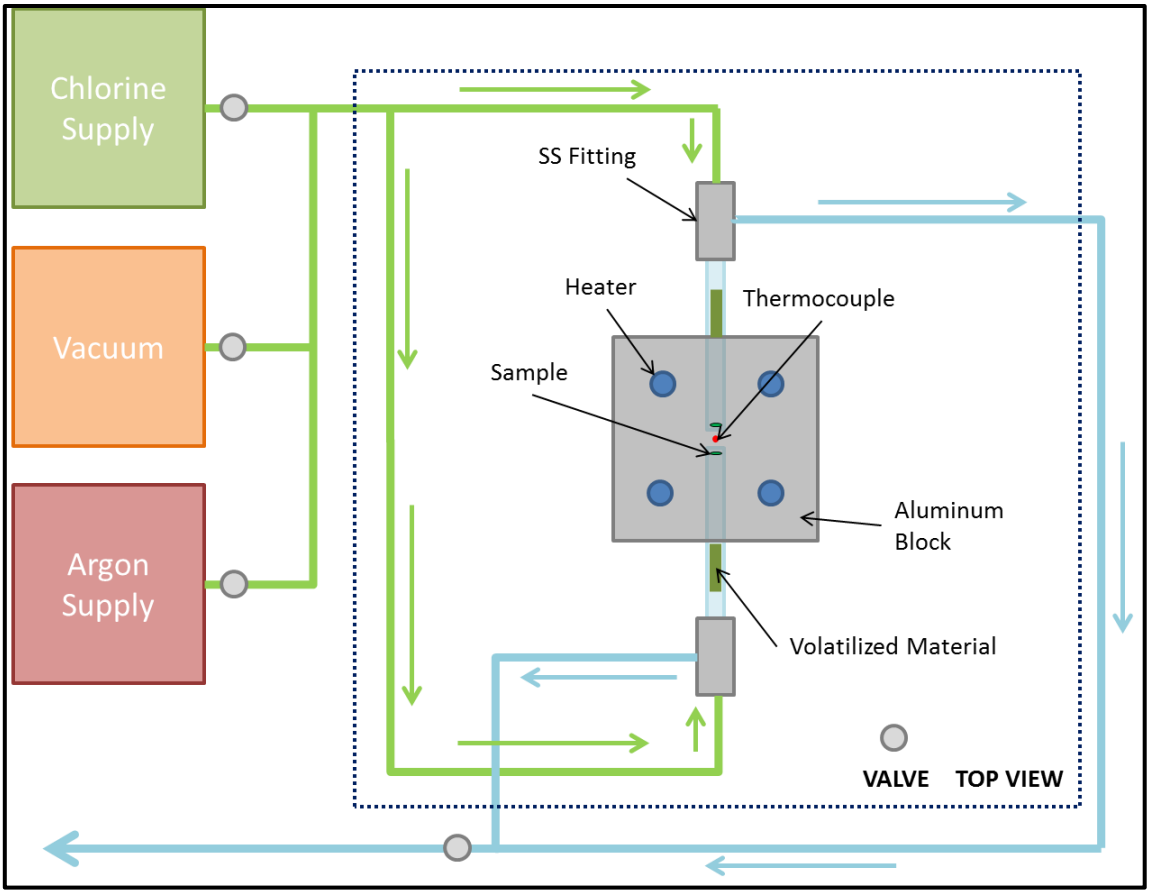

Figure 7: Schematic diagram of the horizontal two-test-tube system assembled for the UT chlorination test series. (Insulation not shown.)

Following the success of the double-test-tube design, a four-test-tube design was constructed as shown in Figure 8. This design contained additional valves which allowed individual samples to be isolated from one another. The advantage of this design is that it allows time information to be obtained for four samples simultaneously while holding all variables constant among samples in each batch. This arrangement was used for the "U50Zr" and "Zr" series described in Sections 4.3 and 4.4.

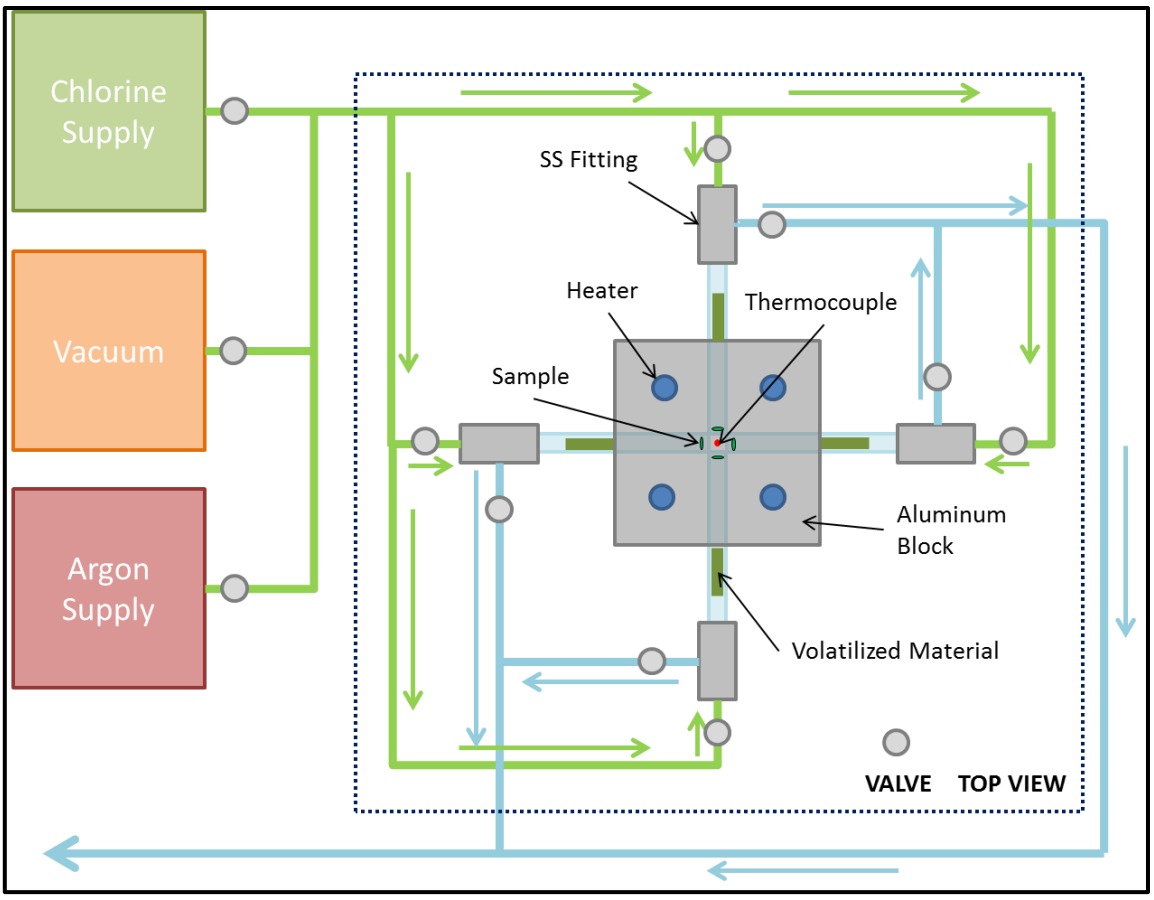

Figure 8: Schematic diagram of the horizontal four-test-tube system assembled for the U50Zr and Zr chlorination test series. (Insulation not shown.)

For the final series of experiments, time data was not obtained. The system was reverted back to a single test-tube configuration so that detailed temperature dependence could be studied. This system is shown in Figure 9 and was used for the "U50ZrFinal" series of experiments described in Section 4.5.

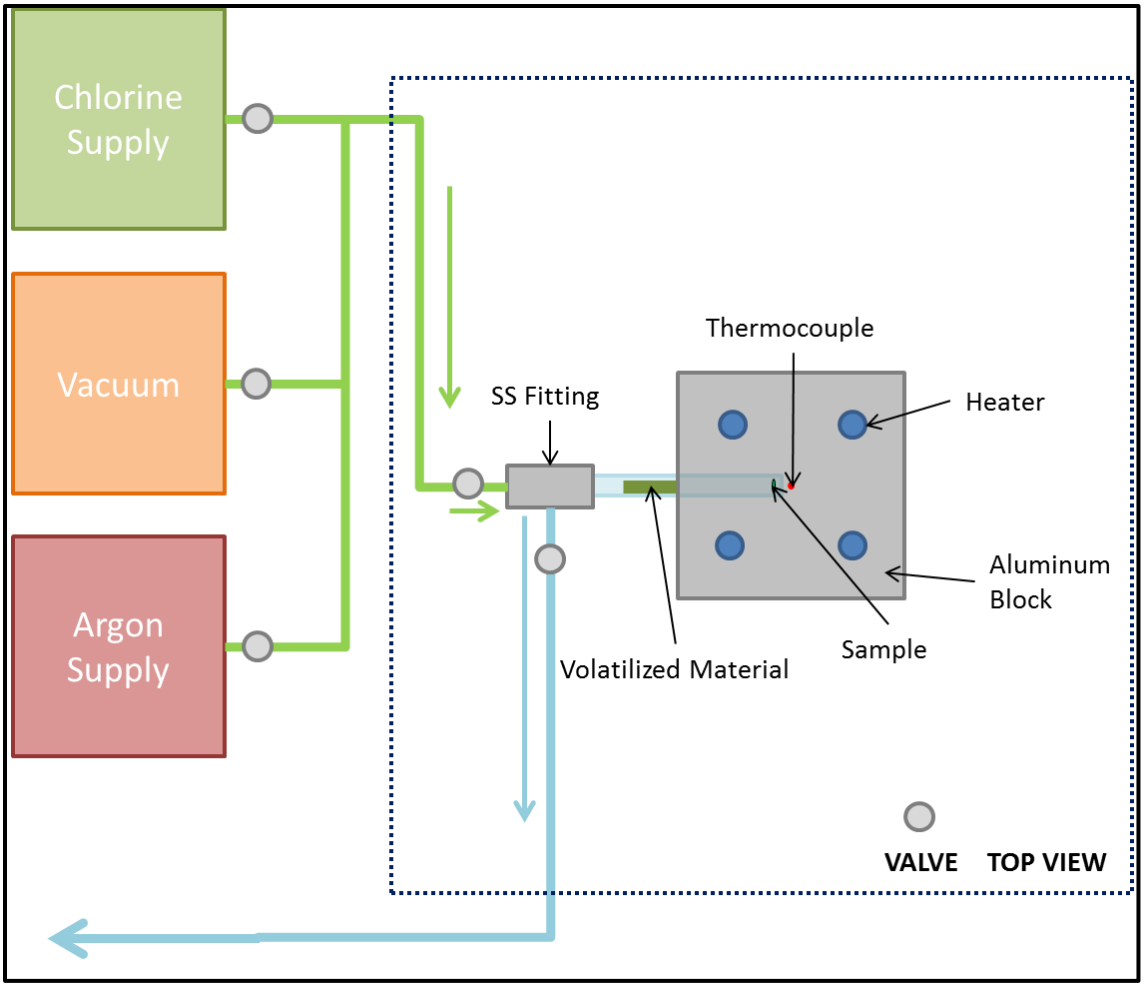

Figure 9: Schematic diagram of the final horizontal one-test-tube system assembled for the U50ZrFinal chlorination test series. (Insulation not shown.)

3.2 Experimental Procedure

As noted in Section 3.1, five experiment configurations were used in the evolution of these processing experiments. The first three configurations (Sections 3.1.1 to 3.1.3) yielded important information, but were not usable for systematic studies. The last two configurations (Sections 3.1.4 and 3.1.5) were used for a sequence of five systematic studies (also noted above) with similar, yet distinct, procedures. The following sections

describe the procedures employed for each of the five systematic studies: 1) Zirconium Test "ZRT" (Section 3.2.1), 2) Uranium Test "UT" (Section 3.2.2), 3) Uranium-50Zirconium "U50Zr" (Section 3.2.3), 4) Zirconium "Zr" (Section 3.2.4), and 5) Uranium-50Zirconium Final "U50ZrFinal" (Section 3.2.5).

The reaction vessels used for the individual tests in each of these series were borosilicate glass tubes contained within a heated aluminum block. All experiments were operated in a static constant-pressure condition. The chlorination reaction was allowed to proceed on solid metal samples, unless otherwise noted, and the volatilized chloride material was deposited on the cold region of the reaction vessel. However, there were some differences among these series. Specific procedures for each of these series are summarized and presented below.

3.2.1 ZRT Series

The ZRT series was carried out using the apparatus described in Section 3.1.4. The purpose was to obtain preliminary data on the volatilization of zirconium in the presence of chlorine. The narrow glass tube reaction vessel system was connected to the gas supply system using stainless steel (SS304) fittings with fluoroelastomer O-ring seals. The reaction vessel was heated by inserting it into a heated aluminum cylinder. The aluminum cylinder contained a K-type thermocouple at its midpoint. This allowed the temperature to be measured at the bottom of the reaction vessel where the sample was located. This system is shown in Figure 10. The samples were prepared from crystal-bar zirconium disks which had been cut into nine pieces. Each disk had a thickness of roughly one millimeter.

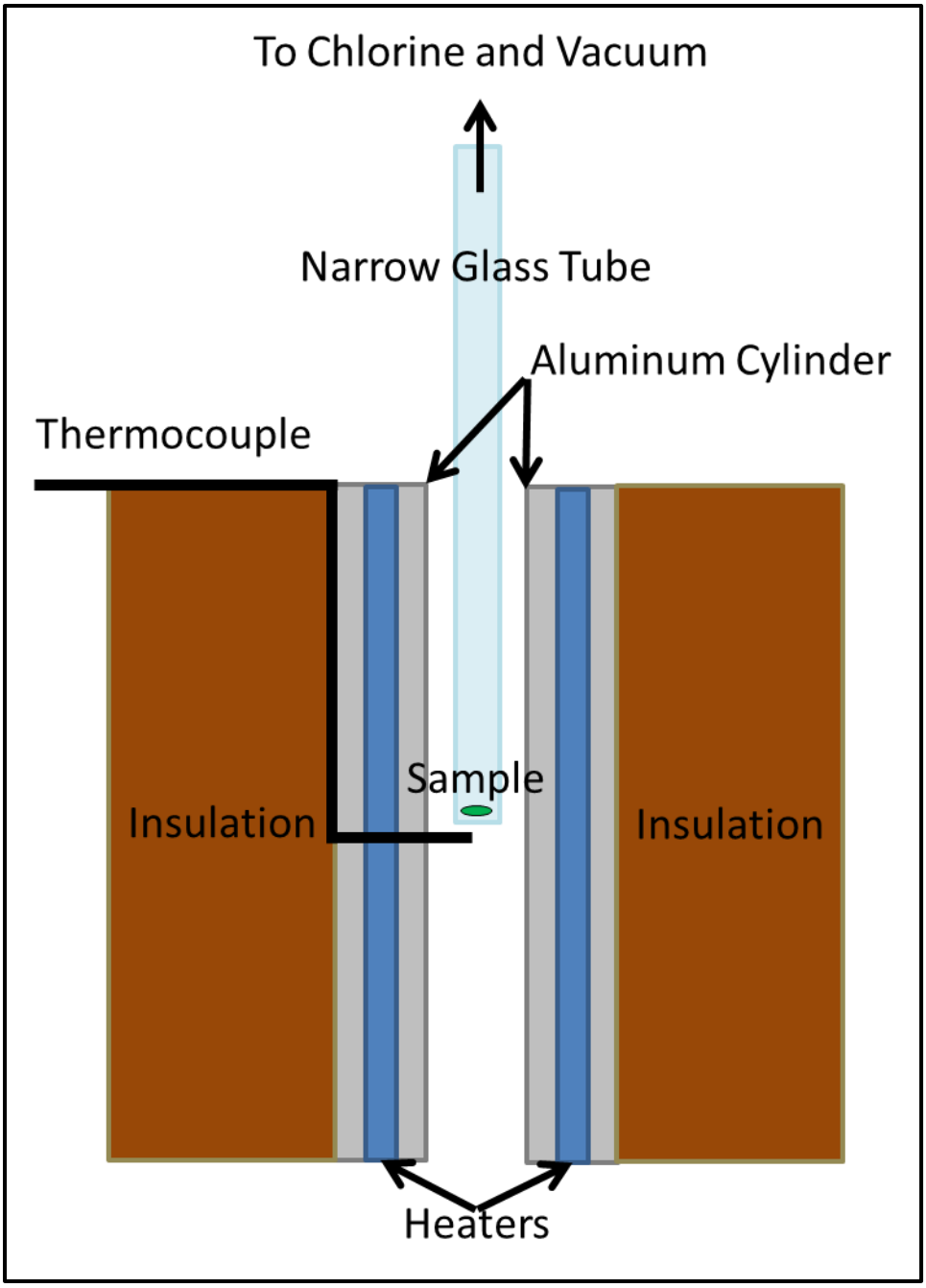

Figure 10: Schematic of narrow glass tube system used for the ZRT experiments.

3.2.1.1 ZRT Procedure

Each test began by recording the mass of the sample to be processed. The sample was loaded into the vessel which was then evacuated using a dry-scroll pump. The vessel was then backfilled with argon. After this purge process was repeated three times, the reaction vessel was pressurized with 14 psig argon. The reaction vessel was then inserted into the preheated aluminum heating block where it was allowed to come to thermal equilibrium at the desired temperature. It was then evacuated using the dry-scroll pump, and the vacuum pressure and sample temperature were recorded. The system was then immediately filled with elemental chlorine gas to the required pressure and the reaction was allowed to proceed. Once the desired reaction time had elapsed, the chlorine gas was shut off, argon gas flow began, and the reaction vessel was removed from the heated zone. The system was cooled under flowing argon until it reached room temperature. The cool-down time was approximately 10 minutes.

3.2.1.2 ZRT Sample Collection

The samples were collected simply by separating the glass reaction vessel from the SS304 fitting. The system was thoroughly washed with ethanol in order to remove all soluble chlorides and any loose material. In the event of volatilized material being stuck to the surface of the narrow tube, which happened often, the tube would be partially filled with ethanol and placed into a sonicator to dissolve all soluble material and to dislodge any insoluble material.

3.2.1.3 ZRT Sample Analysis

The soluble material was physically separated from the insoluble material. The intact solid zirconium left over from the chlorination reaction was weighed using a Mettler Toledo AB204-S scale (0.0001 grams). This enabled the calculation of the measured mass change corresponding to the amount of material which was converted to chloride. Using this method, it was possible to perform a preliminary study of mass change as a function of time, pressure, and temperature, the results of which is presented in Section 4.1. The information was used to guide future system and experimental design.

3.2.2 Uranium Test (UT) Series

The UT series was the first test series carried out using the apparatus described in Section 3.1.5. The purpose was to compare the relative volatilization of the U-50Zr alloy with either uranium or zirconium. A double-test-tube system was used so that two samples could simultaneously be reacted under conditions which would be identical between the two samples, as shown in Figure 7. Experiments UT-1, UT-2, and UT-5 studied the difference in volatilization between U-50Zr and zirconium metal, while experiments UT-3 and UT-4 studied the difference in volatilization between U-50Zr and uranium metal.

3.2.2.1 UT Procedure

The step-by-step procedure for the UT series was identical to that for the ZRT series. Each test began by recording the mass of the samples to be processed. The vessels were then evacuated using a dry-scroll pump and backfilled with argon. This

process was repeated three times and then the reaction vessels were pressurized with 14 psig argon. The reaction vessels were then inserted into the preheated aluminum heating block, and the system was allowed to come to thermal equilibrium at the desired temperature. It was then evacuated again using the dry-scroll pump, and the pressure and sample temperature were recorded. The system was then filled with elemental chlorine gas to the desired pressure and the reaction was allowed to proceed. Once the desired reaction time had elapsed, the chlorine gas was shut off, argon gas flow began, and the reaction vessel was removed from the heated zone. The system was allowed to cool under flowing argon until it reached room temperature. The cool-down time was also approximately 10 minutes.

3.2.2.2 UT Sample Collection

The samples were collected in the same way as in the ZRT series. The glass reaction vessels were both separated from the SS304 fittings. The system was then thoroughly washed with ethanol in order to remove all soluble chlorides as well as any loose material. In the event of material being stuck to the surface of the test tube, the tube would be partially filled with ethanol and placed into a sonicator to dissolve all material. This method also dislodged any intact metal from the walls of the vessel.

3.2.2.3 UT Sample Analysis

The product materials from this series were analyzed in a similar manner as the ZRT series. The intact solid zirconium, uranium, or U-50Zr left over from the chlorination reaction was weighed using a high-precision scale. This resulted in a known mass change corresponding to the amount of material which was converted to

chloride. However, the qualitative comparison between the U-50Zr alloy with pure zirconium or pure uranium was the most useful information gathered in this series. This comparison was largely visual with little meaningful quantitative results.

3.2.3 U50Zr Series

The U50Zr series was designed to enable the performance of a rate study on the volatilization of U-50Zr alloys. The modified four-sample system described in Sect. 3.1.5 was created. An important difference between the U50Zr series and the UT series was that each of the four reaction vessels was able to be isolated from the rest of the system using a system of valves; thus, samples could be selectively isolated and removed from the system at different times. This system is depicted in Figure 8.

3.2.3.1 U50Zr Procedure

Tests U50Zr1-U50Zr5 began by recording the mass of the U-50Zr samples to be processed. The vessels were evacuated using a dry-scroll pump and then backfilled with argon. This process was repeated three times and then the reaction vessels were pressurized with 14 psig argon. The reaction vessels were then inserted into the preheated aluminum heating block, and the system was allowed to come to thermal equilibrium at the desired temperature. It was then evacuated using the dry scroll pump, and the vacuum pressure and sample temperature were recorded. The system was then filled with chlorine gas to the desired pressure and the reaction was allowed to proceed. This series deviates from the previous two series in that the inlet and outlet valves for each independent reaction vessel were closed once the sample of interest had reacted for the desired amount of time. The reaction times were 15, 30, 60, and 120 minutes. After

each time-step, a sample would be isolated and removed from the heated zone. It should be noted that the cooling process took place in the presence of the gasses that were in the reaction vessel prior to isolation instead of cooling under flowing argon as the previous experiments.

Test U50Zr6 was intended to be performed at 250 °C, but it was observed that volatilization would not occur at this low temperature. The temperature was slowly increased so that the onset of volatilization could be recorded. The temperature as a function of time was recorded as was the temperature at which volatilization was first observed. The single sample was then allowed to react for 100 minutes. Test U50Zr7 was designed to more precisely study the onset of volatilization. The single sample was inserted into the reaction vessel in the same way as tests U50Zr1-U50Zr5. The temperature was then increased more slowly than in test U50Zr6, and the volatilization temperature was recorded. The temperature was then increased to 300 °C and the sample was allowed to react for a 90 minutes.

3.2.3.2 U50Zr Sample Collection

The samples in this series were collected in a different manner compared to the previous experimental series noted above. As stated previously, material that becomes volatile during the chloride formation reaction deposits on the region of the reaction vessel which was not heated. This resulted in a separation of the *volatile* and *non-volatile* species. It then became necessary to separate these two materials which were both deposited within the same test tube. A method was developed that allowed the test tube to be cleanly fractured in-between the *volatile* and *non-volatile* materials, resulting

in 100% segregation of these two types of materials. This method is illustrated in Figure 11. The tube was first scored with a file at a location between the *volatilized* and *non-volatilized* material. A heated glass rod was applied at this location, fracturing the test tube; thus, providing a physical separation of the two product streams.

Once this physical separation was complete, the respective chlorides were washed and collected from the reaction vessel using ethanol. The *non-volatile* species were dissolved from the heated end of the vessel using ethanol, and any solid material was separated by decanting. The mass of this solid material was then recorded. The *volatilized* species were also collected from the test tube and SS304 fitting by washing with ethanol. Any solids were then decanted away. The solids in this stream were most likely composed of iron oxide, originating from the chlorine attacking the SS304 fitting. This iron oxide is not relevant to the current study, so its removal and disposal was appropriate.

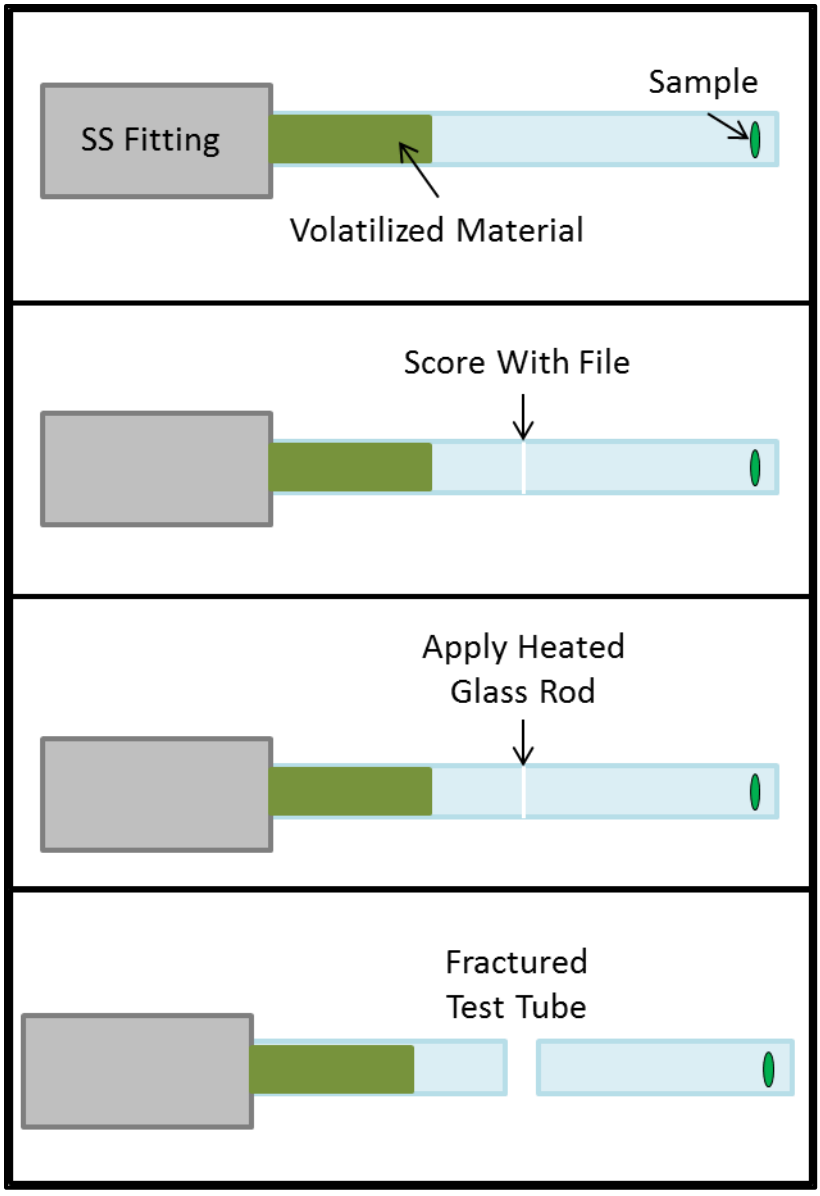

Figure 11: Process to physically separate *volatilized* and *non-volatilized* material.

The ethanol containing dissolved chlorides from the two streams was gently evaporated at ambient temperatures. The chlorides were left behind as a crystalline layer at the bottom of glass beakers. The chlorine was removed from this material by adding an excess of aqueous sodium hydroxide. The solids that resulted from the reaction with

sodium hydroxide were allowed to precipitate, and the aqueous phase was decanted. The solids were then washed and decanted with deionized water until the water was no longer basic. Ethanol (200 proof) was then added and decanted away until most of the water was removed. The material was then dried further by adding and decanting away pure acetone. The dry oxide material of both the *volatile* and *non-volatile* streams was ground to a fine powder using a mortar and pestle, and collected for analysis.

3.2.3.3 U50Zr Sample Analysis

Several methods were considered for quantitative analysis of the two product streams. The first method considered was ICP-MS. This method was eliminated for three reasons. First, the samples must be acidified using, preferably, nitric acid. The nobility of zirconium in nitric acid makes this impossible. Second, the samples must be free of chlorides to be used in the available ICP-MS equipment. This eliminates dissolving the zirconium in aqua regia as an option. Third, the presence of radioactive material greatly limited the number of facilities willing to handle these materials. Therefore, ICP-MS was removed from consideration.

The second method considered was Neutron Activation Analysis (NAA). This method was demonstrated to be capable of providing a reasonably accurate mass measurement of the amount of zirconium and uranium in a given sample. However, this method has several drawbacks which made it unreasonable for this project. The first drawback is that this is a destructive method of sample analysis. It therefore makes it impossible to perform an analysis on the starting alloy prior to being processed with chlorine. That is unless a small sample is taken from the starting alloy and analyzed

using NAA. At the time of these experiments, there was a lab-wide shortage of uranium, so sacrificing any material for destructive analysis became unreasonable. The main factor that eliminated NAA from consideration was the time that must pass between performing an experiment and receiving results. The only way to make NAA economically feasible was to analyze a large number of samples at a time. This meant that a large number of experiments would have to be conducted before any feedback is received. On top of this, NAA requires that samples sit for extended periods of time, often weeks, for the radioactivity to subside to safe levels before an analysis can even be performed. The result would have been an experiment with feedback times on the order of many weeks. This would have made intelligent experimental design virtually impossible within a reasonable timeframe. Therefore, NAA was not used.

The next technique considered was directly counting the gamma rays emitted from uranium in the products. This could be used to determine the amount of uranium contained within a given sample. The zirconium content could then be found by subtracting the mass of uranium from the total mass of the sample. One problem with this technique is that one would have to assume that each sample contains only uranium and zirconium both in their stoichiometric oxide form, which may not be true. One must also assume that the samples contain exclusively uranium and zirconium oxides; this was ultimately proven to be far from true as shown in Section 4.3.2. Even if the samples contained pure uranium and zirconium oxides, a detailed study on matrix correction would have been required to account for gamma shielding as a function of U/Zr ratio. Regardless of these shortcomings, a preliminary study of this technique was conducted.

During this study, it was decided that Wavelength Dispersive X-ray Spectroscopy (WDS) would be used for all analysis in this project.

Wavelength Dispersive X-ray Spectroscopy was selected because of its ability to quantify precise mass-fractions for all elemental species within a given sample. The uranium/zirconium mass fraction obtained using this technique was used as an indicator of the separation that occurred during the chloride volatilization process.

The oxide powders produced during the recovery of the *volatilized* and *non-volatilized* product streams were each prepared for WDS analysis by pelletization. The oxide powders were pressed between two polished hardened-steel cylinders. This resulted in a reasonably dense and handleable powder compact with parallel surfaces mirroring the polished surface of the hardened steel cylinders. Each powder compact was secured onto a sample mount using carbon tape and was carbon coated prior to its insertion into the WDS microprobe.

Analysis of the powder samples was primarily accomplished by performing a wide-beam line scan[1]. This was done by moving a 20 micron beam up to 20 steps in one direction so that a compositional average was obtained along this 400 micron line. This procedure was used because many of the pressed-powder samples were heterogeneous on the 20 micron scale. Therefore, analysis of single points would not produce results representative of the powder as a whole. This line-scanning technique was found to produce results which were reproducible and were considered to be reliable.

[1] The microprobe was operated by Dr. Ray Guillemette, Research Associate Professor at Texas A&M's Department of Geology & Geophysics.

The alloys used in the U50Zr series were also analyzed prior to reaction using the same line-scanning analytical technique. However, the preparation of this material differed from the preparation method employed for producing a pressed-powder sample. A uranium-zirconium alloy was cast and was then remelted to ensure homogeneity. This casting was sectioned into slices with an approximate thickness of one millimeter. These slices were mounted in epoxy and polished so that they could be non-destructively characterized using the microprobe. Once these slices had been characterized, they were removed from the epoxy and quartered for use in the four-reaction-vessel system.

3.2.4 Zirconium (Zr) Series

The Zr series was designed to study the rate of volatilization of pure zirconium metal. The system used was identical to the system used in the U50Zr series and is shown in Figure 8. A four-reaction-vessel system was used which allowed individual reaction vessels to be isolated from the system as needed.

3.2.4.1 Procedure

The Zr series used several different materials and processing methods. Tests Zr-1 through Zr-7 began by recording the masses of the crystal-bar zirconium samples to be processed. The vessels were evacuated using a dry-scroll pump and then backfilled with argon. This process was repeated three times and then the reaction vessels were pressurized with 14 psig argon. The reaction vessels were then inserted into the preheated aluminum heating block, and the system was allowed to come to thermal equilibrium at the desired temperature. It was then evacuated using the dry scroll pump, and the vacuum pressure and sample temperature were recorded. The system was then

filled with chlorine gas to the desired pressure and the reaction was allowed to proceed. The inlet and outlet valves for each independent reaction vessel were closed once the sample of interest had reacted for the desired amount of time. The reaction times were 5, 10, 20, and 40 minutes, later changed to 5, 10, 15, and 20 minutes. After each time-step, one sample would be isolated and removed from the heated zone. It should be noted that the cooling process took place in the presence of the gasses that were in the reaction vessel prior to isolation instead of flowing argon.

Test Zr8 was performed by reacting large sections of crystal-bar zirconium with chlorine gas. The lengths and diameters of the four samples were measured prior to and after the chlorination reaction. The use of large bulk samples was an attempt to gauge the magnitude of the effect of surface area on the reaction rate. The system operation was identical to tests Zr-1 to Zr-7.

Tests Zr-9 through Zr-20 were performed on four machined crystal-bar zirconium samples of near identical starting diameters but with intentionally varied thicknesses, and thus surface areas. The samples were created by machining a section of crystal-bar zirconium into a cylindrical shape. Samples were created by sectioning this large cylinder into smaller cylinders to the desired thickness in order to achieve the required sample surface area. The geometric surface area was determined by taking five diameter and thickness measurements of each of the four samples prior to and after the chlorination reaction. These measurements were collected using a micrometer.

Tests Zr-17 and Zr-20 consisted of one of the four samples being composed of a rectangular prism of Zircaloy-4. The dimensions of these prisms were found by taking

five measurements of each of the three lengths using a micrometer before and after the chlorination reaction. The starting dimensions used for tests Zr-19 and Zr-20 were the final dimensions for tests Zr-18 and Zr-19 respectively. The starting dimensions for the Zircaloy-4 prism used in test Zr-20 was the final dimensions for test Zr-17. This technique allowed samples to be reused between experiments.

Test Zr-14 deviated from the rest in this series in that the purpose of this test was to find the temperature at which chloride volatilization begins for four different samples. The four samples used in this test were a Zircaloy-4 tube, a zirconium crystal-bar disk, zirconium metal powder, and crystal-bar zirconium turnings. The physical dimensions and masses of the Zircaloy-4 tube and crystal-bar disk were recorded both before and after the reaction. The masses were recorded for the zirconium powder and crystal-bar zirconium turnings before the reaction.

Test Zr-14 began by a vacuum-purge process as described previously. The vessels were then filled with chlorine, inserted into the aluminum block at room temperature, and then heaters were then turned on. The temperature was allowed to increase slowly and the temperature was recorded as a function of time. The volatilization temperatures were recorded as soon as chloride deposition was observed on the non-heated zone of the reaction vessels. The reaction rates of both the powder and turnings were so high that these reaction vessels were isolated from the system shortly after volatilization was observed for safety reasons. The system was shut off after all four samples had begun to volatilize, and final dimension measurements were collected for the crystal-bar disk.

3.2.4.2 Zr Sample Collection

The samples were collected in the same way as the ZRT series by separating the glass reaction vessel from the SS304 fitting. The system was thoroughly washed with ethanol in order to remove all soluble chlorides and any loose material. In the event of material being stuck to the surface of the test tube, the tube would be partially filled with ethanol and placed into a sonicator to dissolve all material. This method also dislodged any intact metal from the walls of the vessel.

3.2.4.3 Zr Sample Analysis

The intact solid zirconium samples left over from the chlorination reaction were weighed. This resulted in a known mass change corresponding to the amount of material which was converted to chloride. Where relevant, the dimensions of the samples were measured using a micrometer. The results of these measurements were used to study the effect of surface area on reaction rate.

3.2.5 U50ZrFinal

The U50ZrFinal series was conducted using the system described in Section 3.1.5 and was designed as the definitive demonstration of the ability of the chloride volatilization process to separate zirconium from a uranium-zirconium alloy. Each experiment was conducted on a U-50Zr disk for 45 minutes at varying temperatures.

3.2.5.1 U50ZrFinal Procedure

The alloy samples for the U50ZrFinal tests were created from a melt-cast U-50Zr alloy. This alloy was created by weighing out equal masses of uranium and crystal-bar zirconium. The oxide layer was removed from the uranium through acid-washing in

concentrated nitric acid prior to its placement into the yttrium oxide crucible used to contain the melt. The uranium and zirconium materials were placed into the yttrium oxide crucible with the uranium on top. The uranium was placed on top because of its lower melting point of 1132 °C compared to the melting point of zirconium which is 1855 °C. This has been shown to produce a more homogeneous final alloy because the uranium wets the zirconium prior to the zirconium reaching its melting temperature. The materials were melted in a high-temperature furnace under flowing argon at 1900 °C. After the initial melt, the alloy was removed by fracturing the crucible. Any residual yttrium oxide was removed by sanding the surface of the alloy until all visual indication of yttrium oxide was removed. Experience has shown that it is necessary to remelt U-Zr alloys in order to achieve a fully homogeneous alloy. The alloy was therefore placed upside-down from its previous orientation inside of a new yttrium oxide crucible. The remelt was also performed in a high-temperature furnace under flowing argon at 1900 °C.

The alloy was removed from the crucible by fracture, and any residual yttrium oxide was removed by sanding the surface of the alloy. This final alloy was then cut into slices with an approximate thickness of one millimeter using a diamond saw. These alloys were not characterized by WDS analysis as was done with the U50Zr series, because the results of the U50Zr series indicated that a melt-remelt process produced a homogeneous alloy. It was also believed that the error in U/Zr ratio which may have been introduced during the melt-remelt process is negligible for this series of tests.

Each experiment began by recording the mass of one of the slices. This sample was placed into a reaction vessel which was then evacuated using a dry-scroll pump and backfilled with argon. This vacuum/backfill process was repeated three times and then the reaction vessel was filled with chlorine gas at 6 psig. The reaction vessel was then inserted into the preheated aluminum heating block. This procedure differed from the U50Zr series in that only one vessel was used at a time for the U50ZrFinal series, while four vessels were used simultaneously for the U50Zr series. The samples for the U50Zr series were also preheated before chlorine was introduced. The samples for the U50ZrFinal series were heated under a chlorine atmosphere. The procedure was changed because it was felt that heating the samples under vacuum or argon could potentially affect the alloy due to oxygen and/or nitrogen contamination. This change was further justified because the chlorination reaction shows an incubation period of roughly a minute before any reaction begins. The incubation period was on the order of that required for the sample to reach thermal equilibrium.

The samples were allowed to react with chlorine for 45 minutes at which time the reaction vessel would be removed from the heating block, and argon gas flow was immediately begun. The samples were allowed to cool to room temperature under flowing argon before the vessel was opened and the samples collected.

3.2.5.2 U50ZrFinal Sample Collection

The post-test samples in this series were collected in exactly the same way as in the U50Zr series. As before, material that became volatile during the chloride formation reaction would deposit on the cold region of the reaction vessel. This resulted in a

separation of the *volatile* and *non-volatile species*. It then became necessary to separate these two materials which were both deposited within the same test tube. The same process which is shown in Figure 11 was used to separate the *volatilized* and *non-volatilized* material. Once this physical separation was complete, the respective chlorides were washed from the reaction vessel using ethanol. The *non-volatile* species were dissolved in ethanol, and any solid material was separated by decanting. The mass of this solid material was then recorded. The *volatile* species were also removed from the test tube and SS304 fitting by washing with ethanol. Any solids were then separated by decanting.

The ethanol containing dissolved chlorides from the two streams was then allowed to evaporate. The chlorides would be left behind as a crystalline layer at the bottom of the glass beakers. The chlorine was removed from this material by adding an excess of aqueous sodium hydroxide. The solids that resulted from the reaction with sodium hydroxide were allowed to precipitate out, and the aqueous phase was decanted off. The solids would then be washed and decanted with deionized water until the water was no longer basic. Ethanol (200 proof) was then added and decanted away until most of the water was removed. The material was then dried further by adding and decanting away pure acetone. The dry oxide material of both the *volatile* and *non-volatile* streams was finally ground to a fine powder using a mortar and pestle, and collected for analysis. This process is identical to that which was used in the U50Zr series.

3.2.5.3 U50ZrFinal Sample Analysis

The oxide powders which were produced during the recovery of the *volatilized* and *non-volatilized* product streams were each prepared for WDS analysis by first producing suitable samples. The oxide powder was pressed between two polished hardened steel cylinders. This resulted in a pressed powder with a surface mirroring the polished surface of the polished hardened steel cylinders. The pressed powder was placed and secured onto a sample mount using carbon tape. The sample was then carbon coated prior to its insertion into the WDS microprobe.

Analysis of the powder samples was accomplished by performing a line scan. This was done by moving a 20 micron beam up to 20 steps in one direction so that a compositional average was obtained along this 400 micron line. This line-scanning technique was found to produce results which were reproducible and were believed to be reliable. The sample preparation and analysis processes used for the U50ZrFinal series were identical to the U50Zr series.

4. RESULTS

The following chapter will describe the results obtained from the five experimental series conducted as a part of the research presented here. The first series, the ZRT Series, gathered preliminary data on chlorination of pure zirconium to facilitate the design of future series. The second series, the UT series, qualitatively compared the volatilization behavior between zirconium and U-50Zr alloys, as well as between uranium and U-50Zr alloys. The third series, the U50Zr Series, began to study the selective volatilization of zirconium from U-50Zr alloys. The fourth series, the ZR Series, studies the volatilization of zirconium in greater detail. The fifth and final series, the U50ZrFinal Series, studied the ability of a chlorination process to separate zirconium and uranium from U-50Zr alloys.

4.1 Preliminary Experiments: Temperature, Pressure, and Time (ZRT Series)

The experiments reported in this section (i.e., the ZRT series) were performed to provide parametric data on chloride formation in pure crystal-bar zirconium. While Zr to $ZrCl_4$ volatilization was observed, it was not the focus of this series. The variables of temperature, pressure, and time were systematically studied so that the final effective experimental series (Section 4.5) could be designed and performed. This was accomplished by measuring mass changes as a function of these variables. As described in section 3.2.1, the mass change was measured by weighing the zirconium samples prior to reacting with chlorine and then weighing the mass of the zirconium that was not soluble in ethanol after the chlorine reaction. This provided a measure of the mass of

zirconium which had been transformed into chloride as a function of the variables of interest. This data is presented below in Table 2.

Table 2: Summary of data from ZRT series.

Series	Name	m_I (g)	m_F (g)	T (C)	Pressure (psi)	Time (min)
Temp	ZRT-1	0.1764	0.1308	588	14	60
Temp	ZRT-2	0.2168	0.1797	450	14	60
Temp	ZRT-3	0.1769	0.1043	350	14	60
Temp	ZRT-4	0.1677	0.0636	237	14	60
Temp	ZRT-5	0.1378	0.0482	286	14	60
Temp	ZRT-6	0.1744	0.1363	400	14	60
Temp	ZRT-7	0.2001	0.1612	531	14	60
Temp	ZRT-8	0.1744	0.103	337	14	60
Temp	ZRT-9	0.1749	0.1393	379	14	60
Pressure	ZRT-10	0.1219	0.1008	371	14	30
Pressure	ZRT-11	0.111	0.0871	376	28	30
Pressure	ZRT-12	0.1208	0.0935	377	42	30
Pressure	ZRT-13	0.1565	0.1124	372	56	30
Pressure	ZRT-14	0.1571	0.14	368	2	30
Time	ZRT-15	0.1446	0.1125	366	14	45
Time	ZRT-16	0.1776	0.1638	363	14	15
Time	ZRT-17	0.2213	0.194	364	14	35
Time	ZRT-18	0.2225	0.1848	372	14	60
Time	ZRT-19	0.2134	0.1656	368	14	75
Time	ZRT-20	0.1245	0.0673	371	14	90

4.1.1 Impact of Temperature (ZRT-1 to ZRT-9)

This sequence of tests studied the effect of temperature on the chloride formation rate. The focus was to study the difference in chloride formation at temperatures above the zirconium tetrachloride volatilization temperature (331 °C) and below this temperature. A summary plot showing the composite information from this study is

shown in Figure 12. The experiments in this sequence were conducted at 14 psig and were reacted for 60 minutes.

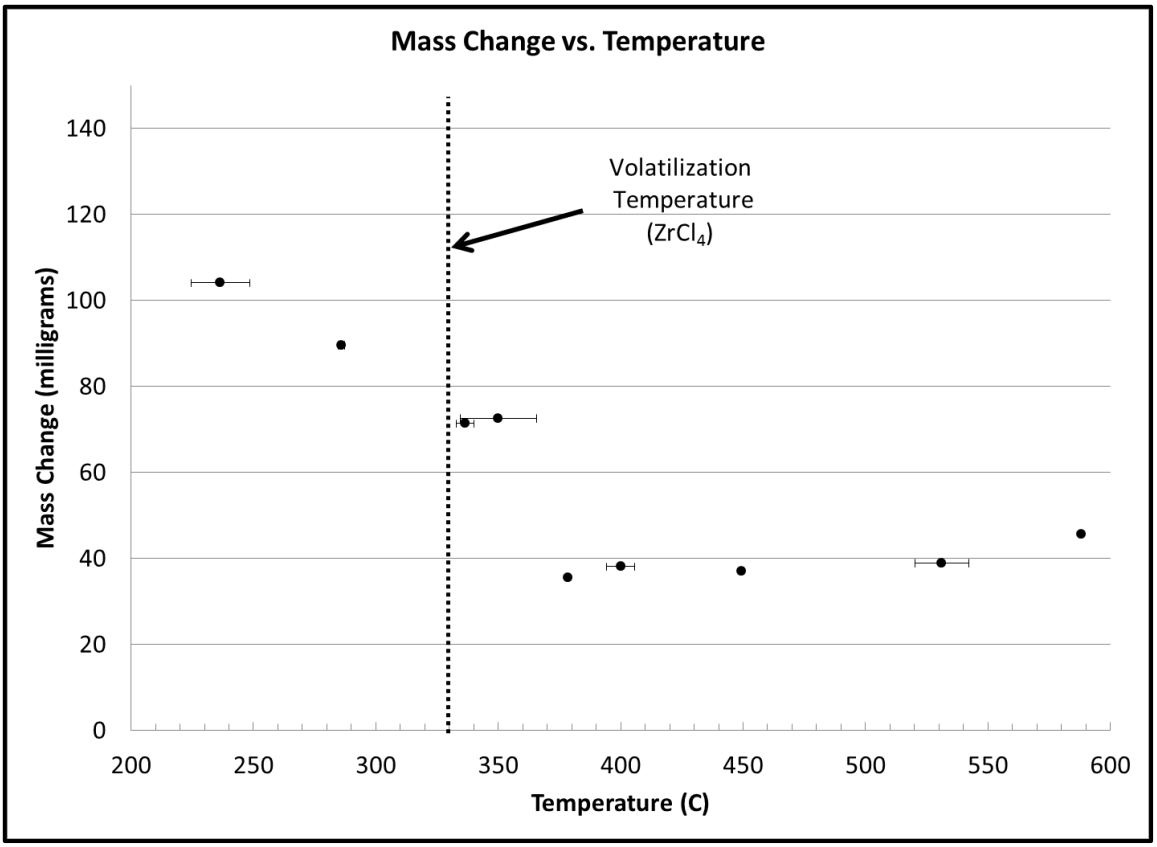

Figure 12: Mass loss of zirconium metal after 60 minute reaction time vs. temperature at 14 psig.

The information in Figure 12 shows a clear difference between behavior that occurred above the volatilization temperature and that which occurred below this temperature. It appears anomalous that the change in behavior occurs at a temperature near ~350 °C, above the 331 °C volatilization temperature of $ZrCl_4$. However, it is most likely due to inaccurate temperature readings caused by poor contact between the vessel

and the heater-block. The result could be an observed temperature at the thermocouple which was not necessarily equal to the sample temperature. Further, and more important, these results are in opposition to expectations. It was expected that there would be increased chloride formation (and mass loss) at temperatures above the 331 °C. The data in Figure 12 show just the opposite. This seemingly contradictory behavior may be explained by considering the geometry of the system. As described in section 3.1.4, these experiments were oriented vertically in a relatively narrow glass tube (Figure 10). This orientation enabled the volatilized material to solidify and fall back into the heated area and onto the sample. This was observed visually as rain-like precipitation of zirconium tetrachloride (speculated composition) within the reaction vessel. In addition to the problems associated with vertical orientation, the narrowness of the reaction vessel resulted in the deposition zone becoming quickly clogged with deposited material. This closed the heated zone and established a reaction zone saturated with gaseous zirconium tetrachloride which may have inhibited the formation of further chloride.

4.1.2 Impact of Pressure (ZRT-10 to ZRT-14)

The desired outcome of this sequence of experiments was to evaluate the need for highly accurate pressure measurement. If the reaction rate remained relatively invariant as a function of pressure, then crude pressure maintenance would be sufficient. However, if the chloride formation rate was highly dependent on system pressure, then the equipment would need to be altered accordingly. The results of these experiments are shown in Figure 13.

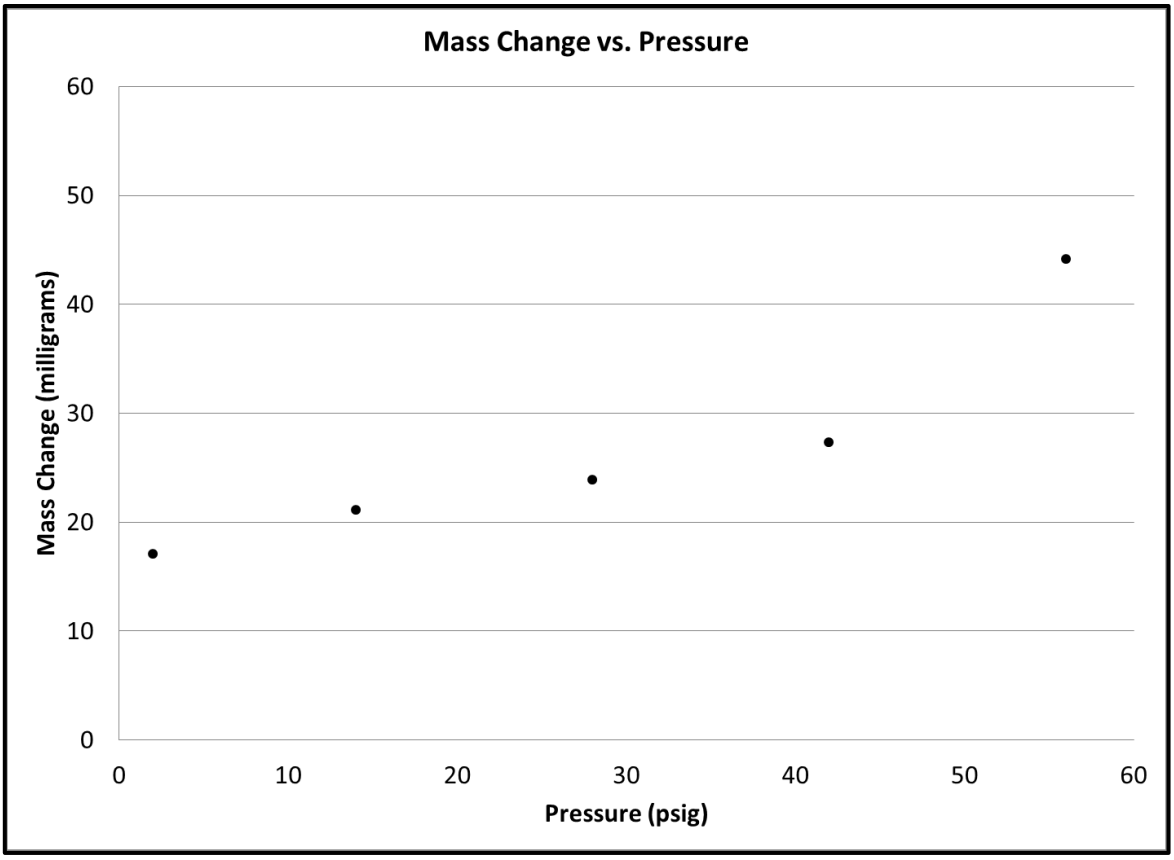

Figure 13: Mass loss of zirconium metal vs. chlorine pressure at 375 °C.

With the exception of the high pressure (56 psig) data point, it is observed that the reaction rate is only weakly dependent on the chlorine pressure. Based on this observation, pressure was eliminated as a variable to be studied in the later experiments and system pressure was regulated and measured using the regulator connected to the gas supply. This pressure sequence was conducted at ~375 °C (tests varied from 368 to 377 °C) which was selected based on the results obtained in the temperature study in Section 4.1.1 (Figure 12). The operating temperature was selected to ensure that temperature fluctuations from the exothermic reaction would have negligible impact. In

an effort to minimize the effect of the tube clogging and influencing results, as was observed in the previous sequence, the reaction time was set at 30 minutes, as opposed to the 60 minute reaction time in the Section 4.1.1.

4.1.3 Impact of Time (ZRT-15 to ZRT-21)

The final sequence of ZRT experiments were performed to investigate the time-dependence of chloride formation. The variables of temperature and pressure were maintained at values which, at the time, were believed to render these variables relatively constant. The temperature was successfully held between 363 and 372 °C and the system pressure was held at 14 psig.

The results in Figure 14 appear to show a linear relation between chloride formation and reaction time. This implies a constant chloride formation rate, which is likely true as long as the volatile chloride is able to freely leave the reaction zone. However, as discussed earlier, the tube was seen to clog once about 40 mg of metal had been turned to chloride. This raises questions regarding the 75 and 90 minute data points, which seem to contradict the “clogging” theory.

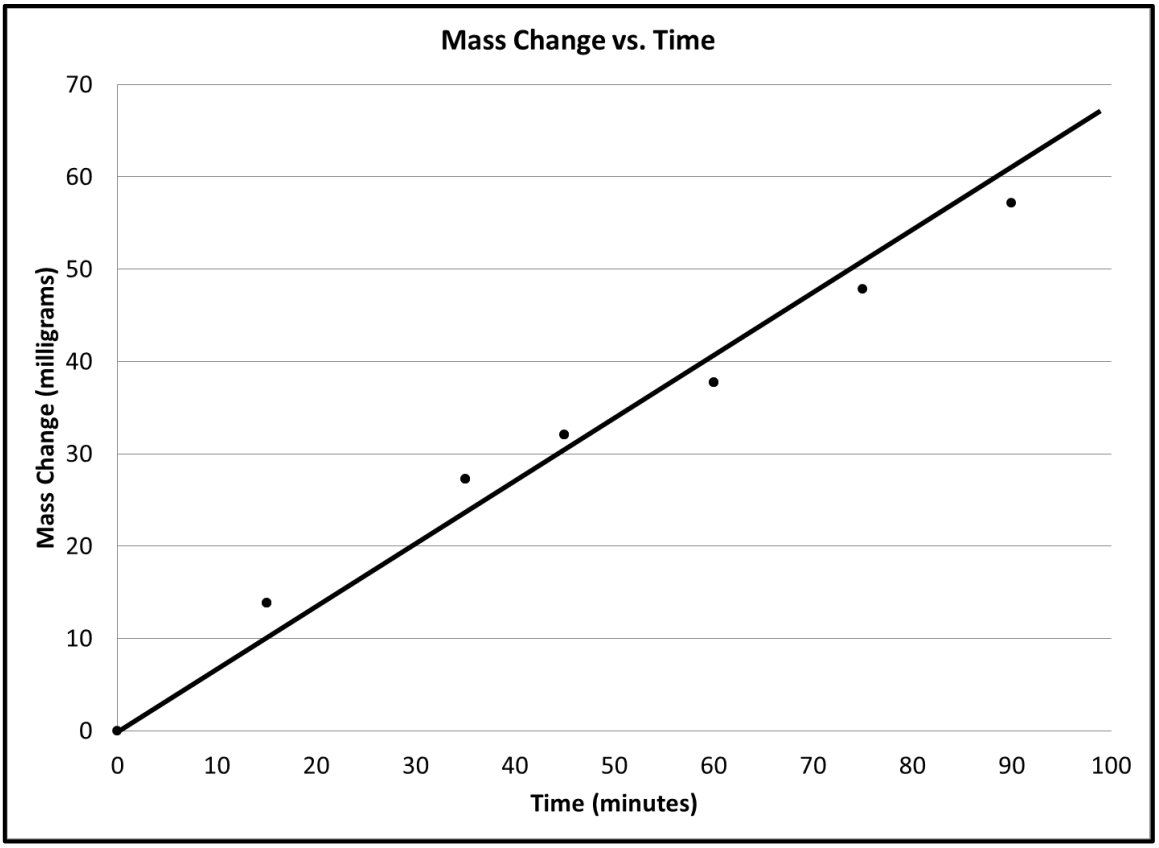

Figure 14: Mass loss of zirconium metal vs. time at 375 °C and 14 psi chlorine.

It can be concluded from the ZRT series that a reaction vessel must be used which allows the volatilized material to freely leave the heated reaction zone. Data gathered from any system which does not allow this, as in this ZRT series, should be interpreted cautiously. That being said, the ZRT data series did provide valuable observations to enable subsequent experiment designs. These observations include (1) the need for a larger diameter reaction vessel, (2) the weak dependence of the chloride reaction rate on system pressure, and (3) the need for more accurate temperature measurement.

4.2 Initial Reactions to Compare Zr, U and Zr-50Zr Reactions (UT Series)

The experiments described in this section (i.e., the UT Series) were performed to generate qualitative understanding of the differences between chloride formation behavior in the U-50Zr alloy along with direct companion experiments with pure zirconium and uranium. As described in Section 3.1.5, the experiments performed in this series took place within the horizontal glass test tube system. This orientation was believed to reduce the "clogging" effect that was seen in the previous ZRT series because of the vessel's larger diameter. All experiments in this series were conducted at 6 psig for one hour and at temperatures ranging between 335 and 370 °C.

Each experiment was set up so that one reaction vessel contained a U-50Zr sample, and the other reaction vessel contained either a uranium or a crystal-bar zirconium sample. The data gathered in this series mostly dealt with visual comparisons between the chloride formation and volatilization of the three materials. Prior to this series, it was not established that chlorine gas would completely extract the zirconium contained within a U-50Zr alloy. It was also not known if the chlorides of uranium would volatilize or if they would stay behind. It was established that the zirconium did indeed volatilize and transport from heated U-50Zr samples and that uranium did remain in the heated zone. The following images and discussion provide the details to support this conclusion and Section 4.5.2 provides data regarding the effectiveness of the separation.

As observed in the ZRT Series, volatilized material would begin depositing immediately after leaving the heated portion of the reaction vessel. Figure 15 shows an

image from test UT-2 showing the volatilized material condensed on the outside of the heated zone. While the larger reaction vessel used here clearly increased the amount of material that could be volatilized before the tube would become clogged, the presence of the internal gas inlet tube that delivered the chlorine gas to the heated end of the vessel limited the amount of material that could be volatilized for each experiment. Figure 16 shows the reaction vessel becoming clogged with material. The gas inlet tube was subsequently removed from all future tests and material was allowed to freely volatilize and deposit.

Figure 15: Reaction vessel containing U-50Zr (UT-2) in heated aluminum block; discoloration from suspended vapor deposited chloride solids.

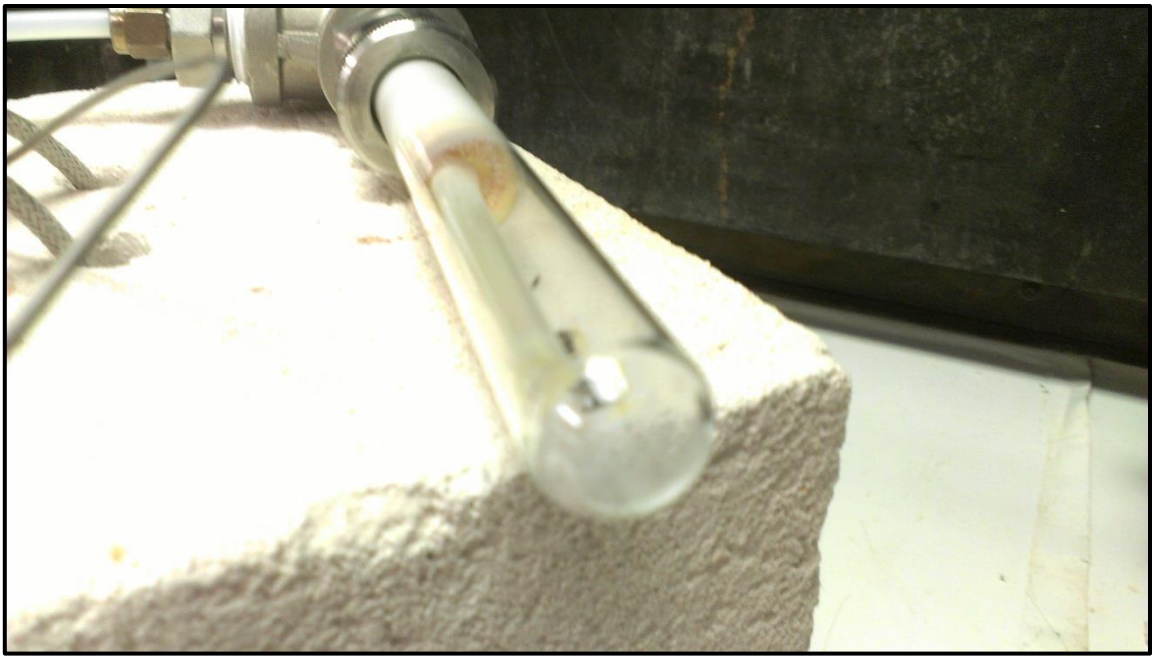

Figure 16: Reaction vessel for UT-5 showing clogging due to deposition of product from chlorinated crystal-bar zirconium.

The original purpose of the gas inlet tube was to provide a gas source directly to the sample in a flowing system. The use of a flowing system was discarded as unreasonable since the flowing supply of chlorine provided a constant feed to the highly exothermic chloride formation reaction that created uncontrollable temperature conditions. Experiment UT-1 allowed chlorine gas to flow for a few seconds into the already heated reaction vessel in an effort to purge the system of gas impurities. Both the U-50Zr and crystal-bar zirconium samples immediately began to glow a bright orange, which was visible even though the reaction vessels remained inside of the heated block. The zirconium sample was completely consumed and volatilized, and the U-50Zr

sample was attacked and reduced to an unrecognizable mass; likely a mixture of chlorides and oxides.

Several important lessons were learned from this series. The first is that a system with flowing chlorine was unreasonable due to safety concerns and because the samples would become uncontrollably heated making it impossible to measure their actual temperature. If the alloy reaches a high, unknown temperature, the uranium chloride may also transport from the hot zone even though the apparent temperature being tested indicates that it should not be volatile. It was also concluded from this series that the gas inlet tube was unnecessary and could be removed from the system, thus removing system clogs for the volatilization of all but the largest masses.

Figure 17 and Figure 18 show the results of the UT-2 test which compared the volatilization of U-50Zr and crystal-bar zirconium. The vessel containing U-50Zr produced a purple product that had volatilized and transported from the hot zone, while the reaction vessel containing zirconium produced a white product typical of zirconium tetrachloride. The purple color is indicative of uranium chlorides being present, and was seen whenever U-50Zr was reacted with chlorine.

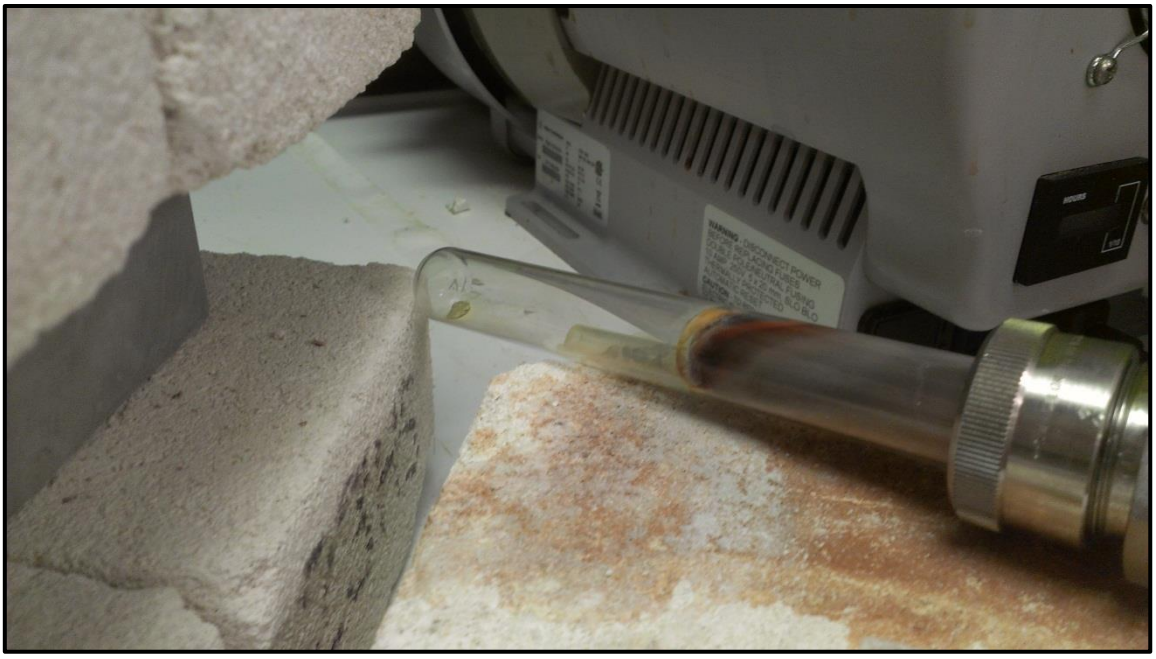

Figure 17: Reaction vessel from experiment UT-2 showing the remnant of the U-50Zr alloy and the purple product on the cold zone wall.

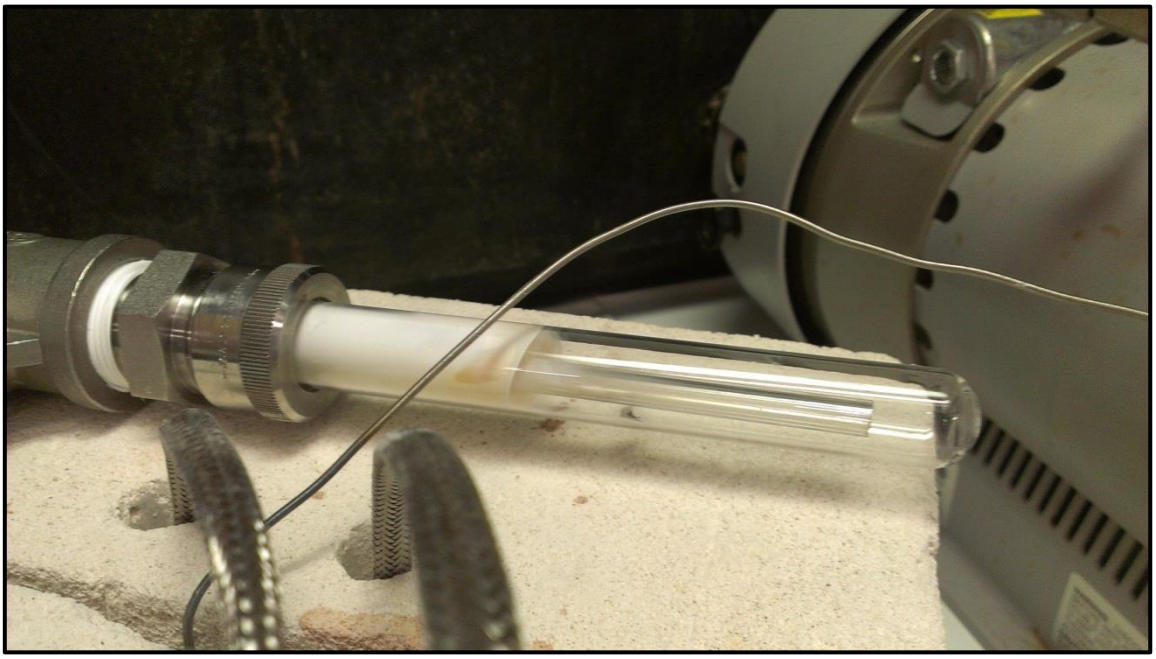

Figure 18: Reaction vessel from experiment UT-2 showing and the white product on the cold zone wall; the Zr sample was completely gone.

Figure 19 and Figure 20 show the results of the UT-3 test which compared the volatilization of pure uranium and U-50Zr. It is evident in Figure 19 that very little, if any, of the pure uranium was volatilized due to chloride formation. In fact, the material which can be seen deposited on the reaction vessel in Figure 19 is very likely due to residual zirconium chloride from the system not being thoroughly cleaned in-between experiments as opposed to material being volatilized from the uranium sample. The sample shown in Figure 20 is identical in appearance to that shown in Figure 17, both of which were volatilization experiments of U-50Zr alloy.

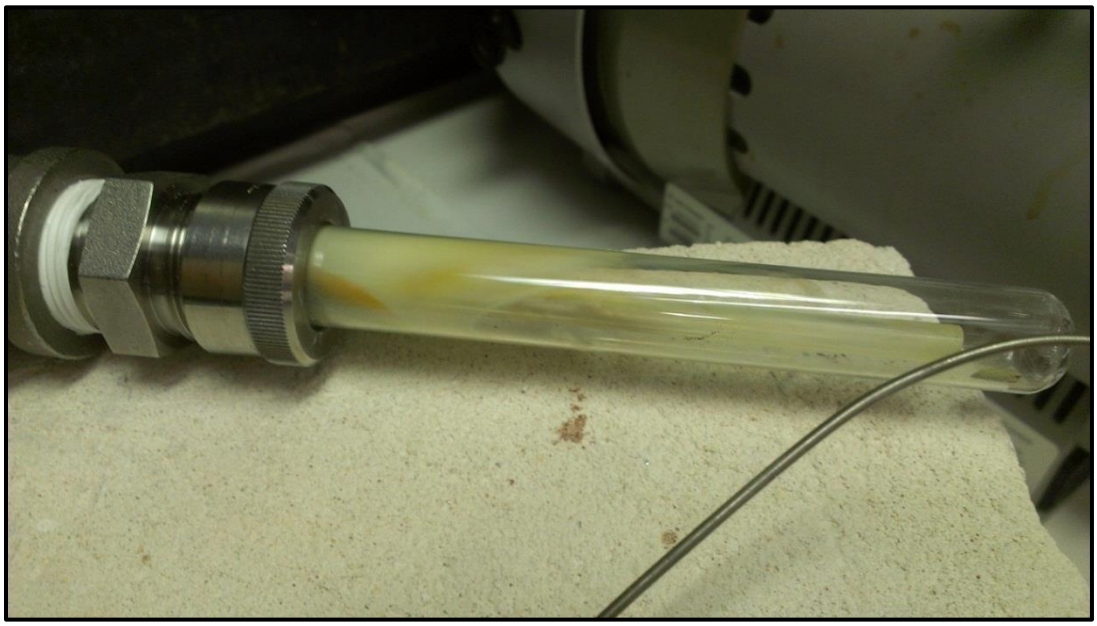

Figure 19: Reaction vessel as removed from heated block. Sample is uranium from experiment UT-3.

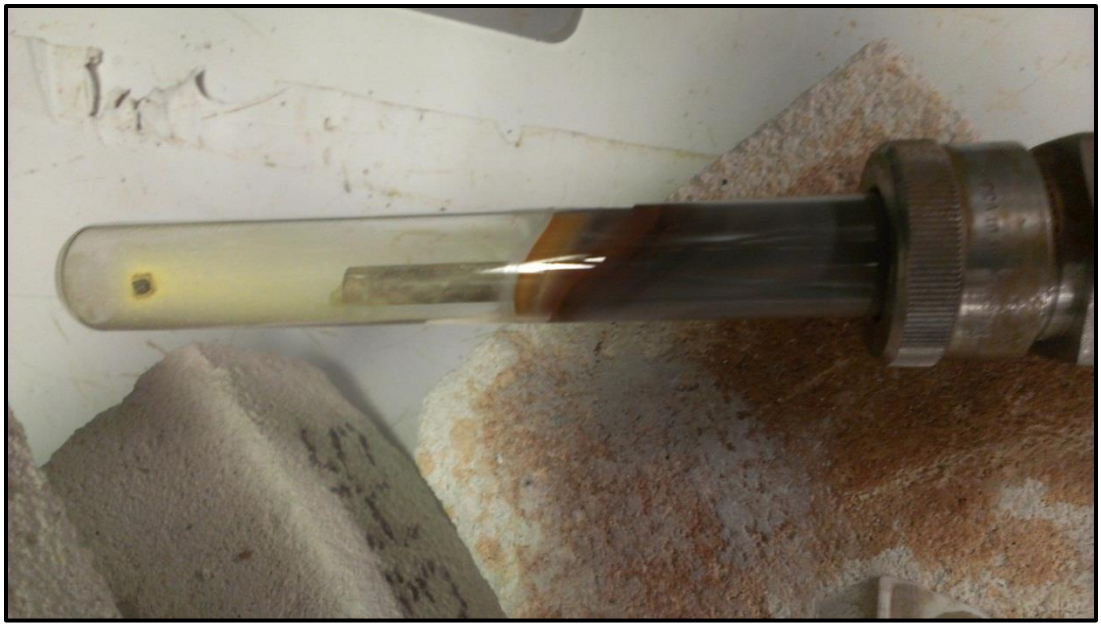

Figure 20: Reaction vessel as removed from heated block. Sample is U-50Zr from experiment UT-3.

As a whole, the UT experiments showed that chlorine could indeed be used to volatilize and separate the components of U-50Zr alloys. These tests demonstrated the resistance of uranium to volatilization by chloride formation. The next step was to perform a quantitative study of the ability of chlorine to separate zirconium from uranium in uranium-zirconium alloys.

4.3 Uranium-Zirconium Separation Demonstration (U50Zr)

The U50Zr series was designed to quantify the selective chloride volatilization of zirconium from uranium-zirconium alloys. The uranum-50 wt% zirconium (U-50Zr) alloy was selected for this study because it contains the δ-phase of the alloy in high concentrations [41]. The δ-phase was anticipated to be the more challenging U-Zr phase to separate Zr from U over uranium and zirconium solid solutions or eutectic 2-phase

mixtures. This is due to the added thermodynamic barrier needed to break the intermetallic bonds. The results of this series are presented below in Table 3.

Table 3: Summary of data from U50Zr series.

Sample Name	%U	%Zr	T	Time (Minutes)
U50Zr1-1NV	99.5	0.5	374	15
U50Zr1-2NV	97.4	2.6	374	30
U50Zr1-2V	58.8	41.2	374	30
U50Zr1-3V	60.0	40.0	378	60
U50Zr2-1NV	77.5	22.5	300	15
U50Zr2-2NV	98.8	1.2	303	30
U50Zr2-3NV	98.4	1.6	312	60
U50Zr2-4NV	99.8	0.2	306	120
U50Zr4-1NV	96.1	3.9	340	15
U50Zr4-2NV	99.7	0.3	340	30
U50Zr4-3NV	99.9	0.1	340	60
U50Zr4-4NV	99.8	0.2	340	120
U50Zr5-1NV	95.3	4.7	360	15
U50Zr5-2NV	96.1	3.9	359	30
U50Zr5-3NV	99.9	0.1	362	60
U50Zr5-4NV	99.9	0.1	360	120
U50Zr6-V	25.8	74.2	265	120
U50Zr7-NV	96.5	3.5	285	90
U50Zr7-V	21.1	78.9	285	90

4.3.1 U-50Zr Alloy Characterization

A pre-fabricated U-50Zr alloy[2] slug was used as the source material for the U50Zr experiments. It was understood that fabricating homogeneous alloys was challenging due to the difference in densities of uranium and zirconium. For this reason, each sample in this series was characterized prior to the chlorination experiments. This was accomplished by sectioning the as-cast alloy into seven slices to be used in seven different experiments. These slices were mounted in epoxy, polished, and characterized using EPMA. The EPMA results can be seen in Figure 21 and Table 4. The alloy composition was seen to vary linearly along the length of the original as-cast alloy. The slight variations, specifically slices 2 and 4, are likely due to the random selection of which surface of the roughly 1mm thick slice was to be characterized.

Table 4: Summary of alloy characterization.

Slice	U%	Zr%
U-50-Zr 1	38.52	61.48
U-50-Zr 2	39.17	60.83
U-50-Zr 3	42.72	57.28
U-50-Zr 4	43.62	56.38
U-50-Zr 5	46.87	53.13
U-50-Zr 6	48.92	51.08
U-50-Zr 7	51.26	48.74

[2] Uranium-50 wt% zirconium alloy was fabricated by Sandeep Irukuvarghula, Texas A&M University, Department of Nuclear Engineering> using melt casting methods in an yttrium oxide crucible at 1900 °C under inert atmosphere.

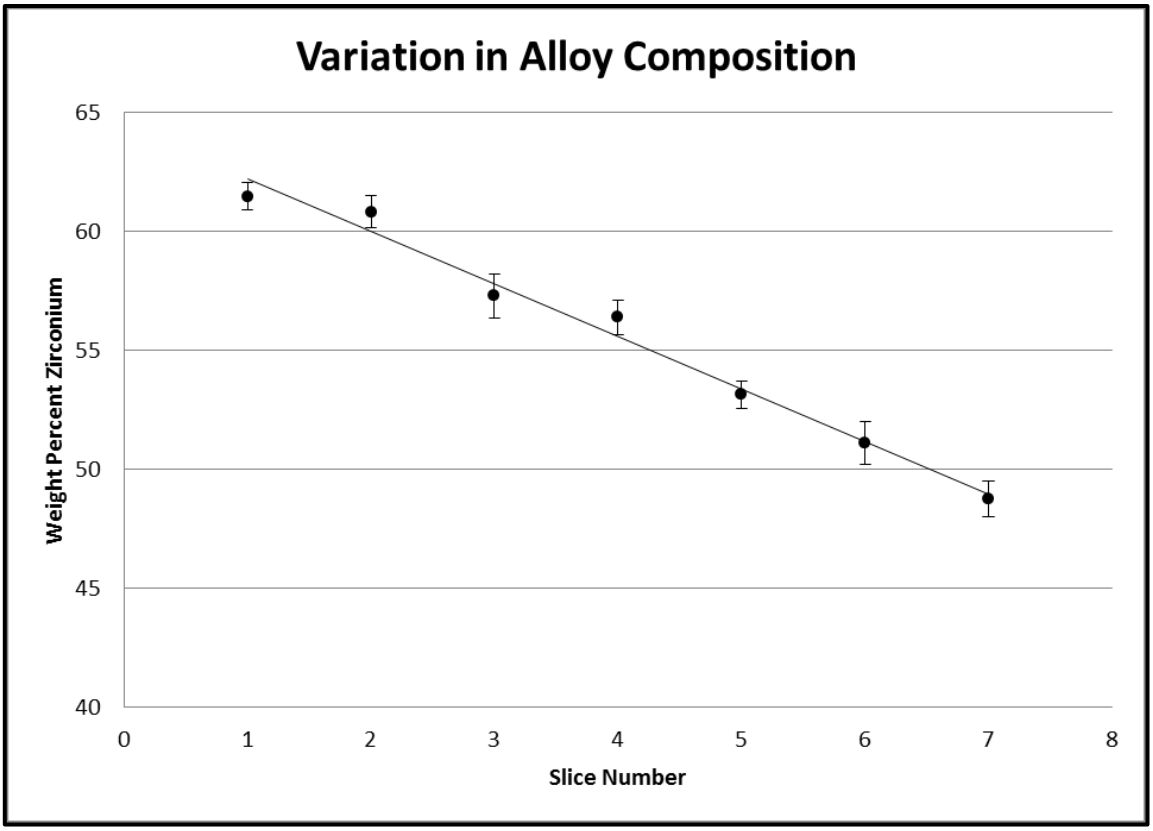

Figure 21: Variation of uranium-zirconium ratio along length of as-cast alloy. Slice 1 was at the top of the alloy, while slice 7 was at the bottom of the alloy.

The observed variation in alloy composition was anticipated to have a negligible impact on the chloride volatilization data obtained using these samples. The alloy microstructure is of greater significance to chloride volatilization than the exact starting composition. It was observed that all seven samples had microstructures which were very similar. Furthermore, it was assumed that slight variations in microstructure are insignificant at the scales being studied in this project. Therefore, a detailed characterization of the U-50Zr alloy microstructure variations was not investigated further.

Even so, the microstructure was examined in some detail for Slice 1, as shown in Figure 22 and Figure 23. It was found that fine α-zirconium phases were present in these samples. These phases were composed of greater than 98% zirconium, with the remaining ~2% being uranium. However, the uranium composition of these precipitates was likely detected erroneously due to the electron beam interaction zone being significant at these scales. It is therefore assumed that the observed zirconium precipitates contain no uranium, although the validity of this assumption is not very important to the outcome of the experiments performed.

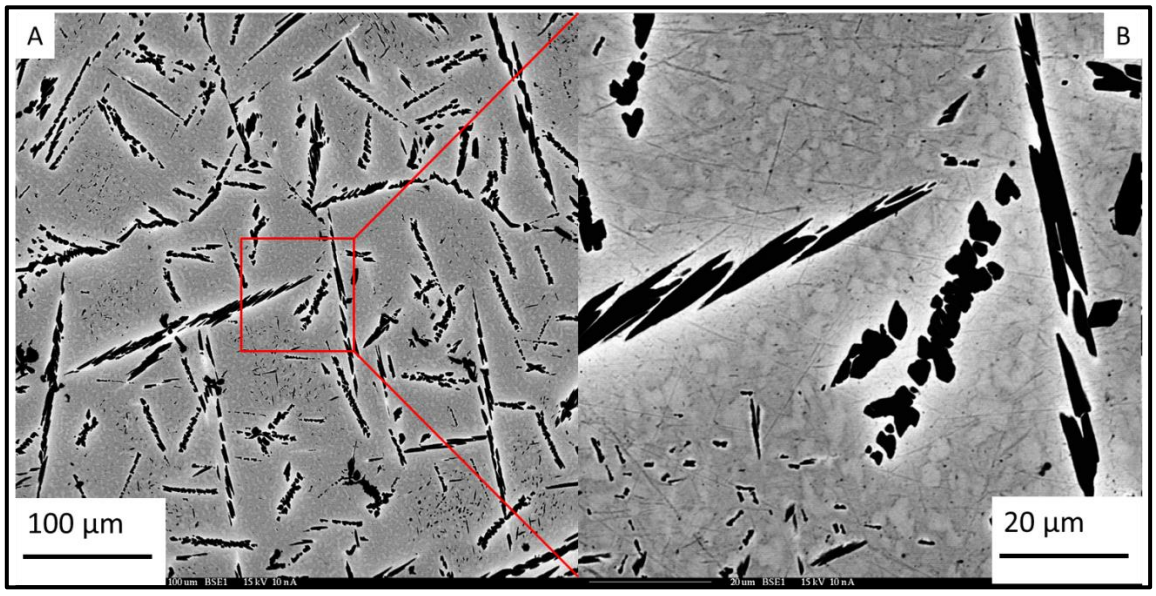

Figure 22: Backscattered electron images of the U-50Zr material (Slice 1) showing a representative microstructure which is common to all slices.

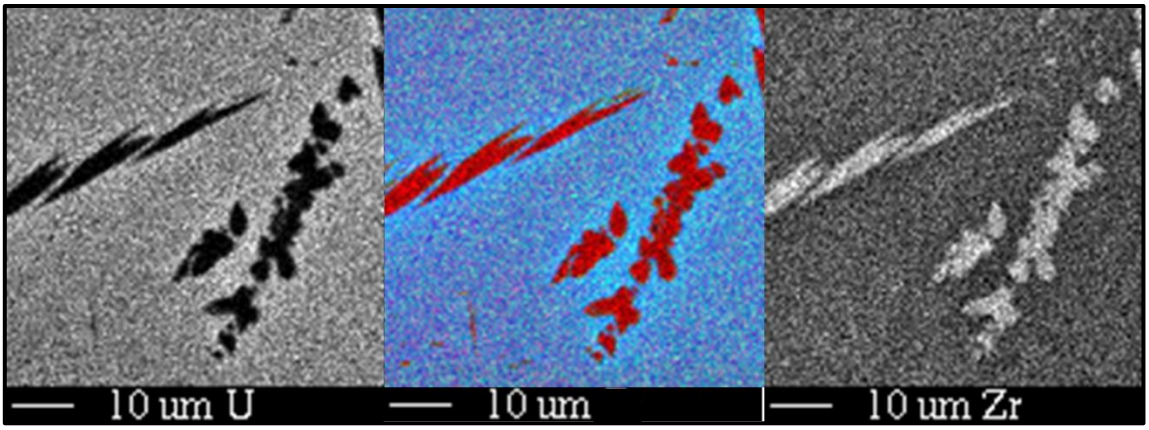

Figure 23: Colorized image (center) from U-50Zr sample in Figure 22-B along with X-ray maps showing the locations of uranium (left) and zirconium (right).

As a further check on the bulk sample uniformity, the U-50Zr slices were compared and found to be homogenous on the macro-scale. This can be seen in Figure 24 for Slices 1-3. This homogeneity is in contrast to that observed for two separate U-10Zr alloys (Figure 25 and Figure 26), neither of which underwent a second remelt step.

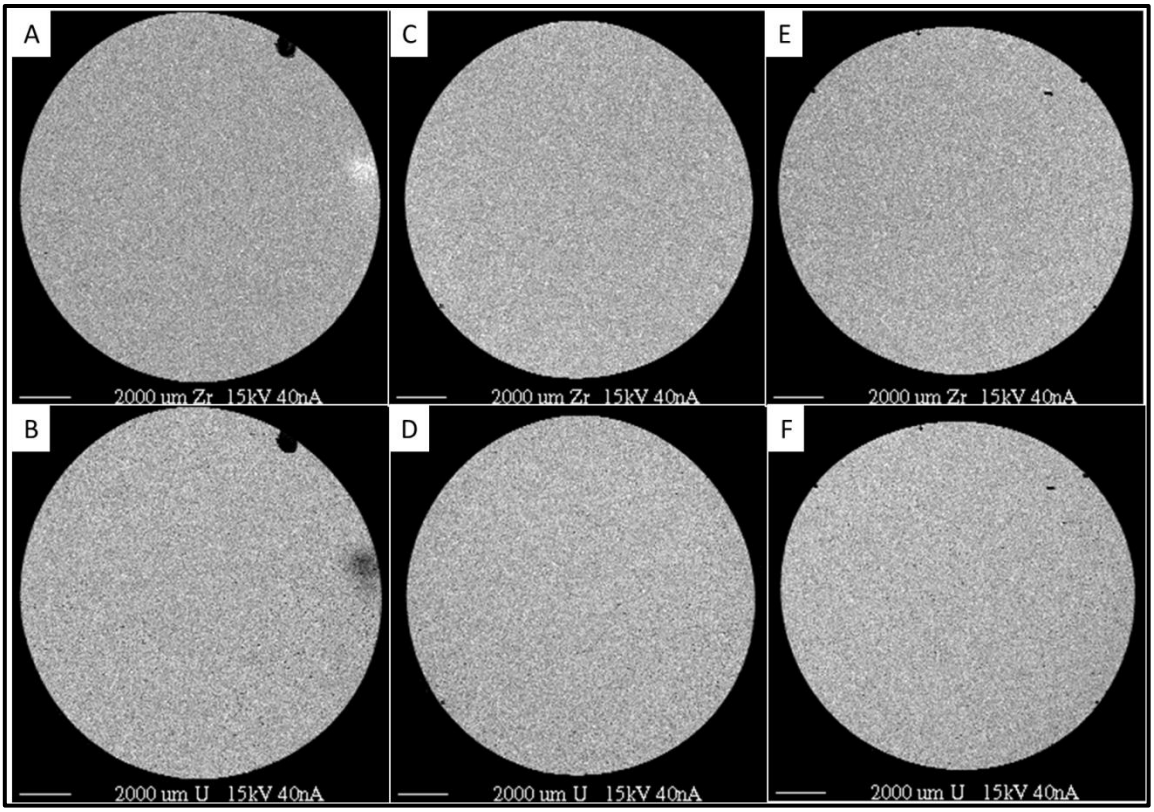

Figure 24: Low magnification backscattered electron images of the U-50Zr alloy slices showing macroscopic homogeneity: The faces of Slice 1 are shown in A-B, Slice 2 in C-D, and Slice 3 in E-F.

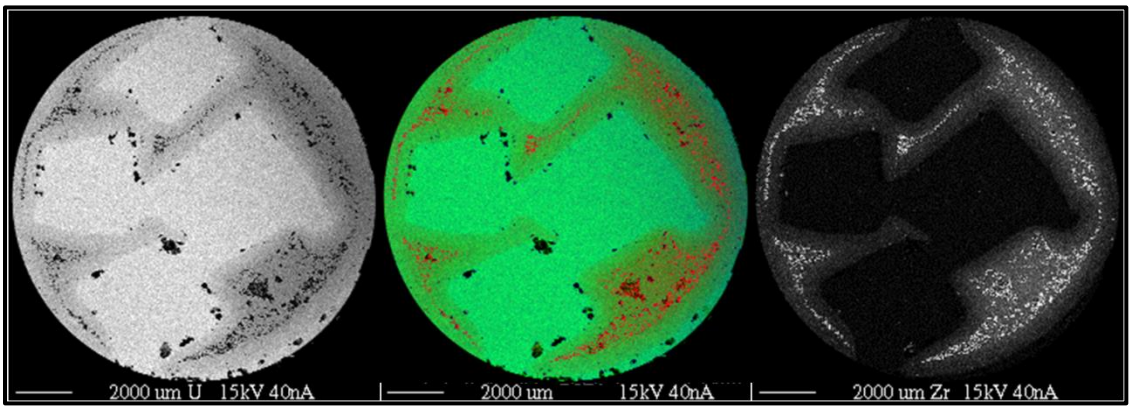

Figure 25: Uranium and zirconium X-ray maps of U-10Zr alloy system showing macroscopic inhomogeneity.

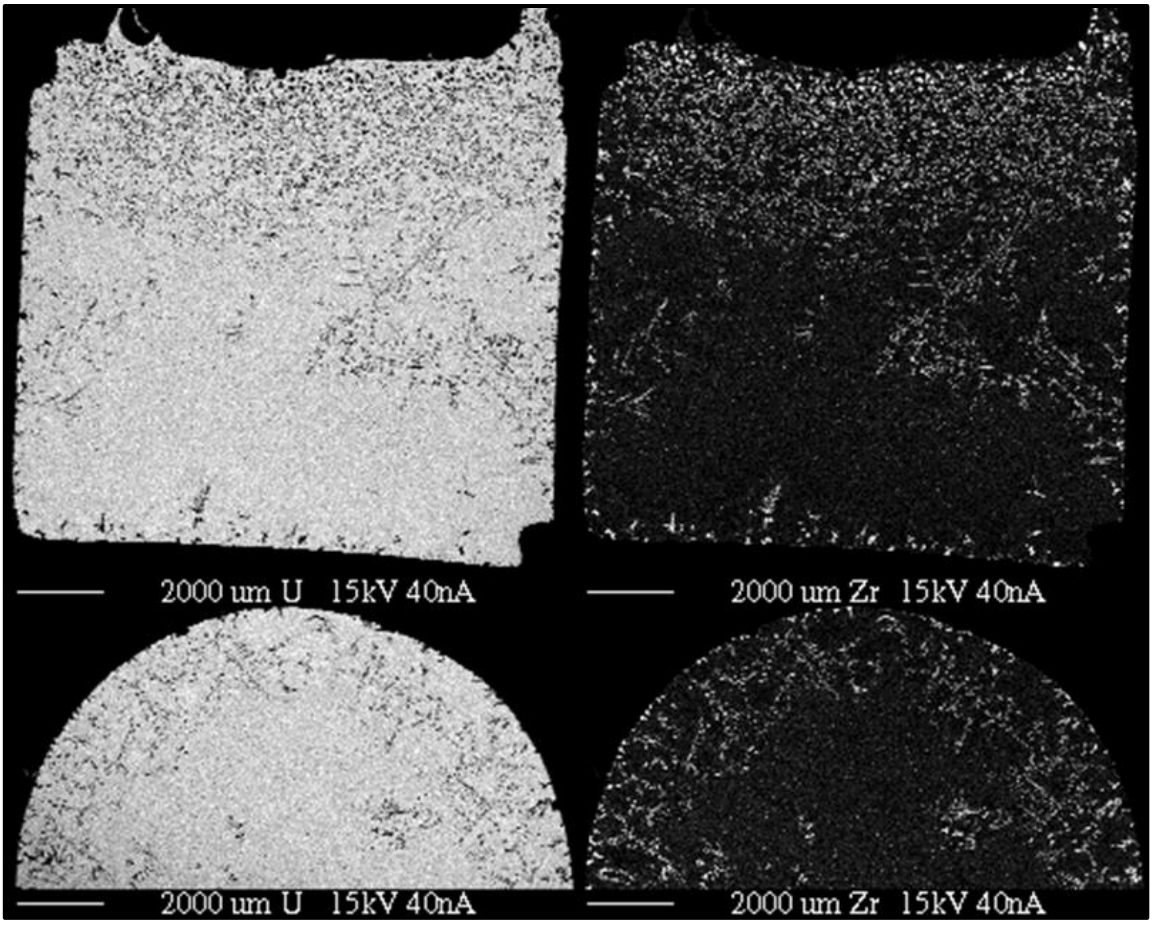

Figure 26: Uranium and Zirconium X-ray maps of U-10Zr alloy-system showing macroscopic inhomogeneity.

4.3.2 Separation Results

After characterization, each disc from the U-50Zr alloy was sectioned into quarters and each quarter was inserted into its own independent glass tube reaction vessel. The samples were then reacted with elemental chlorine for predetermined temperatures and lengths of time according to the procedure in Section 3.2. Each sample was then physically separated into a *volatilized* portion and a *non-volatilized* portion.

This section will present the results of the EPMA analysis for this series of experiments in the order that they were performed.

4.3.2.1 U50Zr-1

This was the first experiment which quantitatively studied the ability of chlorine to separate zirconium from uranium-zirconium alloys. The results are presented in Table 5. Slice 1 of the U-50Zr alloy was sectioned into 4 pieces and exposed to chlorine for 15, 30, 60 and 120 minutes according to the procedures in Section 3.2.3. The *non-volatile* chlorides formed in samples 1-2 were analyzed and was found to contain at least 97% uranium compared to zirconium. This result indicated that the chloride volatilization process is capable of providing some separation in uranium-zirconium alloys.

Table 5: Summary of separation effectiveness from U50Zr1 experiment.

Experiment	U50Zr1	U50Zr1	U50Zr1	U50Zr1
Sample	1	2	3	4
Initial Mass (g)	0.1499	0.1658	0.1259	0.1592
Final Mass (g)	0.0330	0.0079	0.0000	0.0000
Time (Min)	15	30	60	120
Temperature (°C)	374	374	378	381
Percent Zr (Non-Volatilized)	0.5	2.6	NA	NA
Percent U (Non-Volatilized)	99.5	97.4	NA	NA
Percent Zr (Volatilized Grey)	NA	81.5	73.8	NA
Percent U (Volatilized Grey)	NA	18.5	26.2	NA
Percent Zr (Volatilized Bright)	NA	1.9	5.6	NA
Percent U (Volatilized Bright)	NA	98.1	94.4	NA

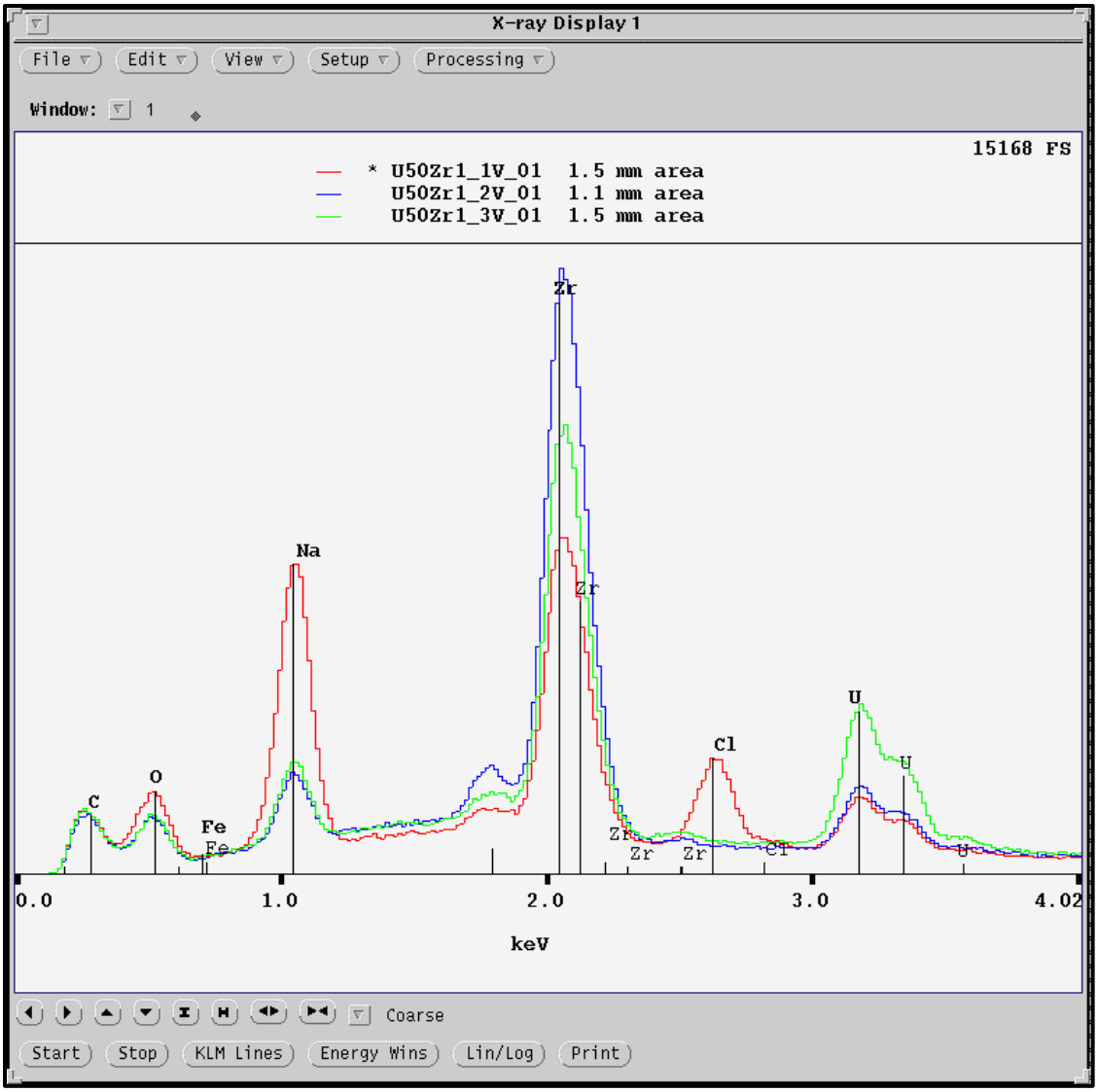

Figure 27: Energy-dispersive X-ray spectrum of volatilized portion of samples 1-3 in experiment U50Zr1 showing sodium contamination and varying U-Zr compositions.

There was some difficulty in analyzing the *volatilized* portions of the samples within this experiment, however. It was observed that the oxide formation process, which utilizes aqueous sodium hydroxide, resulted in a *volatilized* portion which was heavily contaminated with sodium which came from the sodium hydroxide precipitation

process as described in Section 3.2.3.2. This can be seen in Figure 27 which shows the EDS spectrum from the *volatilized* portions of samples 1-3. The sodium contamination is most dramatically seen in sample 1, but was also seen in samples 2 and 3. Greater care was taken to eliminate the effect of sodium contamination in future experiments.

The increasing presence of uranium in the *volatilized* portion of sample 3 can also be seen in Figure 27. This result is expected because nearly 100% of the zirconium is volatilized immediately from the sample, resulting in nearly pure uranium chloride being left behind. The longer the remaining uranium chloride is heated, the more it will move to the volatilized zone simply. In other words, the uranium does transport but at a slower rate to that of zirconium. Therefore, the principal observations from this experiment were the discovery that it is difficult to produce a homogeneous product and that careful kinetic information will be required to optimize the separations. This is important if a reliable measurement of uranium and zirconium content is to be obtained.

Table 5 illustrates this by tabulating the difference in composition between the "bright" and "grey" regions of the *volatilized* portions of samples 2 and 3. Greater care was taken in future experiments to produce a homogeneous product. This was done by grinding the material in a mortar and pestle before being mounted for EPMA analysis. In spite of the dramatic difference in composition between the "bright" and "grey" regions shown in Figure 28, it is believed that the grey regions provide a close approximation to the actual uranium and zirconium content.

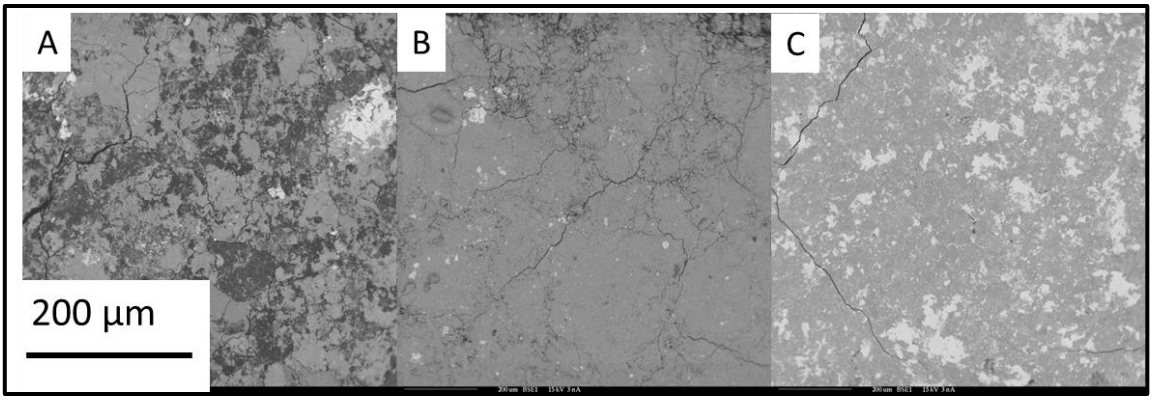

Figure 28: BSE images of volatilized portions of U50Zr1 samples 1(A), 2(B), and 3(C) showing sodium contamination (dark regions), heterogeneity, and increased uranium content (bright regions) in sample 3.

4.3.2.2 U50Zr2

The key feature of this second experiment in the series is that the process temperature was lower than 331 °C, the volatilization temperature of zirconium tetrachloride. In spite of this, it was found that chlorination was able to remove greater than 98% of the zirconium from the uranium-zirconium alloy. These results are tabulated in Table 6. It should be noted that only the *non-volatilized* portions were studied for experiment two through experiment five of this series.

Table 6: Summary of separation effectiveness from U50Zr2 experiment.

Experiment	U50Zr2	U50Zr2	U50Zr2	U50Zr2
Sample	1	2	3	4
Initial Mass (g)	0.2180	0.2467	0.2810	0.2303
Final Mass (g)	0.1934	0.0951	0.1112	0.0577
Time (Min)	15	30	60	120
Temperature (°C)	300	302	312	306
Percent Zr	43.6	1.4	1.6	0.2
Percent U	56.4	98.6	98.4	99.8
Percent Zr (Bright)	2.2	0.9	NA	NA
Percent U (Bright)	97.8	99.1	NA	NA

Sample 1 was found to be very heterogeneous as seen in Figure 29, so both the dark and light regions were analyzed using EPMA and were seen to be composed of very different ratios of uranium and zirconium. This inhomogeneity is likely caused by insufficient mixing of the powdered product, and results in a product which is nearly impossible to accurately characterize. Figure 29 also shows samples 2-4 and the corresponding homogeneity of the product. This is the desired physical appearance of all samples to be analyzed, and this level of uniformity was achieved for the majority of future samples throughout this project. It was found that the heterogeneity seen in sample 1 can be eliminated by thoroughly mixing the products using a mortar and pestle. (Later samples contained small areas of heterogeneity, but the impact on accurate results was negligible.)

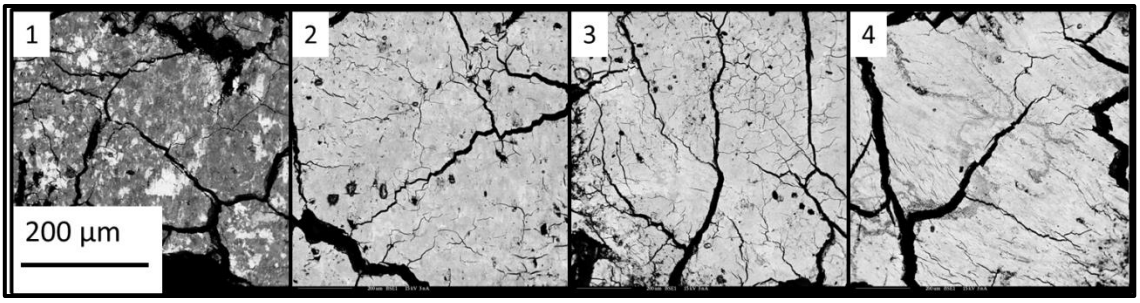

Figure 29: Backscattered electron images of samples 1-4 from the U50Zr2 experiment showing variation in sample homogeneity.

The composition of the sample and homogeneity of the uranium and zirconium can be determined in a rather straightforward manner using EDS. Inspection of Sample 1 in Figure 29 shows clear differences in composition. However, visual inspection of the BSE image is not sufficient to determine if the sample is heterogeneous with respect to uranium and zirconium, only that it is heterogeneous with respect to something. It is possible to use EDS to quickly determine the homogeneity of various regions with respect to uranium and zirconium, as seen in Figure 30. The "bright" and "dark" regions of sample 1 were also analyzed using WDS which, as tabulated in Table 6. It can be seen in Figure 30 that the differences in contrast seen in samples 2-4 are likely not due to actual composition differences between the uranium and zirconium. This is further supported by WDS analysis of the "bright" regions in sample 2 as shown in Table 6, and one can conclude that the contrast differences are unrelated to uranium and zirconium composition. For example, the contrast difference in sample 3 is due to slight variations in sodium composition as seen in Figure 30.

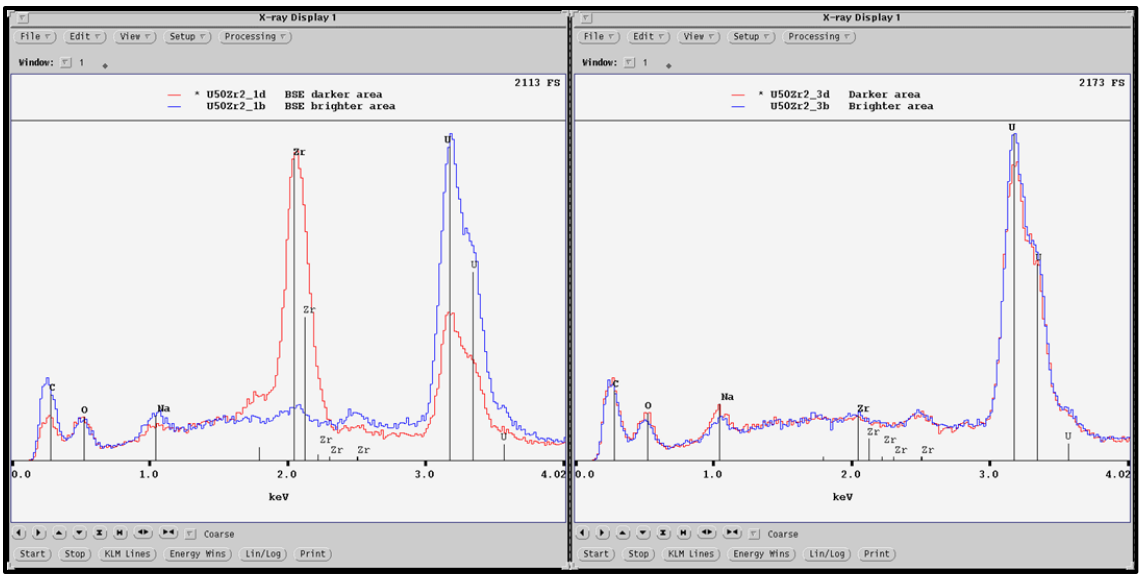

Figure 30: EDS data showing difference in homogeneity between samples 1 and 3 in experiment U50Zr2.

The results obtained in this experiment revealed that obtaining a homogeneous product for analysis is relatively straightforward and that techniques are available to demonstrate the consistent production of homogeneous products. Producing a homogeneous product for composition analysis became routine and will not be discussed further unless it is directly relevant to the results. It was also shown that zirconium can be selectively removed from uranium-zirconium alloys at temperatures below the volatilization temperature of zirconium tetrachloride.

4.3.2.3 U50Zr3 Results

Experiment U50Zr3 was a failed experiment but it will be discussed for the sake of completeness and to illustrate some of the difficulties encountered during the operating the chlorination system. This was the first 4-sample experiment using the setup in Figure 8. Experiments U50Zr1 and U50Zr2 were conducted with sample pairs

while awaiting parts to complete the four-reaction-vessel system. As mentioned above, these systems were operated such that each reaction vessel can be isolated from the rest of the system using a system of valves. All samples were exposed to chlorine simultaneously and the reaction vessels were then isolated from the system at the appropriate time, resulting in a time study of the chloride reaction.

This experiment was abandoned because when it came time to isolate the 15 minute sample, it was noticed that the 120 minute sample was already isolated, and therefore, had never been exposed to chlorine. This means that this 120 minute sample was potentially picking up contaminates from air for 15 minutes while it was not being chlorinated. The 120 minute sample was then opened to the system, thereby introducing chlorine to the 120 minute sample. It was soon decided that this was a mistake because the 120 minute reaction vessel may or may not have contained air contamination which would influence the results obtained for the 30 and 60 minute samples. The entire experiment was therefore shut down and discarded as inconclusive.

4.3.2.4 U50Zr4 Results

Experiment U50Zr2 demonstrated the separation of uranium and zirconium at temperatures below the volatilization temperature of zirconium tetrachloride. Experiment 4 demonstrated separation at a temperature slightly above the volatilization temperature of zirconium tetrachloride. The data shown in Table 7 show that this separation occurs very quickly and results in the effective removal of zirconium (i.e., >96%) from the material in less than 15 minutes. It is worth repeating that the material analyzed to characterize this result is the *non-volatilized* material that was converted to

chloride but remained within the heated zone of the reaction vessel. Experiments were conducted in the U50ZrFinal series which analyzed the *volatilized* material that left the heated zone, and will be discussed in Section 4.5.

Table 7: Summary of separation effectiveness from U50Zr4 experiment.

Experiment	U50Zr4	U50Zr4	U50Zr4	U50Zr4
Sample	1	2	3	4
Initial Mass (g)	0.2769	0.2291	0.3152	0.2975
Final Mass (g)	0.0825	0.0578	0.0651	0.0505
Time (Min)	15	30	60	120
Temperature (°C)	340	340	340	340
Percent Zr	3.9	0.3	0.1	0.2
Percent U	96.1	99.7	99.9	99.8

4.3.2.5 U50Zr5 Results

Experiment U50Zr5 further demonstrated the ability of this process to separate virtually all of the zirconium from a uranium-zirconium alloy in a short amount of time as summarized in Table 8. The experiment was performed to further study the validity of using WDS as an analytical technique for this project. It was again found that WDS produces reliable results as long as proper sample preparation and analytical techniques are used.

Table 8: Summary of separation effectiveness from U50Zr5 experiment.

Experiment	U50Zr5	U50Zr5	U50Zr5	U50Zr5
Sample	1	2	3	4
Initial Mass (g)	0.2833	0.2798	0.3172	0.4087
Final Mass (g)	0.0000	0.0000	0.0000	0.0000
Time (Min)	15	30	60	120
Temperature (°C)	360	359	362	360
Percent Zr	8.4	7.5	0.1	0.1
Percent U	91.6	92.5	99.9	99.9
Percent Zr (Bright)	1.0	2.1	NA	0.1
Percent U (Bright)	99.0	97.9	NA	99.9

It was noted previously that uncertainties complicate the data analysis when analyzing a heterogeneous product due to the phase composition variations (Figure 28 and Figure 29). While large composition differences were not seen in this experiment, there existed were subtle differences in composition across the sample surfaces observed using BSE imaging. These slight differences in composition are evident in Figure 31 as varying shades of grey.

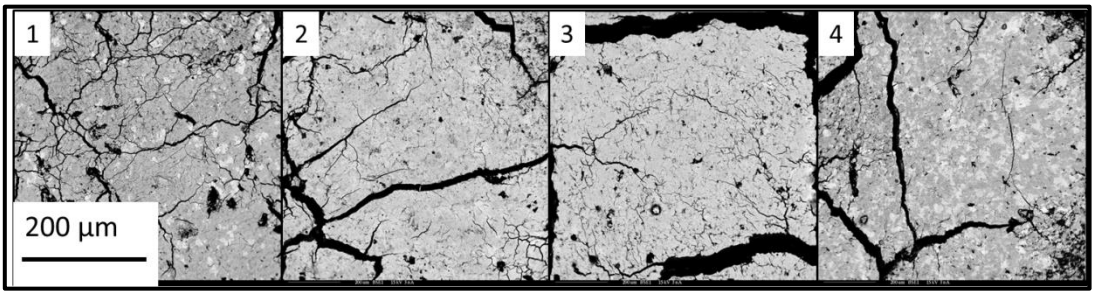

Figure 31: Backscattered electron images of samples 1-4 from the U50Zr5 experiment.

Sample 1 (Figure 31) contains a light phase as well as a darker grey phase. Before further analysis was performed comparing these two phases, it was important to verify that these phases are consistent within a single sample. Figure 32 shows EDS spectra between two random light phase regions, two random dark phase regions, and a comparison between the light and dark regions. It can be seen that the light and dark phases are indeed consistent when examined independent of one another, but differ between each other. This difference was shown to be significant using WDS analysis and is tabulated in Table 8.

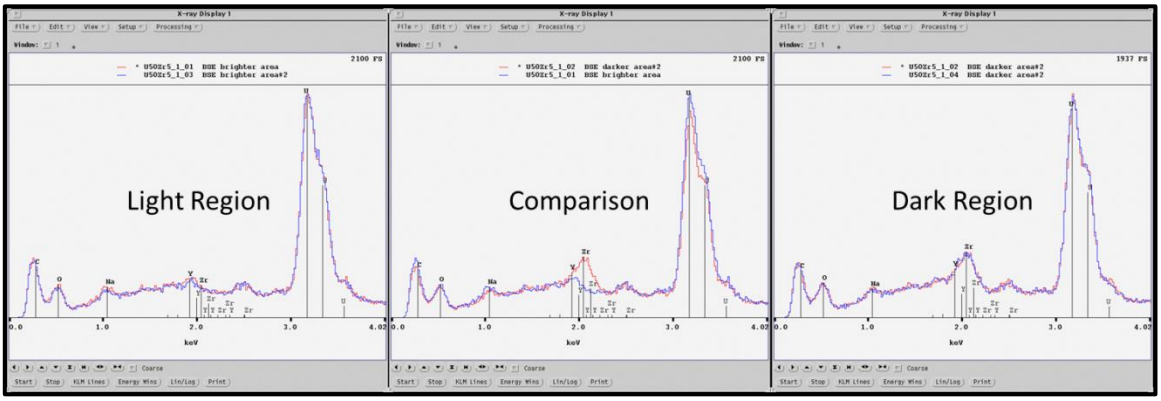

Figure 32: Energy dispersive spectra of sample 1 in experiment U50Zr5 shown in Figure 31. Light phase region (Left). Dark phase region (Right). Light/dark comparison (Center).

Sample 2 can be seen to contain a light area, a grey area, and also a minority darker grey area. The darker grey area was seen to be slightly enriched in zirconium, while the two grey phases were seen to be virtually identical in composition. This can be seen in the EDS spectra shown in Figure 33.

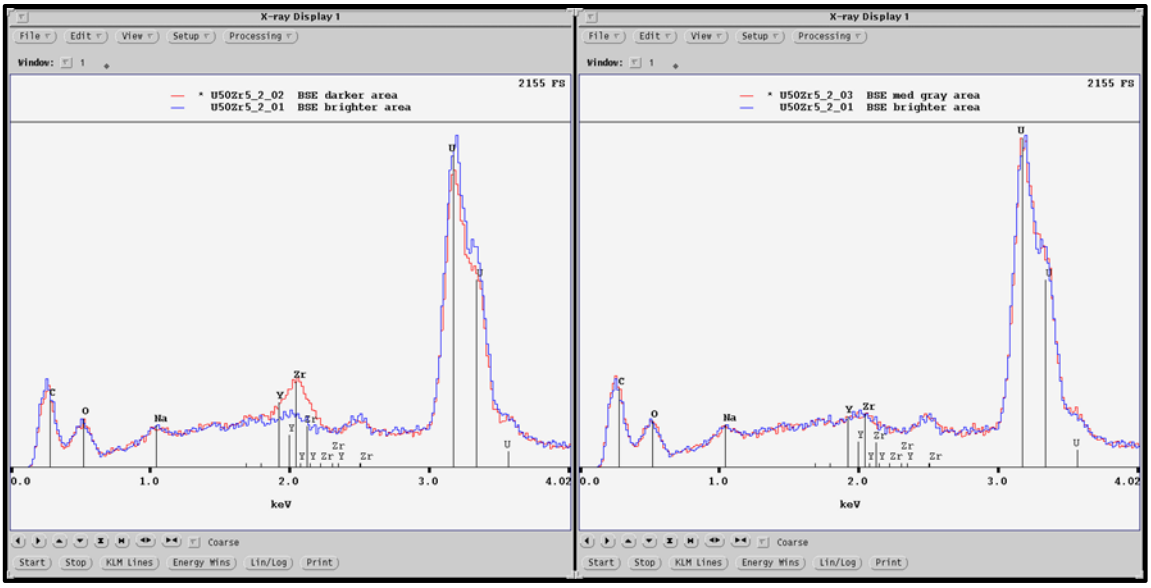

Figure 33: Energy dispersive spectra of sample 2 in experiment U50Zr5.

The pressed product from U50Zr5-3 was clearly observed to be homogeneous. The pressed product from U50Zr5-4, however, appeared heterogeneous with BSE imaging. Backscattered electron observation suggests a product which is heterogeneous in uranium and zirconium; however this is not the case. Upon EDS analysis it was seen that the bright regions were bright only because the rest of the material contained elevated levels of yttrium. This can be seen in Figure 34.

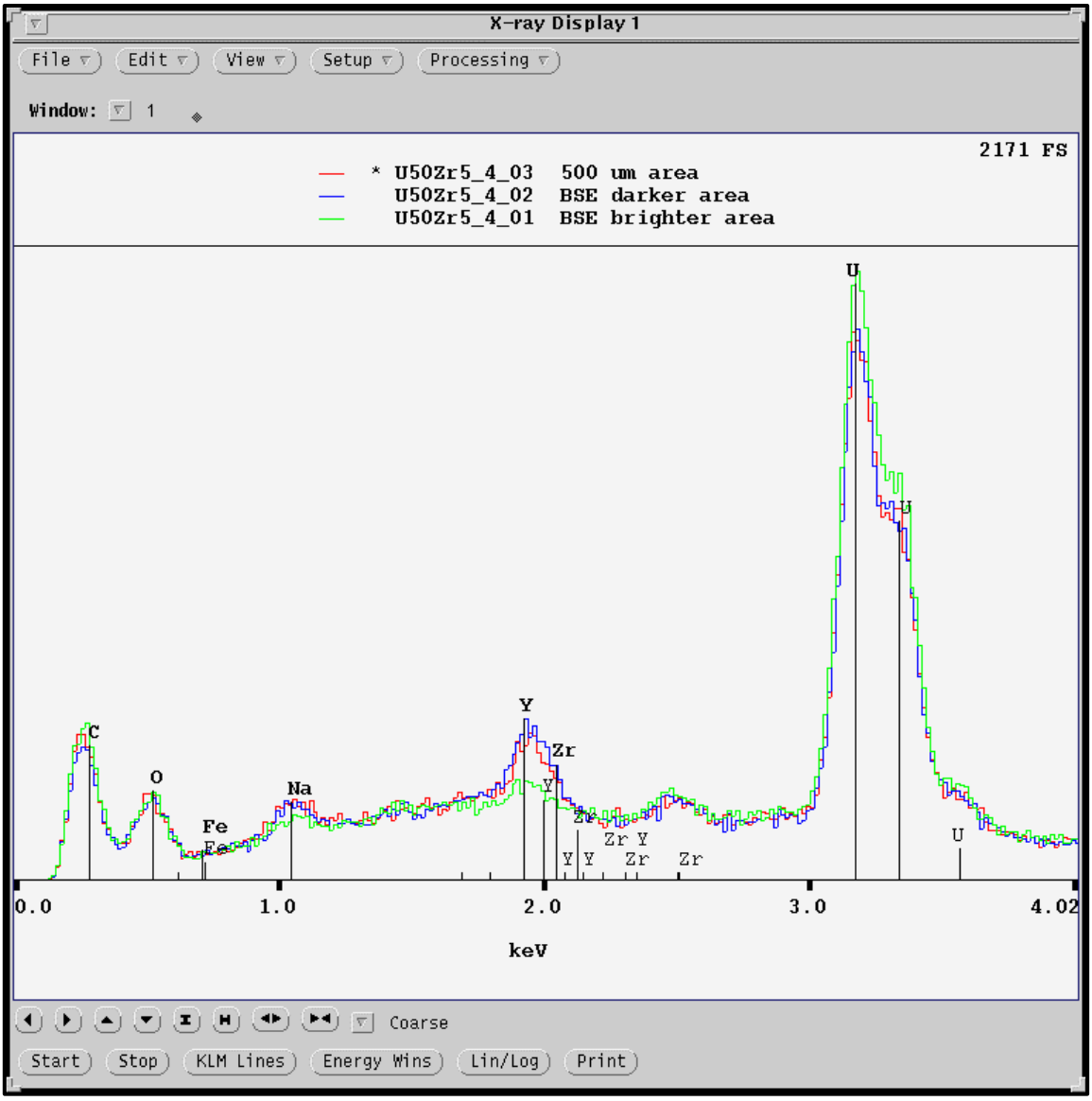

Figure 34: Electron dispersive spectra of sample 4 in experiment U50Zr5.

The yttrium was introduced into the material from the yttrium oxide crucible used to cast the original alloy slug. Its presence can be seen in the X-ray map image of Slice 1 shown as Figure 35. Yttrium was not a concern prior to this experiment, and

does not affect any previous results. This is because the WDS peak of yttrium does not interfere with either the uranium or zirconium peak.

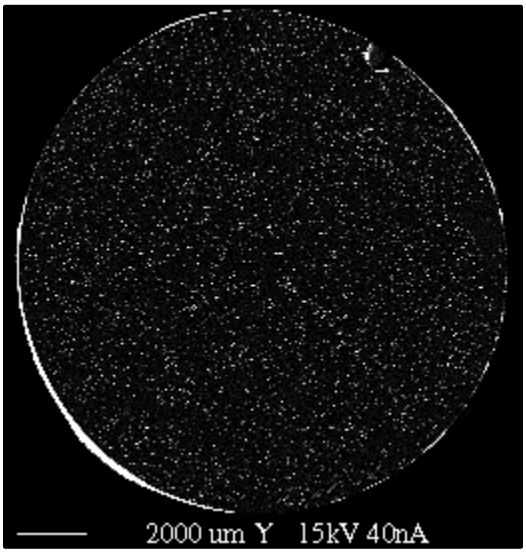

Figure 35: X-ray map of Slice 1 showing presence of yttrium oxide rind.

Even though the heterogeneity of the samples in this experiment was slight, it was present. Therefore a line-scan method was used which produces results representative of the material being examined. A line-scan adds the information gathered over several data points which all lay along a single line. This effectively "smears" any slight heterogeneity which may be present within a sample.

A technique used to determine whether or not a line-scan can be used to produce representative results is to perform an EDS analysis on each region of interest followed by an EDS analysis of a larger representative region that contains all phases in representative area fractions. This technique can be explained using Figure 34 as an

example where it is seen that the bright regions are not likely to contribute much to the bulk analysis of the sample. These comparatively bright regions are in the small minority and are easily avoided with a line-scan of the product, which results in an accurate analysis of the bulk material.

4.3.2.6 U50Zr6 and U50Zr7 Results

These two experiments were single reaction vessel tests performed to determine the temperature at which volatilization would begin in a U-50Zr alloy. This was accomplished by introducing chlorine to a single sample at a temperature where volatilization was not expected. The vessels were then slowly heated to until volatilized material began to deposit on the unheated portion of the reaction vessel. Experiment U50Zr6 began 250 °C and volatilization was noted at temperature of 278 °C after being exposed to chlorine for 20 minutes. The material was then held at 280 °C for 100 minutes. Experiment U50Zr7 was started at 270 °C and volatilization was noted at 271 °C after being exposed to chlorine for two minutes.

This information is useful for establishing the lower temperature limit for the final separation series described in Section 4.5. The fact that experiment U50Zr6 was exposed to chlorine for 20 minutes before it began to volatilize at 278 °C indicates that experiments performed below this temperature will likely have large systematic errors caused by significant differences in onset of chloride formation. Subsequent U-50Zr alloy exposure experiments were therefore performed at temperatures above 280 °C.

While these two experiments were not intended to be processed for EPMA analysis, a rapid characterization was performed. The products were not carefully

prepared but the EPMA results are worth discussing. The conversion to pressed powder was performed in an expedited manner to quickly confirm the qualitative observations. In retrospect, a full conversion would have been preferred, but these imperfect results are worth reporting.

The *volatilized* material from experiment U50Zr6 was processed and analyzed using the method described in Section 3.2.3. A backscattered electron image of this material can be seen in Figure 36. An unusual feature of this product is the presence of large quantities of silicon observed as large darker patches in the image. It is likely that this silicon originates from the glass test-tube used to contain this material in-between its volatilization and eventual analysis. The material was stored in a concentrated sodium hydroxide solution for two weeks. It is possible that the solution leached silicon from the glass test-tube, and this silicon remained in the product as it was washed and dried. The silicon is in the dark regions of Figure 36 were examined using EDS and the resulting spectra is shown in Figure 37. The bright regions in Figure 36 are uranium-rich.

Even though the products of this experiment were not processed carefully, the final uranium-zirconium ratio was very close to that observed in the sixth experiment in the U50ZrFinal series which had similar experimental conditions. The products for the current experiment were found to have a uranium-zirconium ratio of 25.8% uranium to 74.2% zirconium. The products for the sixth experiment in the U50ZrFinal series were found to have a uranium-zirconium ratio of 26.3% uranium to 73.7% zirconium. This

seems to imply that even with large quantities of impurities the uranium-zirconium ratio may be correctly obtained.

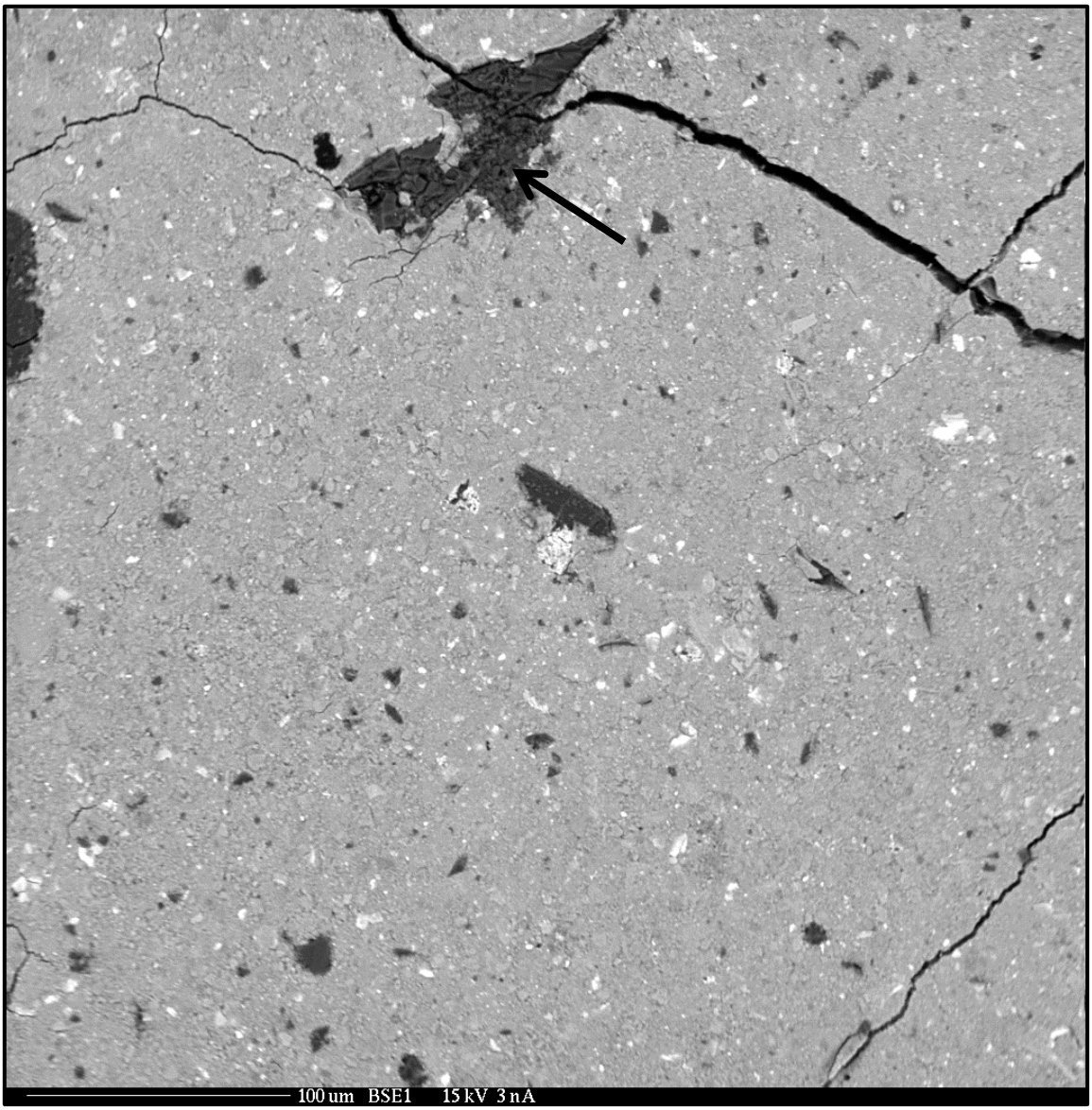

Figure 36: Backscattered electron image of volatilized material from experiment U50Zr6.

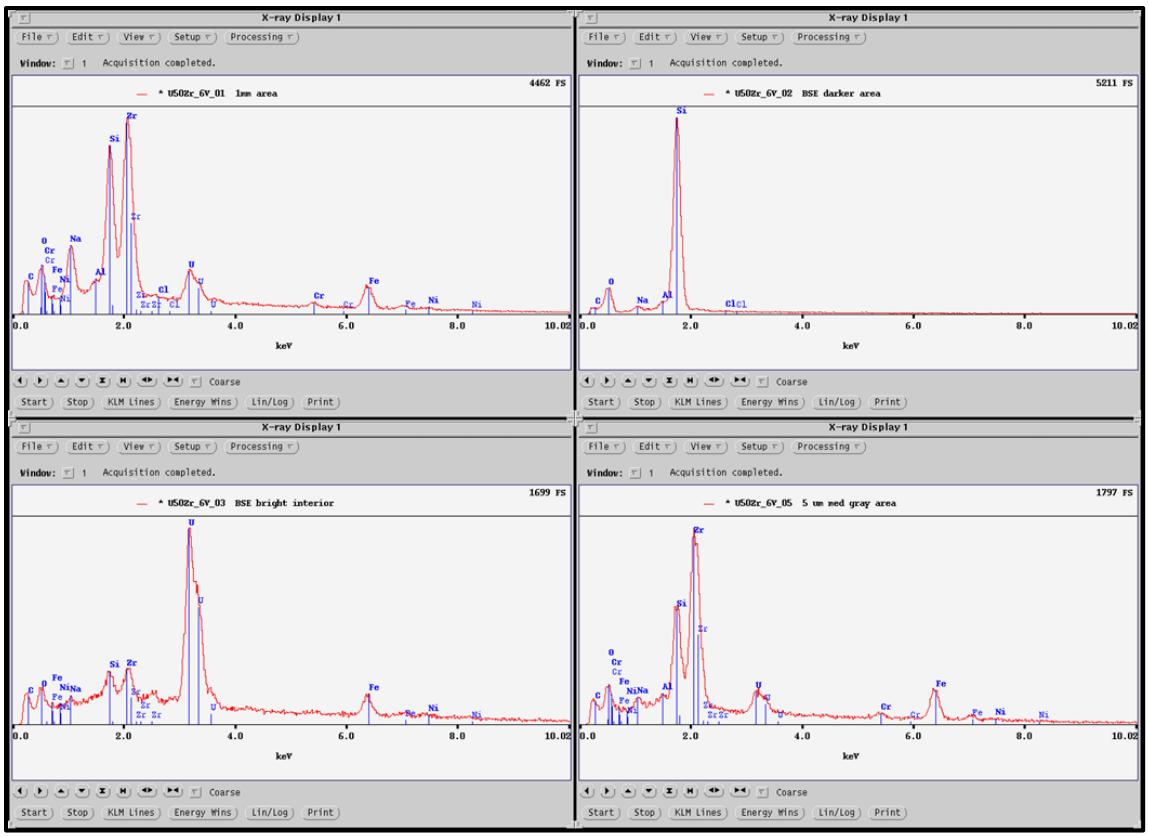

Figure 37: Energy dispersive spectra of volatilized material from experiment U50Zr6.

Both the *volatilized* and *non-volatilized* portions were analyzed from U50Zr7. While this material was not stored in a sodium hydroxide solution as was U50Zr6, it was not washed as thoroughly as the analytical samples noted in previous and subsequent tests. This resulted in a product which was heavily contaminated in sodium. This can be seen as the black phase in Figure 38, which is verified to be sodium-rich in Figure 39. In spite of this heavy sodium contamination, the relative uranium and zirconium concentrations for this *non-volatilized* material were seen to be 96.5% uranium and 3.5% zirconium. This result is consistent with similar experiments.

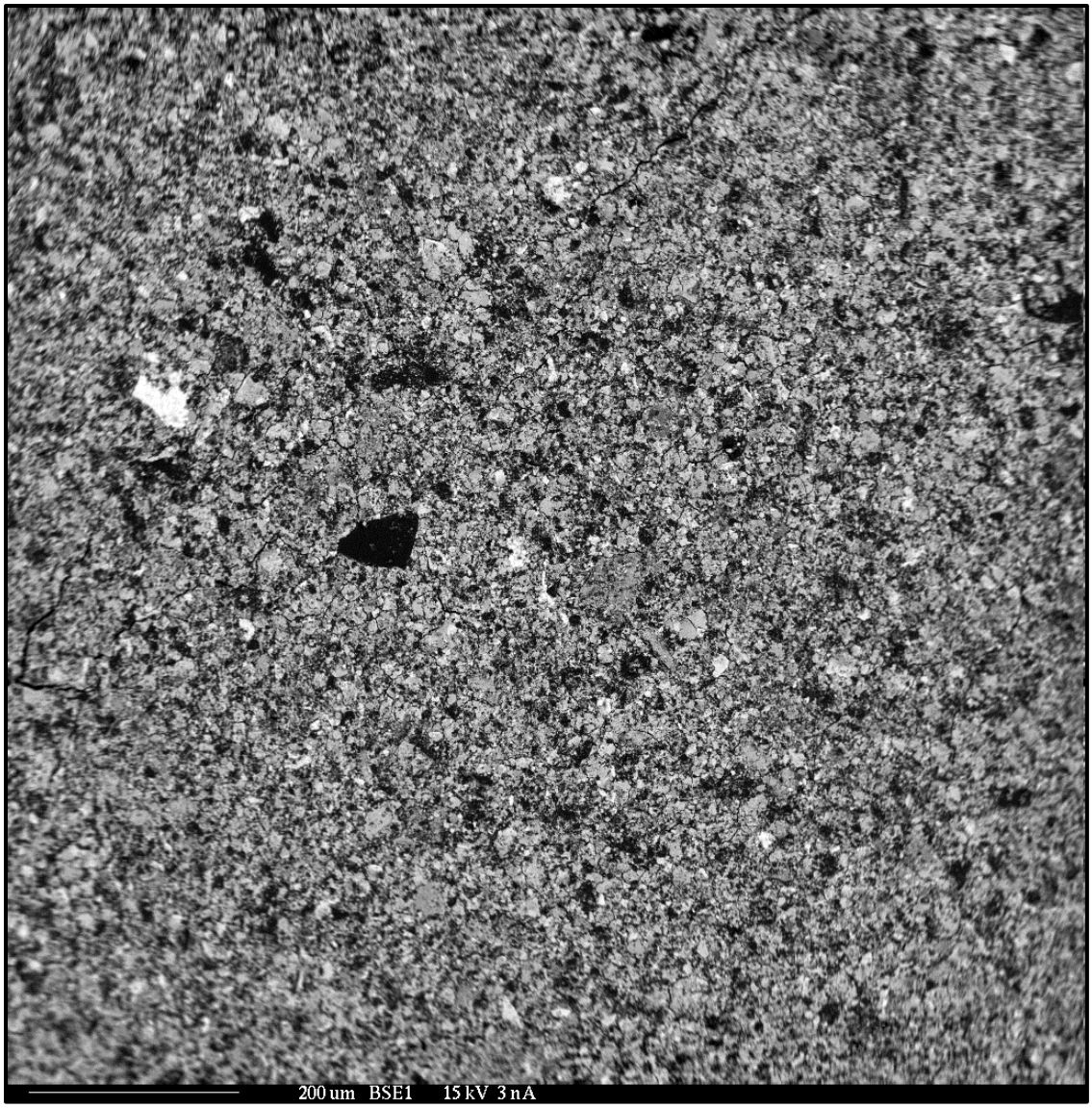

Figure 38: Backscattered electron image of *non-volatilized* material from experiment U50Zr7.

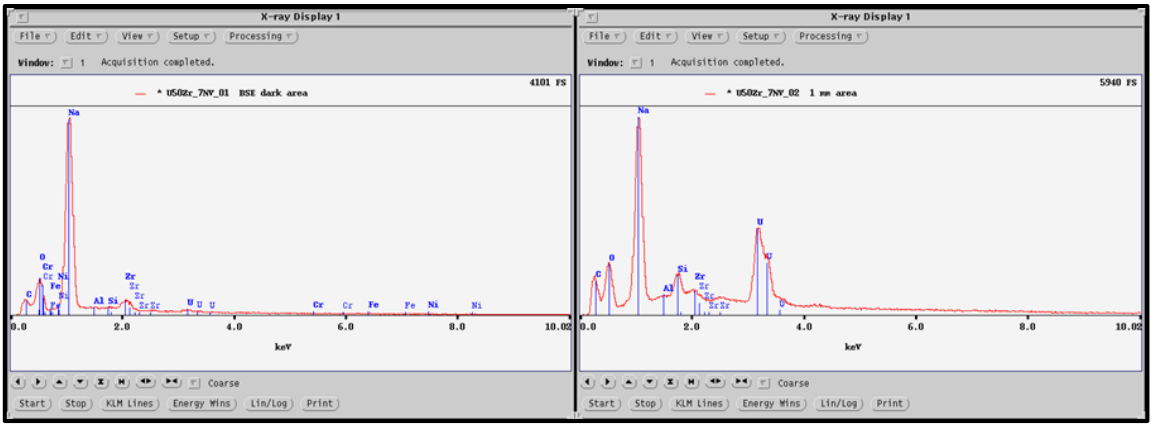

Figure 39: Energy dispersive spectra of *non-volatilized* material from experiment U50Zr7.

The processed product from the *volatilized* portion of U50Zr7 also shows heavy sodium contamination. This can be seen in Figure 40 as dark patches and was confirmed as containing large amounts of sodium via EDS analysis as shown in Figure 41. Wavelength dispersive x-ray spectroscopy analysis of these dark areas show a relative sodium and oxygen mass percentage of 73.7% sodium and 26.3% oxygen. This corresponds to sodium oxide which has a relative sodium and oxygen mass percentage of 74.2% sodium and 25.8% oxygen. This result indicated that the sodium can easily be removed from the product through washing with water. All subsequent products were thoroughly washed in order to convert the sodium oxide to sodium hydroxide and the dissolved sodium hydroxide was then decanted away. Therefore, sodium contamination was not present in the later experiments.

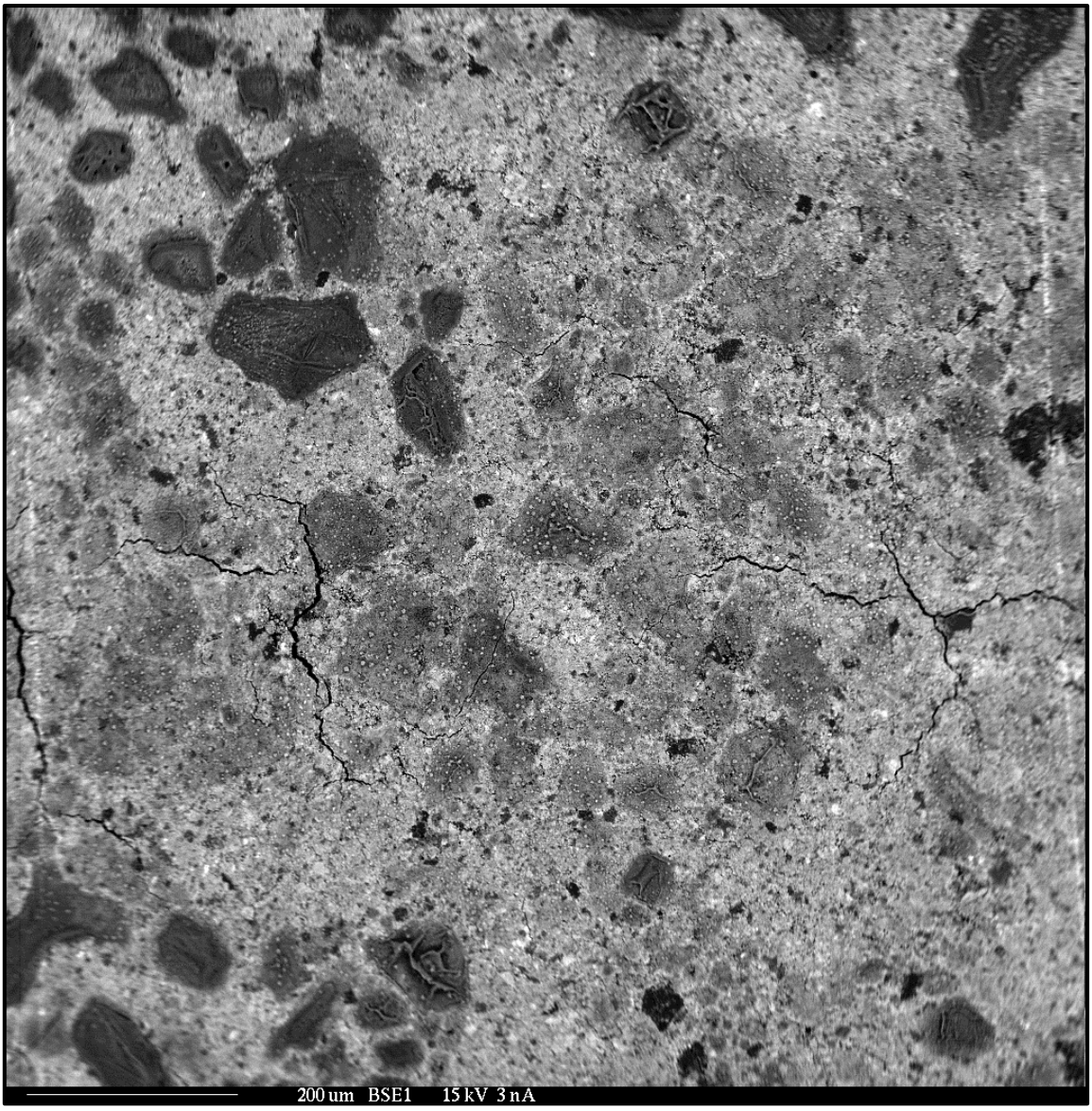

Figure 40: Backscattered electron image of *volatilized* material from experiment U50Zr7.

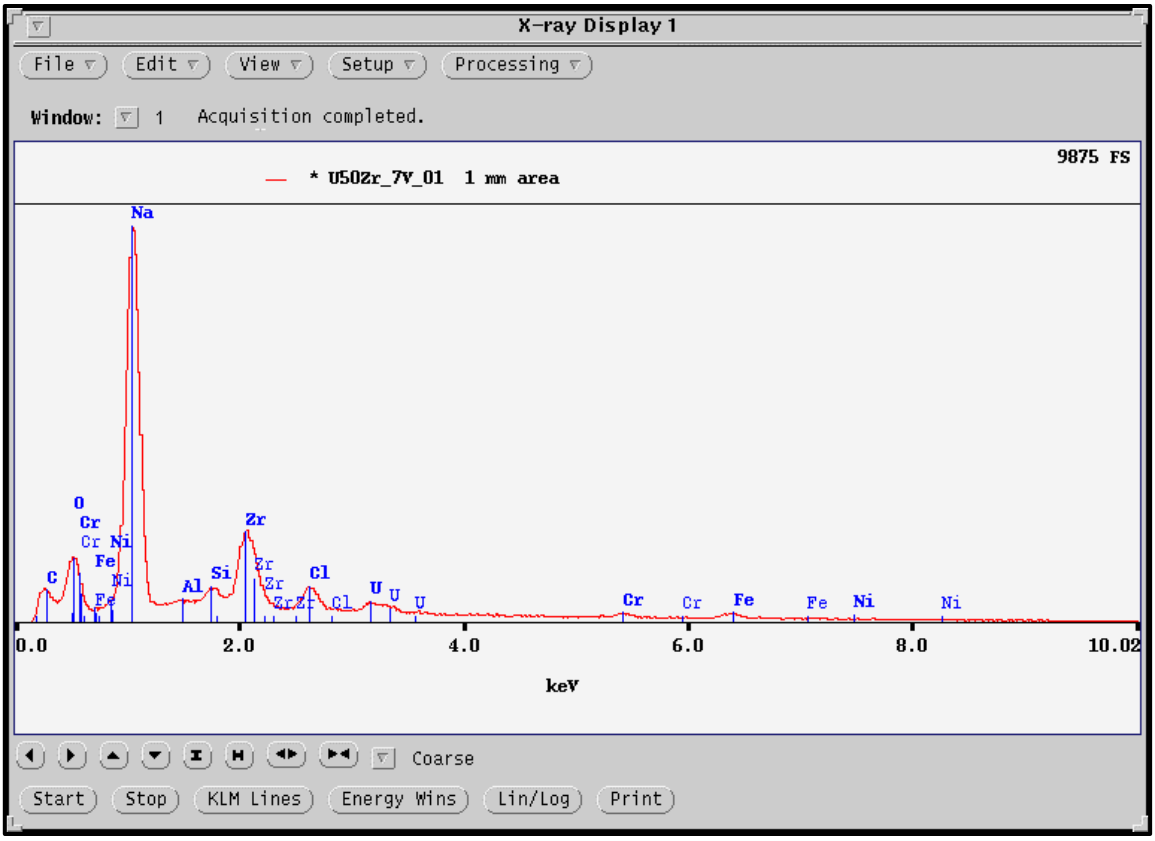

Figure 41: Energy dispersive spectrum of *volatilized* material from experiment U50Zr7.

4.3.2.7 U50Zr Conclusion

The U50Zr experiment series generated insight into the selective volatilization process. It was observed that zirconium is easily removed from U-50Zr alloys, and that this removal occurs rapidly after the chloride is formed. This was even true at relatively low temperatures. This indicates that any temperature above approximately 280 °C is sufficient to remove zirconium. This series did not study the volatility of uranium chloride. This will become important if chlorination is considered for an application

where a pure zirconium product or complete uranium recovery is required. (Uranium transport is addressed as part of the U50ZrFinal series.)

Further, a rough understanding of the times required for separation can be achieved using the data obtained during this series. Figure 42 shows the relative zirconium concentration for *non-volatilized* portions of experiments 1, 3, 4, and 5 in the U50Zr Series plotted as a function of time. This information was used to design the next experimental series.

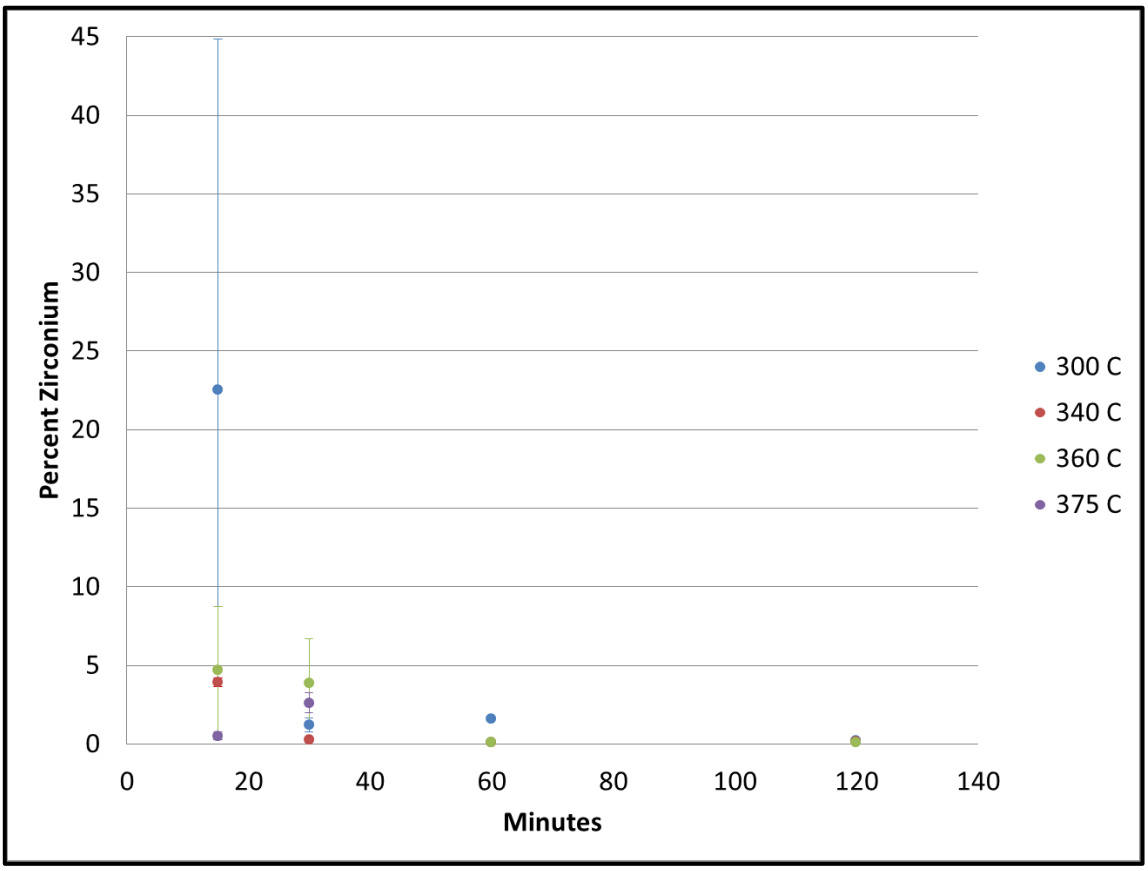

Figure 42: Summary of zirconium volatilization from U-50Zr alloys showing the relative percent of zirconium remaining in non-volatilized products.

4.4 Series Zr

After the U50Zr series (Section 4.3), it was determined that further Zr volatilization data was needed to determine parameters needed for the final separation measurements described in Section 4.5. The first experiments of the Zr series (Zr-1 to Zr-8) were conducted using irregularly shaped pieces of crystal-bar zirconium to study the time and temperature dependence of the volatilization of pure Zr. It was discovered that the reaction rate was highly dependent on surface area, indicating that the irregular shapes were poor starting materials. Therefore, a more careful surface area study was performed in experiment Zr-9 to Zr-20. Finally, an experiment was conducted to determine the onset temperature of volatilization for various zirconium alloys and shapes.

4.4.1 Rate Study (Zr1 to Zr8)

A rate study was performed at temperatures ranging from 300 °C to 400 °C in increments of 20 °C as a probe of the zirconium volatilization process. The results shown in Table 9 were largely inconclusive, other than to say that chloride formation increased as a function of time for all temperatures studied, as seen in Figure 43. This result is trivial. It was determined that the inconclusive results were obtained because of the large unquantifiable irregular sample surface areas noted above. This hypothesis was confirmed by sample Zr7-4, which had a much larger, yet unquantified surface area when compared to the other samples. It was noted that the amount of material volatilized in this sample was higher than that of the rest of the samples in this sequence of experiments.

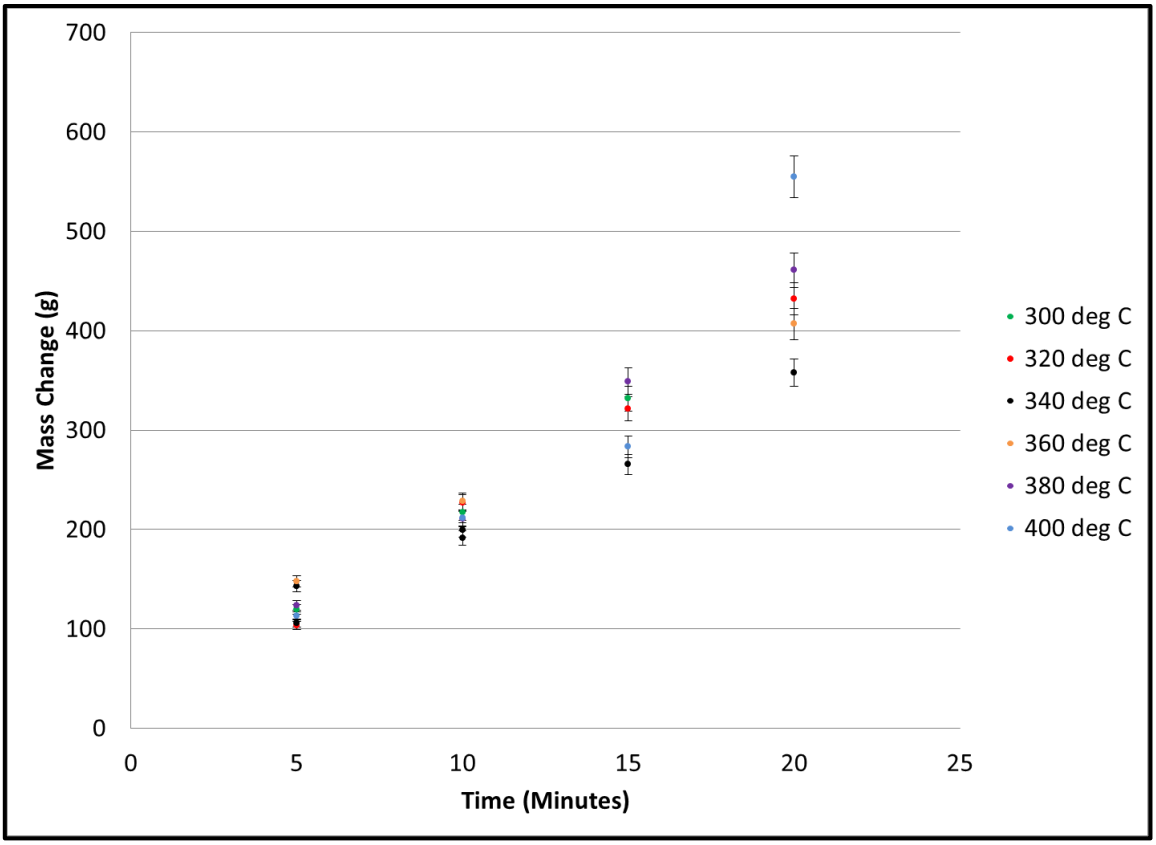

Figure 43: Results from probing experiments showing inconclusive rate study plotted as a function of time.

Table 9: Summary of data from rate study.

Name	m_I (g)	m_F (g)	T °C	P	Time (min)
Zr1-1	0.3325	0.1850	361	6 psi	5
Zr1-2	0.3930	0.1647	360		10
Zr1-3	0.4378	0.0311	358		20
Zr1-4	0.3647	0	360		40
Zr2-1	0.3610	0.2182	339	6 psi	5
Zr2-2	0.2826	0.0831	338		10
Zr2-3	0.3175	0	339		20
Zr2-4	0.3342	0	339		40
Zr3-1	0.2548	0.1491	341	6 psi	5
Zr3-2	0.2803	0.0890	341		10
Zr3-3	0.3750	0.1094	340		15
Zr3-4	0.3984	0.0404	340		20
Zr4-1	0.2760	0.1724	320	6 psi	5
Zr4-2	0.3751	0.1483	318		10
Zr4-3	0.4739	0.1522	318		15
Zr4-4	0.4904	0.0582	319		20
Zr5-1	0.3124	0.1928	301	6 psi	5
Zr5-2	0.3255	0.1084	299		10
Zr5-3	0.3658	0.0342	299		15
Zr5-4	0.3916	0.0068	299		20
Zr6-1	0.4399	0.3161	380	6 psi	5
Zr6-2	0.6127	0.4017	379		10
Zr6-3	0.7807	0.4315	379		15
Zr6-4	0.7959	0.3349	380		20
Zr7-1	0.221	0.1080	401	6 psi	5
Zr7-2	0.2995	0.0878	401		10
Zr7-3	0.4022	0.1190	400		15
Zr7-4	0.8467	0.2920	400		20
Zr8-1	10.226	9.1435	300	6 psi	10
Zr8-2	9.9431	8.8959	300		10
Zr8-3	10.060	9.0491	300		10
Zr8-4	10.537	9.4340	300		10

The inconclusive results of Figure 43 can be shown more clearly in Figure 44, which shows the slope, or rate of chloride formation as a function of temperature. It should be noted that sample Zr7-4 was removed from data presented in Figure 44, due to its uncharacteristically large surface area.

In spite of these inconclusive results, several insights were gathered from this sequence of experiments. First, the chloride formation rate is highly dependent on surface area. Second, the reaction proceeds to completion before 40 minutes have elapsed for the sample sizes of interest. This was noted in Zr-1 and Zr-2 where the entire "40-minute" sample was consumed prior to being allowed to react for the entire 40 minutes. The time-steps studied for these first two experiments were 5, 10, 20 and 40 minutes. In response, the remaining five experiments in this sequence were reacted with time-steps of 5, 10, 15, and 20 minutes.

Experiment Zr8 was conducted to quantify the error inherent in the system. For this experiment larger pieces of crystal-bar zirconium were allowed to react with chlorine gas. These four samples were sectioned from a single piece of crystal-bar zirconium so that their lengths, and therefore their surface areas, were as similar as possible. All four samples were exposed to chlorine for 10 minutes at 300 °C. The results can be seen in Figure 45. It can be seen that the error in mass change is 3.8%, with a variation in surface area measurement of 2.5%. This indicates that as long as the surface area is precisely known; accurate, repeatable results may be obtained for studying the effect of surface area on chloride formation. It should be noted that the samples used in Zr8 were large sections of crystal-bar zirconium. This is important

because there is an inherent variability in measuring the diameter of these samples simply due to the roughness of the samples. This further supports the hypothesis that accurately measured samples can be used to produce data which accurately measures the chloride formation in crystal-bar zirconium. This is because, even with such a large variation in sample surface areas, the systematic error was only 3.8%. It then follows that if samples were to be created with precisely controlled surface areas, then the error in mass change will certainly be less than 3.8%.

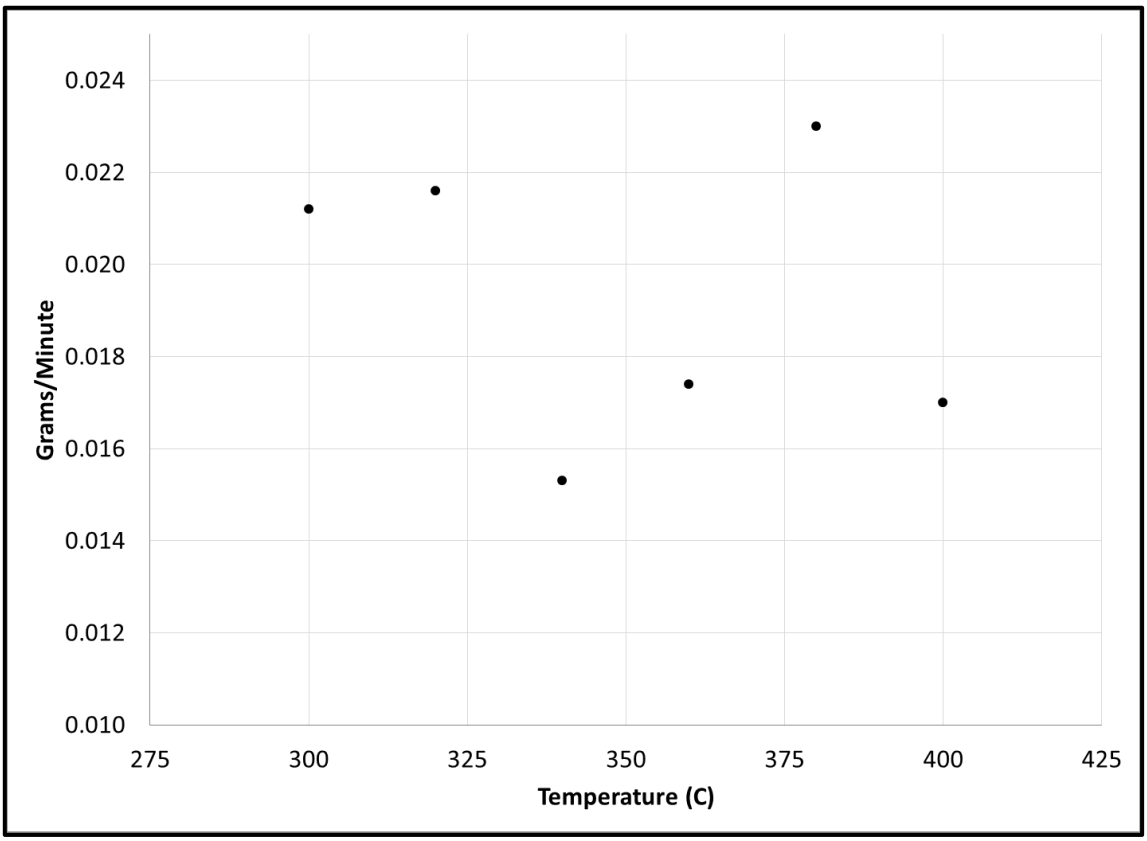

Figure 44: Chloride formation rate from probing experiments.

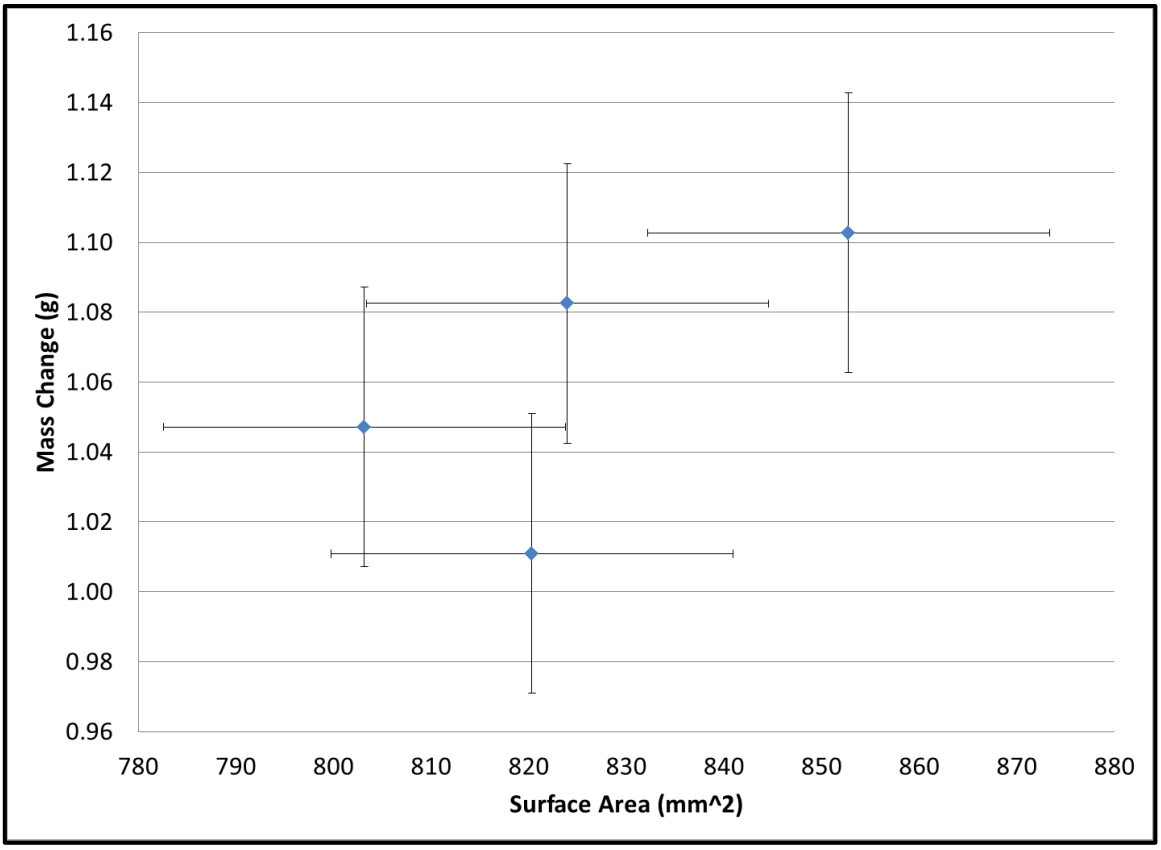

Figure 45: Mass change data from Zr8 showing reproducibility of chloride formation for samples with a similar surface area.

4.4.2 Surface Area Study (Zr9 to Zr20)

The set of experiments was designed to quantify the effect of surface area on chloride formation in crystal-bar zirconium, the results of which are shown in Table 10. The samples were created by machining the source rod of crystal-bar zirconium into a cylindrical shape of uniform diameter. Each sample was then sectioned from this cylinder resulting in samples with nearly identical diameters and precisely measured thicknesses. New samples were used for each of the three temperatures studied, but samples were reused within each temperature. The reuse of samples enabled a more

thorough data set to be obtained because their surface areas decrease by chloride formation after each experiment.

Table 10: Summary of data from surface area study.

Name	Surface Area (mm^2)	Mass Change (g)	Time (min)	Rate (mg/min)	T (°C)
Zr9-1	407	0.1754	2	87.7	320
Zr9-2	351	0.1330	2	66.5	320
Zr9-3	294	0.1312	2	65.6	320
Zr9-4	219	0.0958	2	47.9	320
Zr10-1	396	0.1640	2	82.0	320
Zr10-2	343	0.0590	2	29.5	320
Zr10-3	286	0.0897	2	44.9	320
Zr10-4	207	0.0820	2	41.0	320
Zr11-1	378	0.1152	2	57.6	320
Zr11-2	333	0.0825	2	41.3	320
Zr11-3	268	0.0780	2	39.0	320
Zr11-4	197	0.0349	2	17.5	320
Zr12-1	357	0.6519	10	65.2	320
Zr12-2	317	0.5148	10	51.5	320
Zr12-3	252	0.3830	10	38.3	320
Zr12-4	170	0.3090	10	30.9	320
Zr13-1	312	0.5163	10	51.6	320
Zr13-2	281	0.4229	10	42.3	320
Zr13-3	217	0.3335	10	33.4	320
Zr13-4	NA	NA	10	0.1	320
Zr15-1	385	0.6476	10	64.8	400
Zr15-2	330	0.4653	10	46.5	400
Zr15-3	271	0.3956	10	39.6	400
Zr15-4	206	0.3425	10	34.3	400
Zr16-1	353	0.5907	10	59.1	400
Zr16-2	300	0.4085	10	40.9	400
Zr16-3	242	0.3445	10	34.5	400
Zr16-4	163	0.2851	10	28.5	400

Table 10: Continued.

Name	Surface Area (mm^2)	Mass Change (g)	Time (min)	Rate (mg/min)	T (°C)
Zr17-1	313	0.4953	10	49.5	400
Zr17-2	271	0.3309	10	33.1	400
Zr17-3	211	0.2831	10	28.3	400
Zr17-4	734	1.0205	10	102.1	400
Zr18-1	391	0.4478	10	44.8	500
Zr18-2	335	0.3612	10	36.1	500
Zr18-3	274	0.3027	10	30.3	500
Zr18-4	200	0.2786	10	27.9	500
Zr19-1	371	0.5032	10	50.3	500
Zr19-2	317	0.3804	10	38.0	500
Zr19-3	260	0.2815	10	28.2	500
Zr19-4	161	0.2472	10	24.7	500
Zr20-1	360	0.4220	10	42.2	500
Zr20-2	305	0.3433	10	34.3	500
Zr20-3	247	0.2421	10	24.2	500
Zr20-4	695	0.6604	10	66.0	500

Time was also eliminated as a variable in this sequence of experiments. This was accomplished by reacting each sample for a length of time of 10 minutes. The mass of material volatilized was then divided by 10 to give the reaction rate in units of mg/min. However, the first experiments using this technique were conducted for two minutes. This resulted in a data set with a much variance. Upon observation of this variance, the reaction time was increased to 10 minutes, resulting in much less variance. This can be seen in Figure 46. A reaction time of 10 minutes produced data with a much tighter grouping. This difference in variance is believed to be caused by the incubation time, estimated to be on the order of 10 to 20 seconds, between the introduction of chlorine and the start of volatilization. This lag accounts for an inherent systematic error of up to

~17% for experiments with a 2-minute reaction time compared to an error of up to ~3% for experiments with a 10-minute reaction time.

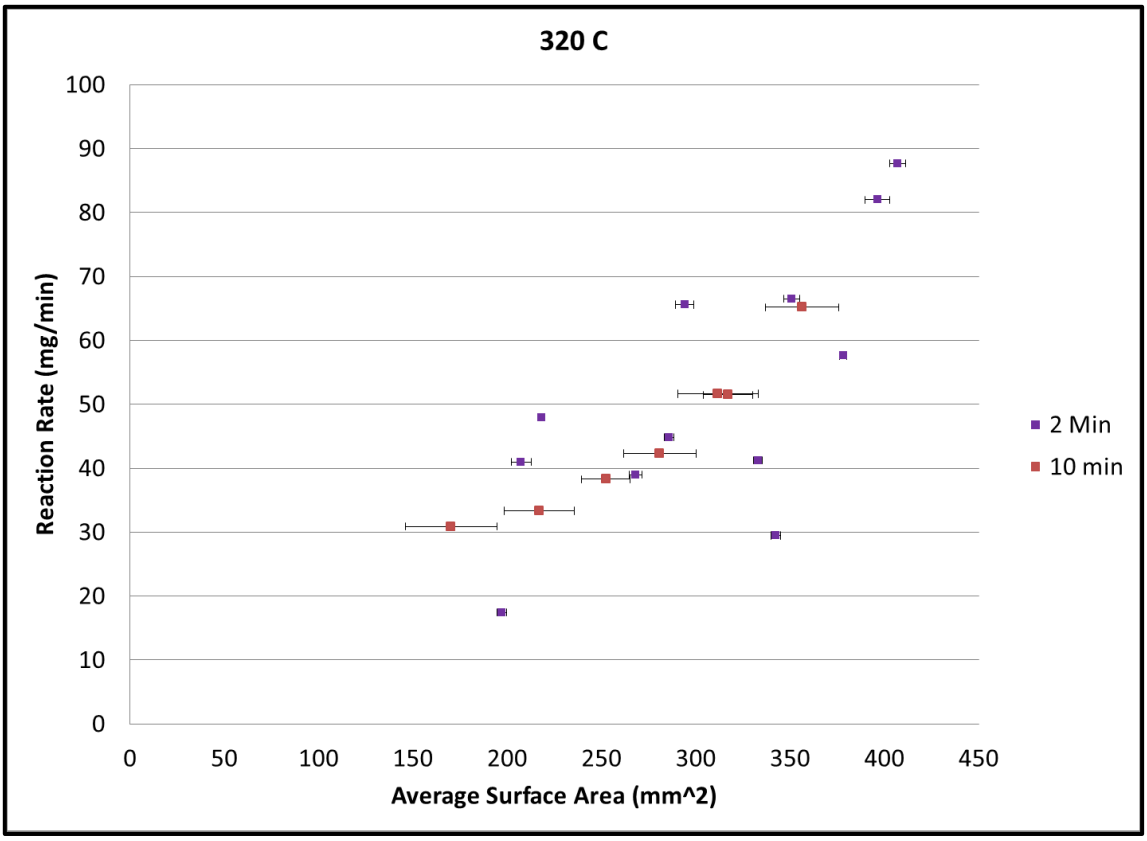

Figure 46: Plot showing relative variance between a 2 minute and 10 minute reaction time.

The reaction rate appeared to accelerate with increasing sample surface area. An increasing reaction rate with surface area is expected, but an accelerating reaction rate deserves some explanation. It is believed that this acceleration is caused by sample heating as the exothermic reaction proceeds. A hotter sample will naturally result in a higher reaction rate, which will result in a hotter sample, etc. This positive feedback was

seen in the nearly instantaneous reactions observed when powder samples were exposed to hot chlorine gas.

The temperature data obtained suggests that the reaction rate of zirconium with chlorine is not dependent on temperature between 320 and 400 °C. However, there seems to be a decrease in reaction rate as the temperature rises to 500 °C. This result is somewhat counterintuitive to what would be expected, and deserves further research.

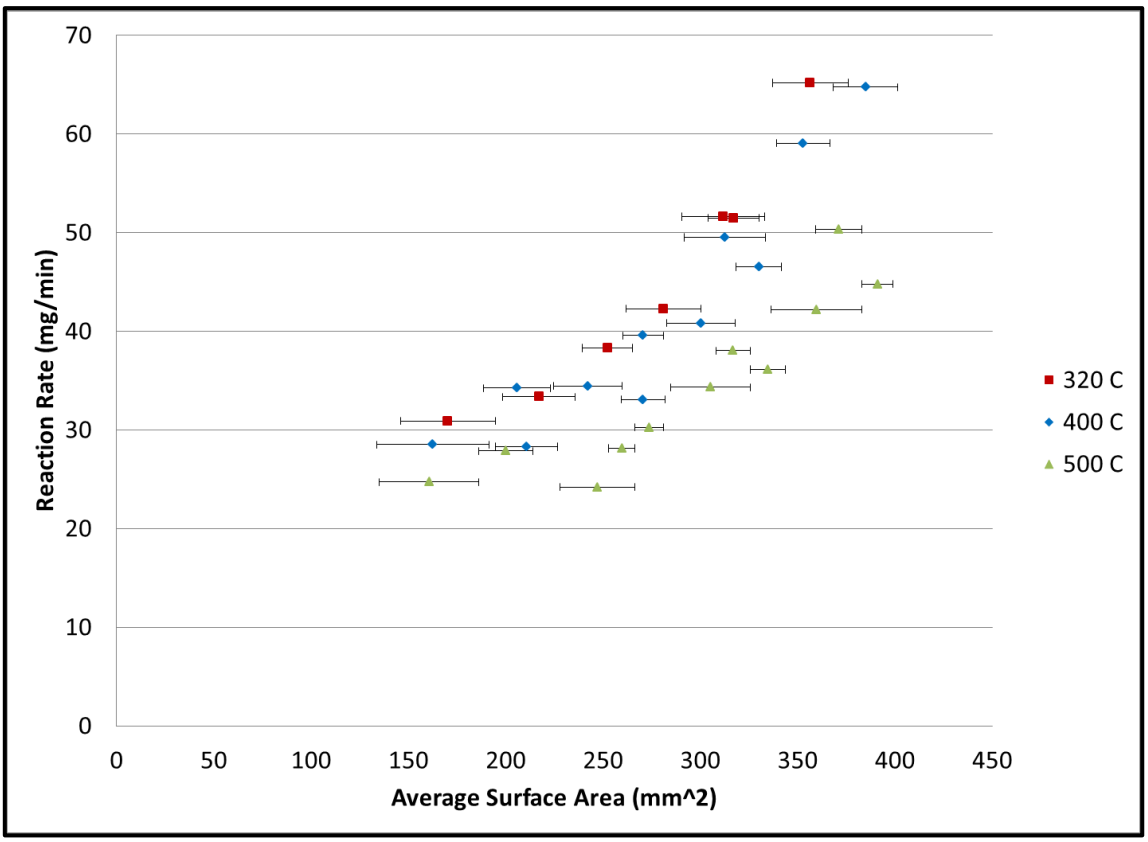

Figure 47: Summary of surface area study showing accelerating reaction rate as a function of surface area, and a decreased reaction rate as a function of temperature.

4.4.3 Study of Composition and Physical Shape (Zr14)

The final Zr experiment (Zr14) was used to determine the initiation temperature for four different sample compositions and/or physical forms. One of the samples was composed of crystal bar zirconium and was identical in shape to the samples used for the surface area study. A second sample was composed of a Zircaloy-4 tube. A third sample was composed of zirconium crystal bar turnings. The fourth sample was comprised of zirconium powder. The samples were loaded into separate reaction vessels and chlorine was introduced at room temperature following the purge process described in Section 3.2.4. The temperature was increased at approximately 5 °C/min, and the time and temperature of volatilization was observed and recorded for each of the four samples and can be seen in Table 11.

Table 11: Volatilization onset temperature.

Sample	T (°C)	Time (min)
Powder	195	30
Turnings	232	40
Zy Tube	302	67
Crystal Bar	310	70

The powder began to volatilize at a system temperature much lower than the volatilization temperature of zirconium tetrachloride (331 °C). This result is consistent with the data seen in Figure 47 which show an accelerating reaction rate with increased surface area. It can then be implied that it is possible to chlorinate a powder at much lower system temperatures than is needed for bulk material. The high-surface-area

zirconium turnings also showed a much lower volatilization temperature than the 331 °C volatilization temperature of zirconium tetrachloride.

The onset of volatilization for both Zircaloy-4 and crystal-bar zirconium were found to be virtually identical. This was not unexpected, because Zircaloy-4 contains 98.5% zirconium. A significantly different volatilization onset temperature would have indicated that the process being proposed in this research might not be suitable for zirconium alloys widely used in the nuclear industry. The fact that the temperatures were nearly identical implies that this process can be carried out on the Zircaloys with little, if any, changes to processing equipment or production methods.

It should be noted that the onset temperatures found for Zircaloy and crystal-bar samples are likely higher than what would be observed in an industrial system. The reason for this is that the Zircaloy-4 tube and crystal-bar zirconium samples were heated for over an hour before volatilization was observed. This incubation period likely allowed these samples to pick up excess oxygen and nitrogen, which may hinder chloride formation. This effect cannot be quantified based on the data obtained, but one can safely assume that the volatilization onset temperatures observed are upper bounds of what can be expected if careful practices are observed.

4.4.4 Zr Conclusion

The Zr-Series demonstrated that the chloride volatilization of zirconium is dependent on surface area. The data suggests that the volatilization rate accelerates with increasing surface area. This property is expected; in fact, it is the motivation behind considering a hydride pulverization process prior to its chlorination. However, the

strong dependence on surface area could possibly indicate that the material does not need to be reduced to a fine powder during the hydride pretreatment step, but simply ground to smaller pieces. This is an important result because a hydride pretreatment step may become the rate-limiting step for the process.

The second important result in this series is in the discovery that Zr volatilization occurred at relatively low system temperatures for samples which had extremely large surface areas. This was evident in dramatic fashion with the zirconium powder samples, but was also notable with the zirconium-turnings. Both of these samples became so exothermic in their reactions with the chlorine that they had to be removed from the system due to safety concerns.

4.5 Series U50ZrFinal

The experiments described here represent the final series of data generated to systematically demonstrate the temperature dependence of the separation of zirconium and uranium from a U-50Zr alloy using elemental chlorine. A U-50Zr alloy was prepared according to the procedure described in Section 3.2.5. This cast alloy was sectioned into cylindrical samples with ~1 mm thickness and 14 mm diameter. Each sample was exposed to chlorine according to the procedure in Section 3.2.5 at various temperatures for 45 minutes and the mass change data are presented in Table 12.

As with the U50Zr series (Section 4.3), the *volatilized* material was physically separated from the *non-volatilized* material, and these separated products were collected and processed for analysis according to the procedures perfected in the previous sections. The products were analyzed using EPMA to determine the relative

compositions of uranium and zirconium contained within the samples. This resulted in data showing the dependence of temperature on the separation of these species.

Table 12: Summary of data from U50ZrFinal series.

Non-volatilized (NV). *Volatilized* (V).

Name	%U	%Zr	T (°C)
U50ZrFinal-1NV	73.9	26.1	300
U50ZrFinal-1V	15.0	85.0	300
U50ZrFinal-2NV	98.5	1.5	400
U50ZrFinal-2V	15.4	84.6	400
U50ZrFinal-3NV	99.5	0.5	500
U50ZrFinal-3V	30.4	69.6	500
U50ZrFinal-4NV	98.8	1.2	360
U50ZrFinal-4V	15.8	84.2	360
U50ZrFinal-5NV	93.2	6.8	340
U50ZrFinal-5V	18.2	81.8	340
U50ZrFinal-6NV	NA	NA	280
U50ZrFinal-6V	26.3	73.7	280
U50ZrFinal-7NV	89.9	10.1	320
U50ZrFinal-7V	17.9	82.1	320
U50ZrFinal-8NV	85.3	14.7	380
U50ZrFinal-8V	20.0	80.0	380
U50ZrFinal-9NV	97.7	2.3	450
U50ZrFinal-9V	26.0	74.0	450
U50ZrFinal-10NV	95.9	4.1	340
U50ZrFinal-10V	14.9	85.1	340

4.5.1 Variable Selection and Justifications

The U50Zr-Final series builds upon all of the data obtained in previous series. The data gathered in previous experiments was used both to justify assumptions used in this series, as well as in the selection of variables and system parameters. The independent variable in this series was temperature, with all other system parameters set

at values based on the previous tests in Sections 4.1 through 4.4 selected to generate reproducible results.

Regarding sample fabrication, it was seen in the U50Zr series (Section 4.3) that as-cast alloys had slightly variable compositions along their axial length and experience has shown that the addition of a remelt step will decrease this compositional variation. Even with a possible variation in composition among samples, the microstructure was seen to be invariant even when the zirconium weight percent varied from 48-62%. It is assumed that the volatilization reaction will be relatively independent of alloy composition as long as the zirconium weight percent is roughly 50% along the length of the as-cast alloy. Therefore, the U-50Zr alloy was cast, recast, and sliced, and the samples were chosen at random among these slices.

The previous experiments also provided useful information regarding product recovery and preparation for analysis following each successful experiment. The techniques developed produce representative samples relatively free of impurities and their compositions were readily obtained using EPMA. The result is a data series which is believed to be of high quality.

In order to isolate temperature as the only process variable, all other possible potential process variables were fixed. The possible variables include system pressure, reaction time, and sample shape. It can be seen in Figure 13 that volatilization of $ZrCl_4$ is only weakly dependent on system pressure. Therefore, the system pressure was maintained at 6 psig out of convenience since the previous experience at that pressure indicated functional operation of the chlorination system. The primary requirement was

that the system be operated at a positive pressure in order to avoid contamination from the atmosphere. (Such a low positive pressure was selected to minimize the amount of leakage out of the system, thus better simulating a totally static system.)

The reaction time was fixed at 45 minutes based on the data shown in Figure 42. Those data show that the zirconium tetrachloride formation reaction is mostly complete between 30 and 60 minutes for all temperatures of interest. In order to eliminate time as a variable, 45 minutes was chosen because the reaction would likely have reached a steady state at all temperatures studied within this timeframe.

The samples were prepared as thin disks of near-identical dimensions in order to eliminate surface area as a variable. As shown in Figure 45, the variation in zirconium chloride formation is negligible in samples of similar dimensions. The thin-disk shape itself is used to justify the assumption that each sample's surface area will change little throughout the course of each 45 minute experiment as material is actively removed through volatilization.

The temperatures for this series were also selected based on the data obtained in the previous data series. The lowest temperature selected for this series was 280 °C, which is slightly higher than the 271 °C to 278 °C threshold temperature noted in Section 4.3.2.6 for experiments U50Zr6-U50Zr67. Previous experiments showed that the most interesting temperatures for zirconium volatilization are those around the tetrachloride volatilization temperature of 331 °C. Temperatures of 280, 300, 320, 340, 360, and 380 °C were studied in this final series resulting in a data set which contains three temperatures above, and three temperatures below the volatilization temperature of

zirconium tetrachloride, spanning 50 °C in either direction. In addition, the temperatures 400, 450, and 500 °C were included to gain further insight into the volatilization of uranium tetrachloride at higher temperatures. This test matrix results in a data set which studies in detail the separation of zirconium from U-50Zr alloys at the temperatures most relevant to an industrial process, as well as a rough study of the level of uranium contamination which might be expected in the volatilized zirconium in the case of elevated temperatures, accidental or otherwise.

4.5.2 U50Zr Final Results

Figure 48 and Figure 49 show representative sample surfaces of the *non-volatilized* and *volatilized* samples, respectively. Throughout this series, the product collection and conversion method developed for this research produced uniform analytical samples that provided repeatable and reliable data. It should be noted that the differences in contrast are simply due to different contrast settings during image acquisition, and do not reflect compositional differences. That being said, it can be seen that the predominately uranium samples shown in Figure 48 contain dark zirconium spots, while the predominately zirconium samples shown in Figure 49 contain bright uranium spots. This segregation is caused by the process which converts the chlorides to their respective oxides. It was observed that the uranium and zirconium would begin to segregate while in solution. In an effort to compensate for this, the samples were ground using a mortar and pestle prior to final preparation. However, there would always be "inclusions" in spite of these efforts. These spots are not believed to result in any significant error due to their size when compared to the size of the 20 μm beam width

and 400 µm scanned beam length. Each of these line-scans was repeated three to six times for each.

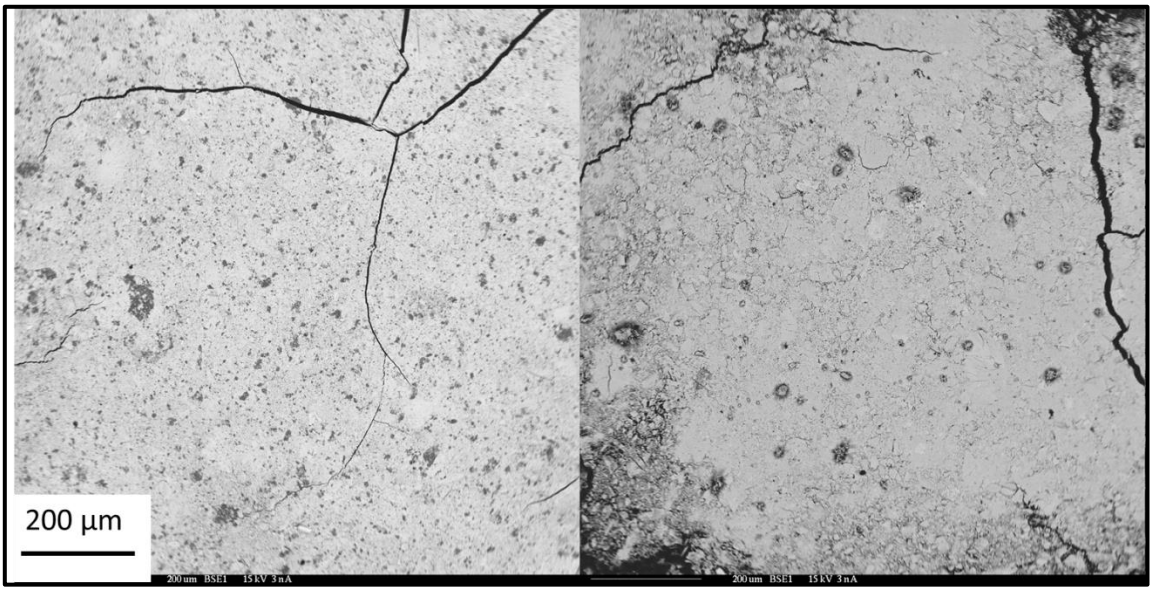

Figure 48: Backscattered electron image of *non-volatilized* samples. Experiment U50ZrFinal-8 on left, experiment U50ZrFinal-10 on right.

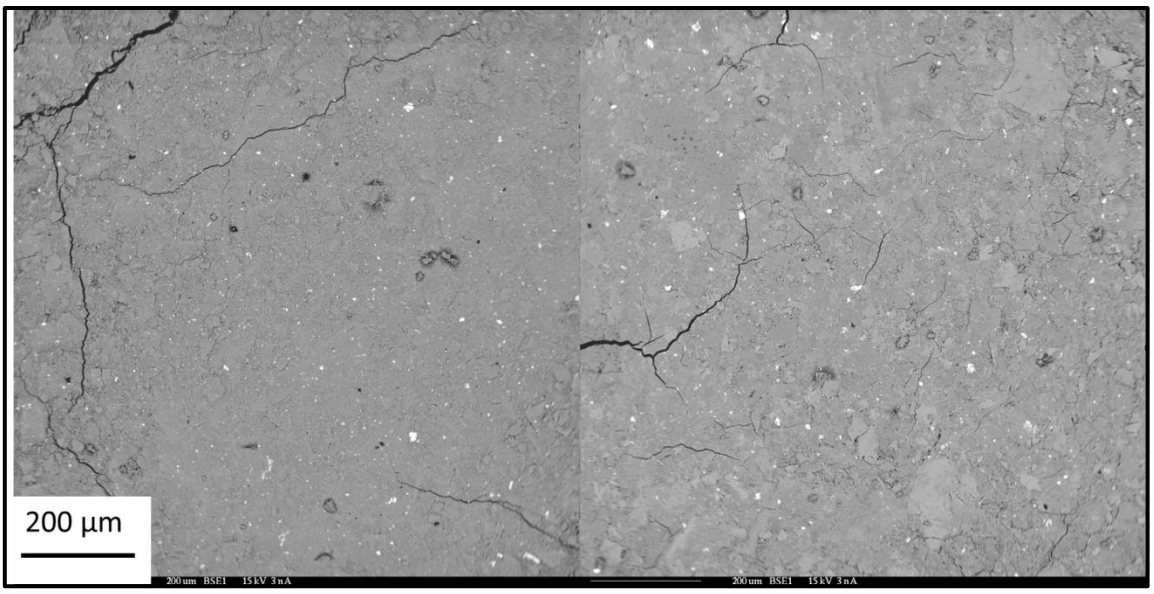

Figure 49: Typical backscattered electron image of *volatilized* samples. Experiment U50ZrFinal-7 on left, experiment U50ZrFinal-10 on right.

It can be seen in Figure 50 that the samples still contained some sodium. This figure shows large-area EDS spectra of the *non-volatilized* and *volatilized* samples showing large qualitative differences in the U/Zr ratio. The figure also shows an EDS spectrum of one of the bright uranium "inclusions" seen in Figure 49. While these areas contain a different composition when compared to the bulk material, the line-scan technique is believed to eliminate the effect that this difference would cause when analyzing the samples for this series.

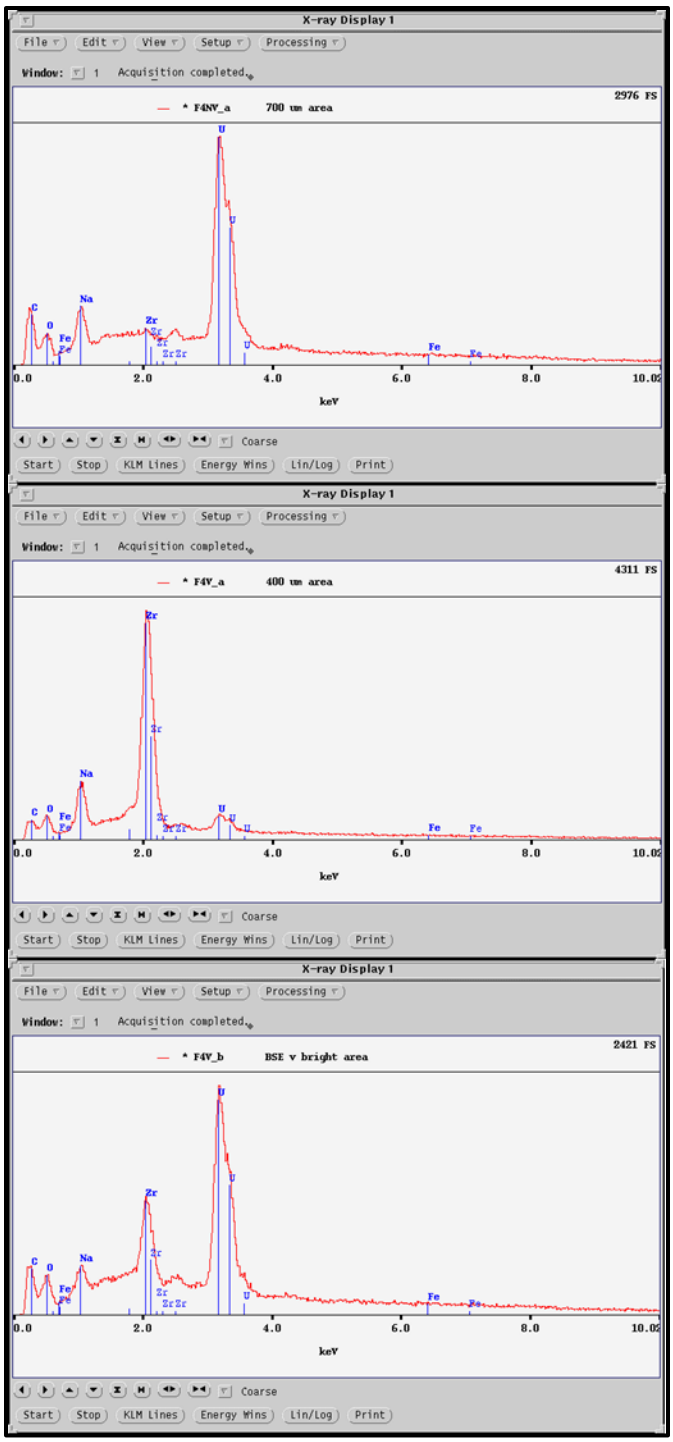

Figure 50: Energy dispersive spectra of *non-volatilized* samples, *volatilized* samples, and the bright portion within the volatilized samples. Plots are from experiment U50ZrFinal-4.

As mentioned previously, all samples prior to experiment U50ZrFinal-5 contained no significant levels of contamination outside of a slight sodium contamination. Experiments performed after experiment U50ZrFinal-4 marked a departure from this trend. Experiments U50ZrFinal-5 and U50ZrFinal-6 especially showed stainless steel contamination in the *volatilized* samples. The only source for this contamination is from the stainless steel fitting which the glass reaction vessel was connected to. This is further supported by Figure 51 which shows the difference in stainless steel contamination for the *non-volatilized* and *volatilized* portions of experiment U50ZrFinal-5. As can be seen, the *non-volatilized* portion contains no contamination, while the *volatilized* portion shows significant Fe, Cr, and Ni contamination. This is consistent with the geometry of the system. The *volatilized* samples are collected from both the glass reaction vessel as well as the stainless steel fitting which would inevitably have material deposited on it. In hindsight it would have been better to have a system geometry which did not allow material to deposit within the stainless steel fitting.

The stainless steel contamination is not believed to have had any effect on the U-Zr ratio neither from an analytical standpoint nor is it believed to have affected the volatilization of the material being studied. Checks were made to determine if the stainless steel components would produce any interference in EPMA analysis, and no interference effect was found. The stainless steel is not believed to affect the volatilization because it is assumed that the steel contamination came from steel leaving the surface of the fitting in the form of rust. This rust was never a volatilized component

nor was it even chlorinated and would therefore have no impact on the chlorination process being studied. Experiments U50ZrFinal-5 and U50ZrFinal-6 contained the highest levels of steel contamination. Once this was discovered, efforts were made to clean the surface of the inside of the fitting with the effect of virtually eliminating any traces of steel contamination from all future experiments.

The reason that this is mentioned is not so much because of its effect on experimental results as much as because it is relevant to future system design. One of the assumptions in developing this process was that a large portion of the equipment could likely be constructed of low-cost stainless steel. This is in contrast to the exotic materials which must be used for fluorination processes, for example. The fact that the stainless steel fittings were actively corroded throughout the project indicates that the previous assumption may not be valid after all. However, it should also be mentioned that these fittings were continuously cycled between being exposed to chlorine, metal-chlorides, water, ethanol, and acetone. It cannot be concluded that the chlorine or metal-chlorides alone were responsible for the corrosion. That being said, it can also not be concluded that the chlorine or metal-chlorides were NOT responsible. This is an area where future research is needed.

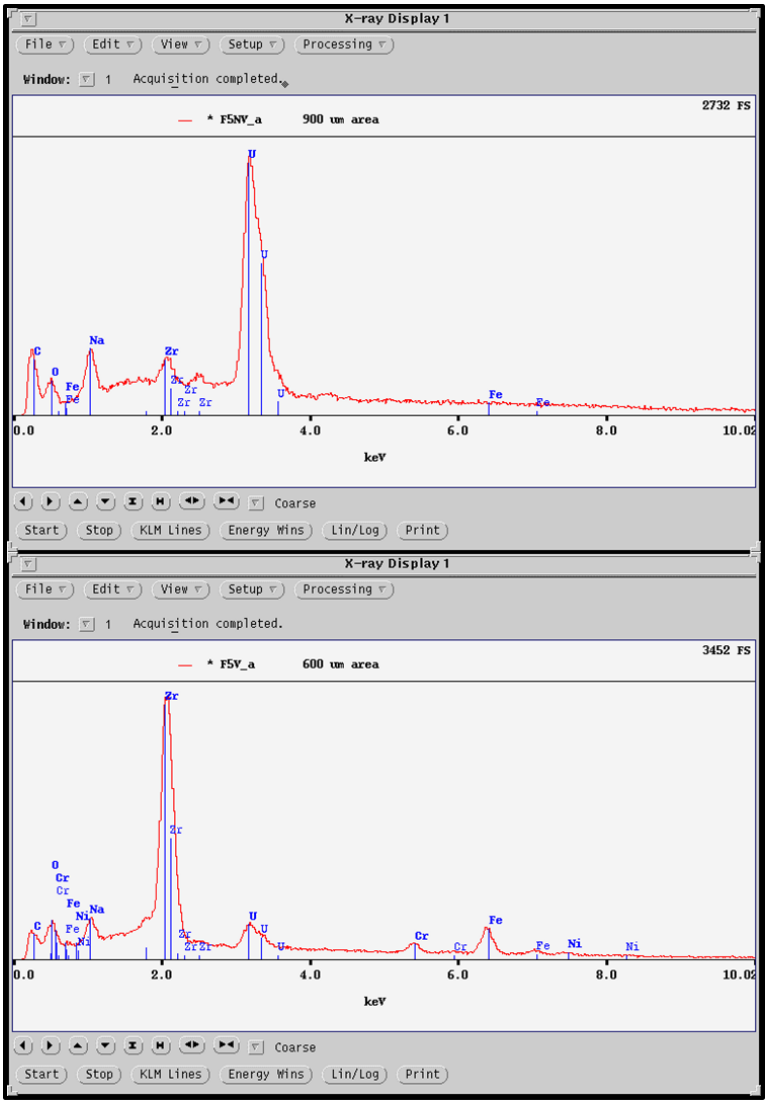

Figure 51: EDS spectrum showing contamination of *volatilized* samples from stainless steel fittings. Plots are from experiment U50ZrFinal-5.

It should be noted that the conditions of experiment 5 were repeated in experiment U50ZrFinal-10. The reason for this was because the initial samples size for experiment U50ZrFinal-5 was small enough that the entire sample was reduced to chloride over the 45 minute time period. This is in contrast to all other experiments

which always had some bulk material which was not consumed after the experiment was concluded. This was done intentionally so that there would always exist an excess amount of the alloy starting material. Even so, the differences in results between experiments U50ZrFinal-5 and U50ZrFinal-10, as seen in Table 12, are minimal and virtually insignificant.

Another item worth discussing is that there is no data for the *non-volatilized* portion of experiment U50ZrFinal-6. The sample was barely attacked by the chlorine. This resulted in extremely small sample sizes. Enough material was collected for the *volatilized* portion, but there simply was not enough *non-volatile* chloride present after the experiment to be analyzed. It may be valid to assume that the *non-volatilized* portion of experiment U50ZrFinal-6 is 50% Zr and 50% U, but this was not confirmed. However, it fits with logic because this is the composition of the starting material, and it also fits the trend of the data seen in Figure 52.

The final thing of note is that experiment U50ZrFinal-8 appears to be anomalous. There is no obvious reason for its departure from the observed trend of the data, especially for the *non-volatilized* sample. This experiment will therefore be ignored in all future discussions.

The data from Table 12 are presented graphically in Figure 52. It can be seen that, under these conditions, the uranium can be purified to nearly 99% at temperatures exceeding 360 °C and to nearly 90% at temperatures as low as 320 °C. It is therefore unlikely that any industrial-scale process will be required to operate at temperatures greater than 360 °C. This is especially true considering that these experiments were

conducted on bulk specimens, where the proposed process suggests the use of metal powder as the feed material. The reason that this is important is because the only reason to increase the temperature above 360 °C is to speed up the process. If the starting material is a metal powder, the process will likely occur instantaneously, as seen in previous experiments, and an increase in temperature will have little to no effect on the throughput of a facility. . It can also be seen that the removal of zirconium drops of dramatically at temperatures lower than 320 °C. This suggests that the ideal temperature for achieving purified uranium from a U-50Zr alloy is between the temperatures of 320 °C and 360 °C.

The data shows that the uranium content of the *volatilized* product stream remains relatively constant at temperatures at and below 400 °C, and begins to increase at temperatures above 400 °C. This is consistent with the increased vapor pressure of uranium chloride at higher temperatures. It appears that the uranium-zirconium ratio for the *volatilized* material is independent of temperature at the most likely temperatures of operation, namely 320 to 360 °C. This seems to indicate that the recovery of a pure zirconium product might not be possible under these conditions. However, it is possible that the observed volatilization of uranium is more a product of the small size of the system than it is to variables such as temperature. More research is needed before this process can be used to produce a purified zirconium product.

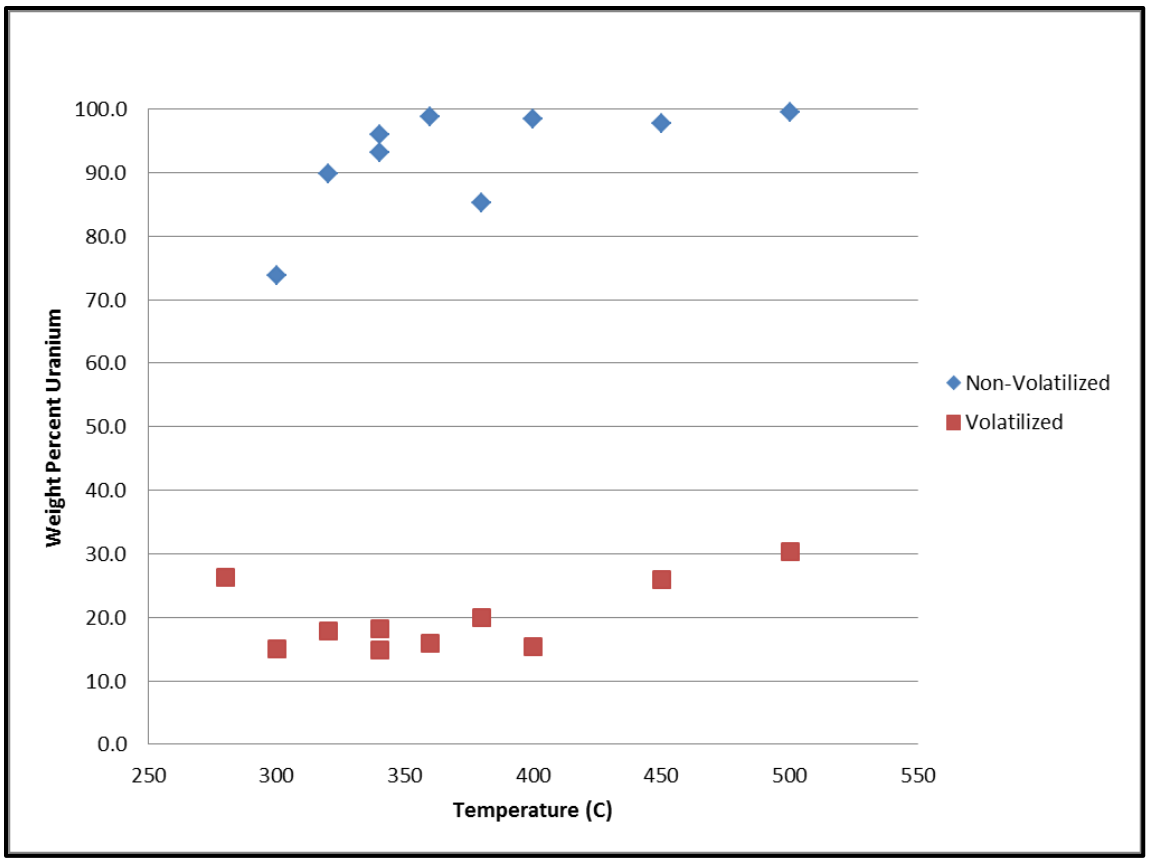

Figure 52: U50ZrFinal data plotted as a function of temperature.

5. SUMMARY OF EXPERIMENTAL RESULTS

5.1 Motivation

The research presented in this dissertation was performed in order to gather preliminary data for use in designing an industrial prototype system. This system would take advantage of hydrogen's ability to embrittle and pulverize both zirconium and uranium. Previous research has shown that this pulverization occurs rapidly and at temperatures which are on the same order as those needed for a chloride volatilization process as shown in this dissertation. This means that it may be possible to add a hydride pulverization pretreatment step to a chloride volatilization process with only minimal changes to any existing equipment and process techniques. It is believed that this pulverization step will result in a near instantaneous formation of volatile chloride, which may then be selectively distilled based on the goals of the facility utilizing the process. The production rate of the facility therefore becomes limited by the hydride formation rate instead of the chloride formation rate.

It is believed that a hydride pulverization process will result in simpler plant design because it allows for more precise control of system temperatures and reduces the risk of local hot-spots forming. The formation of hot-spots was observed throughout the course of this project, most notably during the initial testing of experimental systems. It was seen that if chlorine were allowed to flow continuously over solid zirconium samples, that they would become hot enough to glow orange and melt through the borosilicate-glass reaction vessel. While the temperature of these samples was not

measured directly, the combination of an orange glow with the fact that the borosilicate glass melted provides a conservative estimated temperature of at least 800 °C. It should be noted that this temperature was achieved very rapidly; on the order of a few seconds. This would greatly reduce the amount of material that an industrial facility could process if it had to be designed to account for these hot-spots. The presence of hot-spots would also all but eliminate the use of metallic alloys in the heated zone. As far as is known, there are no existing alloys capable of surviving an 800 °C elemental chlorine environment long-term.

Pulverizing the material prior to chlorination would result in a system who's temperature can be controlled in a more reliable and safe manner. It is proposed that the chloride formation process would take place with material that has been fluidized. As was seen in this project, the chlorination reaction occurs very readily for powdered material, and at much lower temperatures than are needed for chloride volatilization. Again, this suggests the use of a fluidized bed reactor with cooled walls for the initial chloride formation process. The material would actively be deposited on the walls of the reactor until the distillation process is to begin. This means that the equipment itself will not be exposed to elemental chlorine at temperatures nearly as high as would otherwise be needed if bulk material were processed with chlorine. This allows much greater flexibility in equipment design and much longer lifecycles for all equipment used. While the distillation temperatures might push the limits of fluorocarbons, they should certainly be considered as being one of the primary construction materials. In fact, the results obtained in this research suggest a distillation temperature as low as 320 °C,

which is pushing the limits of, but not outside of the realm of possibility for some of the more exotic fluorocarbons.

The separation process itself will likely be a simple distillation process. Unlike the experiments conducted for this dissertation, an industrial process will likely consist of separate chlorination and distillation processes. This recommendation is a result of consistent observations which indicate that the heat generated, and thus temperature increase, by the chlorination reaction is not insignificant. This local temperature increase would limit the control that a facility would have on the distillation products. It seems much more likely that a process would achieve better separation results if the chlorides are formed and then distilled in separate processing steps. The data obtained in this research shows the results of a combined chlorination/distillation process. It was seen that, while the non-volatilized portion of the material was virtually free of zirconium, the volatilized portion contained significant uranium contamination. The volatilized portions were enriched in zirconium and the uranium could likely be further removed through the use of multiple distillation steps. However, the temperatures studied were far below those at which one would expect to see uranium volatilization. The fact that uranium volatilization was observed is believed to be a result of local heating from the chloride formation process itself coupled with the simple geometry of the system. The data gathered in this project will now be used to provide recommendations for researchers and engineers who may wish to utilize this process in the future.

5.2 Pulverization Process

The pulverization process itself is highly dependent on the nature of the alloy being processed. It is for this reason that certain assumptions need to be made. This project studied the volatilization of U-50Zr, however it is worth restating that the process is certainly not limited to this exact alloy composition. Regardless, U-50Zr will be the basis for the recommendations presented here.

5.2.1 Rate of Pulverization

Previous research has shown that the hydride formation rate is higher for pure uranium compared to the rate of hydride formation in zirconium. While the hydride formation rate is not known for U-50Zr alloys, a conservative estimate can be made by using the rate of hydride formation in zirconium as the benchmark. It is important to keep in mind that complete hydride formation is not necessary. Rather, sufficient hydrogen embrittlement is all that is required to enable pulverization. Previous research on hydride pulverization was conducted on Zircaloy-4 tubes which had a thickness of 0.83 mm. The results of this research showed that this material can be pulverized in less than an hour. Because the inside and outside of these tubes were exposed to hydrogen, it can be conservatively assumed that the pulverization will take place at a rate of 0.4128 mm/hour at each exposed surface. It is worth repeating that this reaction rate was observed for the Zircaloy-4 alloy system. The hydride pulverization rate for U-50Zr alloys will almost certainly be higher, perhaps dramatically higher.

Assuming a fuel-pin has a 10 mm diameter, one can safely expect total pulverization to occur in no more than 12 hours. This time estimate assumes that the

fuel pins will remain fully intact until the hydride formation reaction is allowed to consume the pin in its entirety. Not only is it unrealistic to assume that the material will remain intact, it was observed in previous research that Zircaloy-4 would become fully pulverized even at 50% hydride formation. This result reduces the maximum hydride formation time to 6 hours. Even this estimate assumes the material remains intact until 50% hydride is formed, which is likely to be unrealistically conservative. Again, these estimates are using the hydride formation rate as was observed in Zircaloy-4, where the reaction rate, and thus pulverization rate, in U-50Zr is likely to be much higher. This belief is due to the nature of the respective hydrides of uranium and zirconium; uranium forms a naturally-spalling hydride, while zirconium does not.

The hydride pulverization rate can be further accelerated through mechanical agitation of the material. This can be achieved through various well-known methods, and it is the belief of the author that, in doing so, the gross pulverization rate can be increased by an order of magnitude or more. The reason for this belief is that the surface area will increase exponentially as the reaction proceeds, thus exponentially increasing the reaction rate. While not supported by direct data, it is the educated opinion of the author that pulverization of a 10 mm diameter fuel-pin can be achieved in less than an hour. It is also important to note that this pulverization rate is independent of the amount of material within any given reaction vessel, as long as an over-pressure of hydrogen is maintained. Rather, the pulverization reaction is dependent on the surface area of the material being reacted. It follows that the amount of material processed per batch is not

limited by the chemistry of the system; however, criticality concerns may limit the batch size, depending on the type of material being processed.

5.2.2 Criticality Limits

As stated previously, the isotopics of the material to be processed is totally dependent on the needs of the user, and assumptions cannot be made of the exact composition of the material to be processed at this time. However, analysis can be performed on the "worst-case" situation from a criticality standpoint. Although an identical process can be used to remove gallium from plutonium-gallium alloys, the focus of this discussion will be on U-235 as the main fissile isotope of interest. This is not meant to imply that other fissile isotopes, such as Pu-239, may not be present in material being processed using this method. In fact, it will certainly be present if irradiated U-Zr fuel is to be processed, such as that originating from a breeder reactor fuel cycle or the Traveling Wave Reactors (TWR). However, the isotopics of these materials is entirely dependent on the irradiation history and time after irradiation, making selection of a single specific material composition impossible.

5.2.2.1 Irradiated Fuel

A safety analysis of irradiated fuels is the most difficult situation to consider from a criticality standpoint. The source of this material may be irradiated LEU/DU or HEU fuel, each presenting its own unique challenges. The isotope of concern for irradiated LEU/DU fuel is Pu-239. In this case, the system should be designed such that the material is not able to achieve criticality due to the Pu-239 content. These concerns are virtually independent of the chemical processes being employed, because the critical

mass of Pu-239 is lowest in its metallic state. It would be relatively straightforward to design the system such that it incorporates material which contains neutron-absorbing species. The neutron-absorbing material may be built into the equipment itself, or it may be introduced into the hydride process as neutron-absorbing chemically-inert milling balls, for example. This, combined with careful design of system geometry, can be used to prevent criticality.

In the case of irradiated HEU, the situation is somewhat different, but not prohibitively so. The critical mass of U-235 is appreciably reduced through the formation of its hydride. The critical mass reaches a minimum at a hydride composition of UH_2, where the full hydride conversion of uranium is reached at UH_3. This suggests that all equipment and process design should be done with UH_2 in mind, rather than metallic uranium. Regardless, these concerns may be alleviated in a manner identical to those used for material containing significant amounts of Pu-239. In the case of irradiated fuel, the concerns due to potential criticality are reduced because of the likely presence of significant quantities of poisoning fission products. Again, the exact quantities and composition of this irradiated material is dependent so much on the history of the material, that further discussion would be mere speculation.

5.2.2.2 Unirradiated HEU Fuel

If U-235 is the primary constituent and the only fissile isotope present, then the situation gets more complicated. This is because the critical mass of uranium hydride is appreciably less than that for uranium metal. This should be accounted for when determining batch sizes for the hydride process. It can be shown that the minimum U-

235 critical mass is obtained for a hydride composition of UH_2. As stated previously, this result implores those performing equipment design to assume a presence of 100% UH_2 for all criticality calculations.

This case is perhaps the most critical from a criticality perspective. While Pu-239 is certainly more sensitive to accidental criticality, realistically, any material containing this isotope will be heavily contaminated by U-238 as well as an abundance of neutron-absorbing fission-products. This is in contrast to virgin HEU material, which has the potential to go critical at much smaller batch sizes. It is for this reason that it may be prudent to consider hydride batch sizes of less than 18 kgU for unirradiated HEU. This will be sufficient to prevent criticality even without the addition of neutron-absorbing material. Although not directly studied in this project, it may be possible to add hafnium directly to the reaction vessel in order to prevent criticality, thereby increasing the batch size considerably. This hafnium is likely to be volatilized along with zirconium during the volatilization process, but this has not been confirmed. This means that the separated zirconium will require further processing if it is to be used again for nuclear applications. Again, this decision is dependent on the needs of the facility.

5.2.2.3 Unirradiated LEU/DU Alloy

Criticality is much less of a concern for unirradiated LEU alloys, and is not a concern at all for DU. In fact, in the absence of a moderating material, uranium enriched to less than 5.4% U-235 will never go critical under any normal circumstance. The critical mass of 20% enriched uranium metal is 766 kg, which is likely near or

surpassing the amount of material which may be efficiently processed in a single batch. The hydride process batch size for LEU/DU will therefore likely be limited by the material-handling limits of the facility rather than those imposed by criticality limits.

5.3 Separation Process

The experimental aspect of the research presented in this dissertation focused on the separation of uranium and zirconium through chloride volatilization. These experiments were intended to demonstrate that this technique was capable of this separation, and what conditions might be ideal to facilitate such a separation. Not only was this shown to be possible, but it was seen that one may achieve near total removal of zirconium from uranium-zirconium alloys using this method. While the non-volatilized portion left behind following processing did contain between 1 and 2% zirconium even in the best-case, this is still a dramatic reduction in zirconium content compared to the starting material which contained 50% zirconium. It is not unreasonable to assume that the zirconium content which was left behind is at least partially due to the formation of chemically-inert surface-oxide on the alloy prior to reaction with chlorine. This suggests that if material were to be processed which contains a lower surface area to volume ratio, that the zirconium removal may be even greater. The samples being studied in the U50ZrFinal experiments had thicknesses and diameters of 1 mm and 15 mm, respectively. This corresponds to a surface area to volume ratio of 2.26 mm^{-1}. It is unlikely that material being processed using this technique will have such a high initial surface area to volume ratio. Assuming the material takes the form of a pin, as is common for nuclear fuels, this ratio will decrease tremendously. If a pin of 10 mm

diameter and 100 mm length is processed, its surface to volume ratio will be 0.024 mm^{-1}, a reduction of surface area to volume ratio of greater than two orders of magnitude. It is proposed that this may translate to a corresponding reduction in zirconium content by two orders of magnitude. For all practical intents and purposes, this would result in a total elimination of zirconium from the alloy. To be clear, the intent of the hydride pulverization process is to increase the surface area to volume ratio; however, preventing the formation of surface oxide on this pulverized material is a straightforward matter.

Experimental evidence shows significant uranium contamination in the *volatilized* portion which suggests that improvements should be made to the process. It is likely that the recovery of uranium will be the primary concern for any facility utilizing this process, especially if the uranium species involved is the valuable U-235 isotope. It follows that zirconium contaminated with up to 20% uranium may be an unacceptable final product.

First, it should not be lost to the reader that the experiments conducted in this research took place in standard test tubes whose dimensions are far from being representative of an industrial-scale facility. The experiments were set up such that the volatilization reaction would take place in a carefully controlled heated zone, and the condensing of products would take place in an area outside of this heated zone, the temperature of which was neither controlled nor recorded. Further, the physical separation between the sample being reacted and the deposition zone was on the order of 10 cm, hardly characteristic of the equipment likely to be used in an industrial facility. The reason why this matters is that the volatilization of uranium, and thus contamination

of the zirconium product, will be driven by several factors which were not controlled in these experiments, but could easily be controlled in a larger system which is designed to take advantage of a pulverized starting material.

The first difference in the experimental system presented in this dissertation and an industrial system is that the experimental system was oriented horizontally. An industrial process will likely take advantage of the buoyancy difference between the chlorides of uranium and zirconium, whereas a horizontally oriented system is unable to do so. It would be relatively easy to accomplish this task through the use of a larger system with a condensation zone which is physically located above the initial reaction or distillation zone. It may be possible to achieve greater separation and the creation of a more pure zirconium product through the introduction of temperature-controlled physical bottlenecks which would selectively allow zirconium chloride through, while inhibiting the passage of uranium chloride. The temperature of this structure can be maintained at a temperature slightly above the volatilization temperature of zirconium tetrachloride thus encouraging condensation of uranium tetrachloride but allowing the zirconium chloride to pass unimpeded. Distillation processes such as this are well established and understood, and need not be discussed further.

The second major difference between the experimental system and an industrial system is in the physical makeup of the starting material. The material used in the experiments was a bulk alloy, whereas that used in the proposed industrial process will be a metal powder. The importance of this distinction is that a bulk material is likely to reach temperatures which exceed the desired system temperature for extended periods of

time, where a powder system can be designed such that the material is instantly turned to chloride and subsequently deposited on the temperature-controlled vessel walls. This is in addition to the clear advantages of eliminating local hot-spots as discussed earlier. The small size of the experimental system, coupled with the use of bulk alloy, likely resulted in material becoming volatilized due to temperatures which were higher than that of the vessel walls, and the small system size gave preference to the now volatilized uranium chloride to deposit in the cool zone instead of the heated zone. Again, this can be eliminated through careful control of temperatures throughout a larger reaction/distillation system, especially if these high local temperatures are not permitted to exist in the first place.

5.4 Conclusion

The experiments performed during the course of this research showed that a combined hydride/chloride-volatilization process can be used to separate zirconium from uranium-zirconium alloys. The results obtained can be directly applied to designing an industrial prototype system with expected batch sizes on the order of several kilograms instead of the gram batch sizes which were studied for this project.

It was observed that a powdered material would be chlorinated nearly instantaneously, while a bulk sample required a non-trivial reaction time before it was fully consumed. This result supports the hypothesis that pulverizing the material prior to chlorination may decrease the total processing time, thus increasing the throughput of an industrial facility. Previous research has shown that both uranium and zirconium are easily pulverized using a hydride/dehydride process.

It was also seen that selective volatilization of the chlorides can be used to produce a uranium product which is nearly devoid of zirconium. This near-total separation was seen to take place at temperatures above 320 °C. The zirconium product was seen to be heavily contaminated with uranium, however. It is believed that this result can be easily improved upon through careful equipment design.

REFERENCES

1) B. Lustman and F. Kerze Jr., The Metallurgy of Zirconium, McGraw-Hill Book Company, Inc, New York: 1955.

2) J. Saling and A. Fentiman, Radioactive Waste Management, Taylor & Francis, New York: 2001.

3) T. L. Yau, "Zirconium for Nitric Acid Solutions," Industrial Applications of Titanium and Zirconium, Philadelphia: 1986, Volume 4, pp. 57-68.

4) W. B. Lanhan and T. C. Runion, "PUREX Process for Plutonium and Uranium Recovery", ORNL-479, Oak Ridge National Laboratory: 1949.

5) J. L. Snelgrove, G. L. Hofman, C. L. Trybus, and T. C. Wiencek, "Development of Very-High-Density Low-Enriched Uranium Fuels," Nuclear Engineering and Design: 1997, Volume 178, pp. 119-126.

6) T. Ellis, R. Petroski, P. Hejzlar, G. Zimmerman, D. McAlees, et al., "Traveling-Wave Reactors: A Truly Sustainable and Full-Scale Resource for Global Energy Needs," Proceedings of ICAPP: 2010, Paper 10189.

7) G. D. Moon and P. Rudling, (Eds).: "Zirconium in the Nuclear Industry: 13th Int. Symposium," ASTM International, West Conshohocken, PA: 2002.

8) J. M. Markowitz: ''Internal Zirconium Hydride Formation in Zircaloy Fuel Element Cladding under Irradiation,'' WAPD-TM-351, Westinghouse Electric Corporation, Bettis Atomic Power Laboratory, Pittsburgh, PA: 1963.

9) K. Une, K. Nogita, S. Ishimoto, and K. Ogata, "Crystallography of Zirconium Hydrides in Recrystallized Zircaloy-2 Fuel Cladding by Electron Backscatter Diffraction," Journal of Nuclear Science and Technology: 2004, vol. 41, pp. 731–740.

10) S. Yamanaka, K. Yoshioka, M. Uno, M. Katsura, H. Anada, et al., "Thermal and Mechanical Properties of Zirconium Hydride," Journal of Alloys and Compounds: 1999, vols. 293–295, pp. 23–29.

11) H. M. Finniston and J. P. Howe, "Metallurgy and Fuels," Progress in Nuclear Energy, Pergamon Press, New York: 1956.

12) W. L. Mudge Jr., "Effect of Hydrogen on the Embrittlement of Zirconium and Zirconium Tin Alloys," Zirconium and Zirconium Alloys, American Society of Metals, Cleveland, OH: 1953, pp. 146-167.

13) A. J. Parkison and S. M. McDeavitt, “Hydride Formation Process for the Powder Metallurgical Recycle of Zircaloy from Used Nuclear Fuel,” Metallurgical and Materials Transactions A: 2011, vol 42, pp. 192-201.

14) W. M. Mueller, Metal Hydrides, Academic Press Inc., London: 1969.

15) A. J. Parkison, “Hydride Production in Zircaloy-4 as a Function of Time and Temperature,” Texas A&M University: 2008.

16) S. M. McDeavitt, A. J. Parkison, A. R. Totemeier, and J. J. Wegener, "Fabrication of Cermet Nuclear Fuels Designed for the Transmutation of Transuranic Isotopes," Material Science Forum: 2007, vols. 561–565, pp. 1733–1736.

17) S. M. McDeavitt, D. T. Kraemer, A. Parkison, A. R. Totemeier, and J. J. Wegener, "Zirconium Matrix Cermet Storage Form and Transmutation Fuel for Transuranics," Proceedings of American Nuclear Society Winter Meeting, Washington D.C.: 2005, vol 93, pp. 743.

18) W. Sames, "Uranium Metal Powder Production, Particle Distribution Analysis, and Reaction Rate Studies of a Hydride-Dehydride Process," Senior Honors Thesis, Texas A&M University: 2011.

19) P. Chiotti and B. A. Rogers, “The Production of Uranium and Thorium in Powder Form,” United States Atomic Energy Commission: 1950, AECD-2974.

20) H.H. Hausner and J. F. Schumar, Nuclear Fuel Elements, Reinhold Publishing Corporation, New York: 1959.

21) M. A. Hunter, “Metallic Titanium,” Journal of the American Chemical Society: 1910, vol. 32 (3), pp. 330–336.

22) W. J. Kroll, “Method for Manufacturing Titanium and Alloys Thereof,” Germany Patent No. 217,773, Luxemburg: 1938.

23) C. Bodsworth, The Extraction and Refining of Metals, CRC Press, Ann Arbor, MI: 1994.

24) W. J. Kroll, “The Production of Ductile Titanium” Transactions of the Electrochemical Society: 1940, vol. 78, pp. 35–47.

25) P. Korbel and M. Novak, Encyclopedia of Minerals, Ribo International, Lisse, the Netherlands: 1999.

26) A. E. van Arkel and J. H. de Boer, "Darstellung von reinem Titanium-, Zirkonium-, Hafnium- und Thoriummetall," Zeitschrift für anorganische und allgemeine Chemie: 1925, vol. 148 (1), pp. 345–350.

27) J. Bigeleisen, M. G. Mayer, P. C. Stevenson, and J. Turkevich, “Vibrational Spectrum and Thermodynamic Properties of Uranium Hexafluoride Gas,” Journal of Chemical Physics: 1948, vol. 16, pp. 442.

28) E. P. Ney and F. C. Armistead, “The Self-Diffusion Coefficient of Uranium Hexafluoride,” Physical Review: 1947, vol. 71, pp. 14–19.

29) G. D. Oliver, “The Vapor Pressure and Critical Constants of Uranium Hexafluoride,” Journal of the American Chemical Society: 1953, vol. 75 (12), pp 2827–2829.

30) C. D. Harrington and A. E. Ruehle, Uranium Production Technology, D. van Nostrand Company, Inc., New York: 1959.

31) L. J. Anastasia, E. L. Carls, A. A. Chilenskas, J. E. A. Grane, A. A. Jonke, et al., “Fluoride Reprocessing of Breeder Fuels,” U.S. Patent No. 3,753,920, United States: 1971.

32) M. A. Thompson, R. S. Marshall, and R. L. Standifer, “Pilot Plant Experience on Volatile Fluoride Reprocessing of Plutonium,” Nuclear Metallurgy: 1969, vol 15, pp. 163-176.

33) J. J. Schmets, “Reprocessing of Spent Nuclear Fuels by Fluoride Volatility Processes,” Atomic Energy Review: 1970, vol 8, pg. 3-126.

34) Y. Kani, A. Sasahira, K. Hoshino, and F. Kawamura, “New Reprocessing System for Spent Nuclear Reactor Fuel Using Fluoride Volatility Method”, Journal of Fluorine Chemistry: 2009, vol 130, pp. 74-82.

35) J. Uhlir and M. Marecek, “Fluoride Volatility Method for Reprocessing of LWR and FR Fuels,” Journal of Fluorine Chemistry: 2009, vol 130, pp. 89-93.

36) L. J. Anastasia, P. G. Alfredson, and M. J. Steindler, “Reaction Model for the Fluorination of Uranium and Plutonium Compounds in Fluidized-Bed Reactors,” Industrial & Engineering Chemistry Process Design and Development: 1971,vol 10 (2), pp 150–157.

37) L. P. Hatch, J. J. Reilly, and W. H. Regan, “Fluidized Solids Process for Recovery of Uranium from Zirconium-Type Fuel Elements,” U.S. Patent No. 3,149,909, United States: 1964.

38) W. B. Blumenthal, The Chemical Behavior of Zirconium, D. van Nostrand Company, Inc., New York: 1958.

39) R. F. Rolsten, Iodide Metals and Metal Iodides, John Wiley & Sons Inc., New York: 1961.

40) G. L. Miller, Metallurgy of the Rarer Metals: Zirconium, Academic Press Inc., New York: 1957.

41) R. Sheldon and D. Peterson, “The U-Zr (Uranium-Zirconium) system,” Journal of Phase Equilibria: 1989, vol 10, pp. 165-171.